University of Kent

Establishing a metabolite extraction protocol and elucidating the fate of pyruvate in *Blastocystis*

A thesis submitted for the degree of MSc by research in Microbiology for supervisors Anastasios D Tsaousis and Jose Ortega-Roldan

Jamie Newton
8/16/2019

Contents

Acknowledgements

I would like to thank my supervisors Dr Anastasios Tsaousis and Dr Jose Ortega Roldan for the opportunity to write and work on this thesis as well as for their support, guidance and advice. I would also like to thank Dr Gary Thompson for his help, guidance and diligence with the NMR and data analysis and use of the spectrometer to perform the experiments, and would also like to thank the other members of Dr Tsaousis' lab for their help and support with the experimental procedures.

Abbreviations

ADH	Alcohol dehydrogenase
ASCT	Acetate : succinate CoA transferase
ATP	Adenosine triphosphate
COSY	COrrelated SpectroscopY
ETC	Electron transport chain
Fefe-Hyd	Iron-Iron hydrogenase
FRD	Fumarate reductase
FUCA	alpha-L-fucosidase
fucP	L-fuculose-phosphate aldolase
FUM	Fumarase
GC	Gas chromatography
GTP	Guanosine triphosphate
HIHS	Heat inactivated horse serum
HSQC	Heteronuclear single quantum coherence
IBD	Inflamattory bowel disease
IBS	Iritable bowel syndrome
IMDM	Iscove Modified Dulbecco Media
LC	Liquid chromatography
LGT	Lateral gene transfer
M:W	Methanol Water
MAS	Magic angle spinning
MDH	Malate Dehydrogenase
MRO	Mitochondrial related organelle
MS	Mass spectrometry
MTBE	Methyl tert-butyl ether
NADH	Nicotinamide adenine dinucleotide
NMR	Nuclear magnetic resoanace
OAA	Oxaloacetate
PDC	Pyruvate decarboxylase
PDH	Pyruvate dehyrogenase
PFO	Pyruvate ; ferredoxin oxidoreductase
PNO	Pyruvate ; NADPH oxidoreductase
RT	Room tmperature
SCS	Succinyl-CoA synthetase
SDH	Succinate Dehydrogenase
ST	Subtype
TOCSY	TOtal Correlation SpectroscopY
β1,GalT	Beta-1 1-galactosyltransferase

Abstract

Blastocystis is an extremely prevalent gut colonising eukaryotic microbe which has a global distribution. *Blastocystis* is extremely genetically diverse and encompasses 17 different subtypes 9 of which have been detected in humans. This genetic diversity along with the fact that most *Blastocystis* cases are asymptomatic, have resulted in its pathogenicity being hotly disputed. *Blastocystis* is transmitted via the faecal-oral route and has been linked with irritable bowel syndrome (IBS) and inflammatory bowel disease (IBD). Recently the theory that *Blastocystis'* impact on the gut microbiome is the basis for its pathogenicity has garnered much support and this is likely to be facilitated by its metabolism. Pyruvate metabolism is central to the metabolic pathways of all eukaryotes and *Blastocystis'* pyruvate metabolism is extremely unique, as it possesses three enzymes which convert pyruvate to acetyl-CoA. This study establishes a method to analyse *Blastocystis'* metabolome using 1D ^{1}H and 1D ^{1}C nuclear magnetic resonance (NMR) spectroscopy. A method to lyse the *Blastocystis* cells and extract its metabolites is developed. Methanol was determined to be a better extraction solvent than ethanol, bead beating was a better lysis method than sonication and temperature did not have an impact on metabolite extraction. The method developed was then applied to analyse *Blastocystis'* pyruvate metabolism. *Blastocystis'* metabolic footprint following supplementation with ^{13}C-Glucose and then ^{13}C-pyruvate was also analysed. We extracted evidence of lactate, ethanol and xylitol production in *Blastocystis*. Lactate in past studies has been demonstrated to have probiotic effects, ethanol has been demonstrated to have negative effects on the gut microbiome and xylitol has anti-adhesion effects which could also have an impact on the gut microbiota. The three different molecules detected could all have an important impact on gastrointestinal health.

Chapter 1 – Introduction

1.1 *Blastocystis*

Blastocystis Is the most commonly occurring gut dwelling eukaryotic microbe worldwide and infects humans and some animals. Its highest prevalence rate in humans is in the developing world and in faecal samples it has a reported prevalence of 30 to 50% in some developing countries [1]. *Blastocystis* true taxonomy has only quite recently been confirmed as a stramenopile and is the only known member of this group to reside in the human gut and potentially inflict pathogenicity [2]. Other members of this phylum include brown algae and mildew and are mostly marine biflagellates. *Blastocystis* has some interesting unique characteristics amongst stramenopiles as it is non-flagellated and has low motility [2].

Analysis of the genome of various *Blastocystis* isolates has determined that despite being almost morphologically identical, *Blastocystis* organisms encompass a huge amount of genetic diversity which facilitates the individuality of each subtype. Phylogenetic studies have grouped them down into 17 clades each representing a subtype [3]. Divergence in sequence between *Blastocystis* isolates is up to 3% within STs and 5-15% between STs [4].

The *Blastocystis* life cycle still requires some elucidation. However, it is widely understood to enter the host in the metabolically inactive dormant cyst form via the faecal oral route (**figure 1**). The faecal oral route involves a food or water bourne source with bad sanitation being the primary cause of the spread of *Blastocystis*. There is however strong evidence for zoonotic transmission as well. Once transmission is complete excystation occurs in the large intestine into the vaculoar form and can then further morph into the granular or ameboid form. At this stage *Blastocystis* can replicate by binary fission and can start to proliferate. The organism encysts in the large intestine. The cyst further develops in the faeces losing a fibrillar layer it initially possesses. Once it is released into the faeces it is free to enter another host [5].

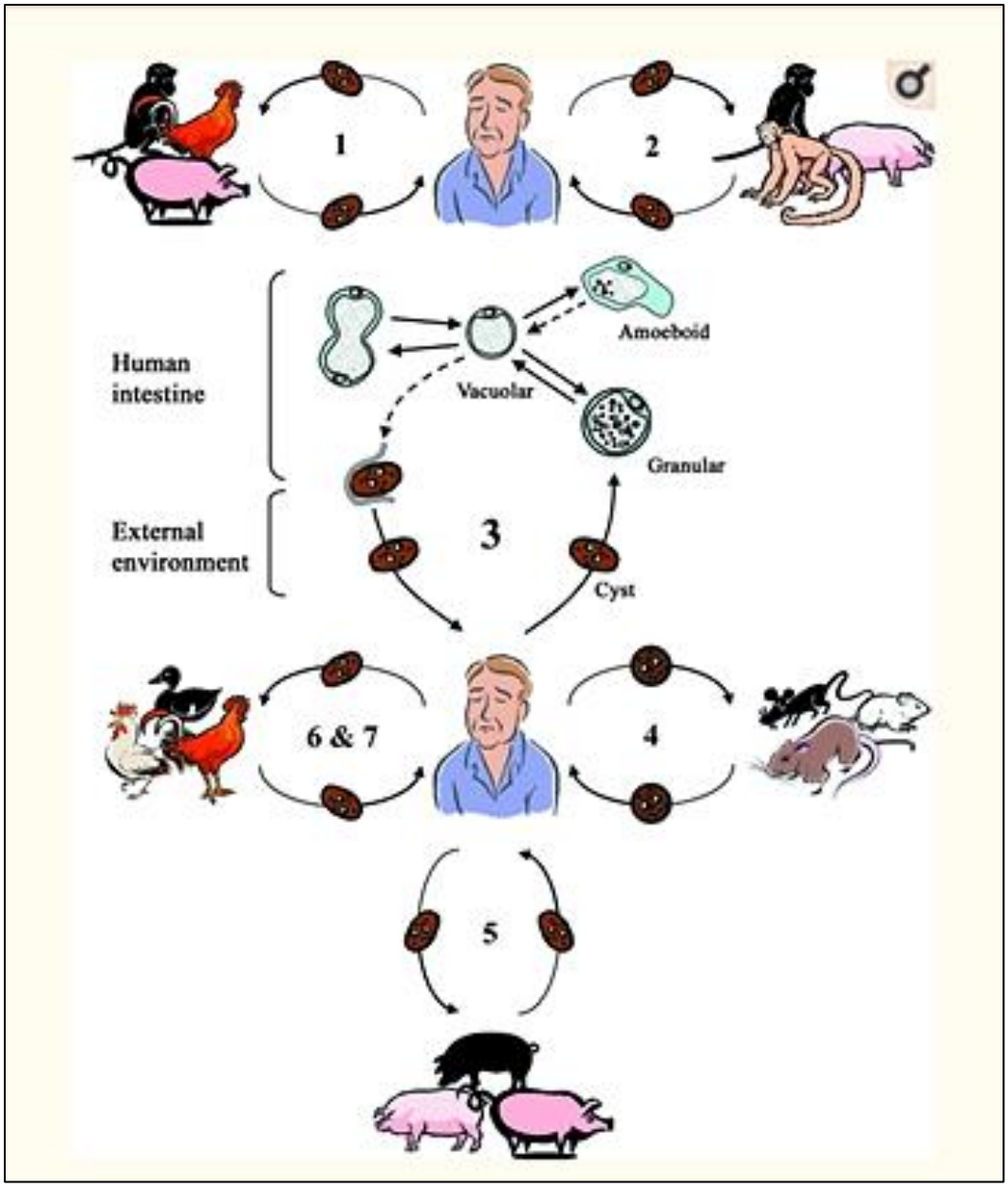

Figure 1 *Blastocystis* life cycle and origins of different subtypes involved in zoonotic infections [5]. *Blastocystis* resides in cyst form in the external environment and morphs into vacuolar form in the human intestine. It can then further develop into amoeboid or granular form and reproduce by binary fission. Subtype 1 is cross-infective among birds and mammals including humans. Subtype 2 is cross-infective between humans, other primates and pigs. Subtype 3 is cross-infective between humans, cattle and pigs. Subtype 4 is cross-infective between humans and rodents. Subtype 5 is cross-infective between humans, cattle and pigs. Subtypes 6 and 7 are cross-infective between birds and humans.

1.2 *Blastocystis* distribution

Blastocystis has a global distribution in humans, and although its highest prevalence is in the developing world it can still be isolated from 5-10% of stool samples in the developed world. The poor hygiene, cramped conditions and often higher temperatures in the developing world help facilitate this distribution as *Blastocystis* is

transmitted via the faecal-oral route [1]. A study on soldiers returning from peace keeping missions predominantly in Iraq and Afghanistan produced a 15.3% positive diagnosis, an increase on the normal prevalence in the west. This data suggested that the cramped conditions and poor hygiene the soldiers endured in these countries yields a higher transmission rate [6]. *Blastocystis* can be found in both immunocompetent and immunocompromised individuals. However it shows a significant rise in immunocompromised patients with a 38-44% prevalence in AIDS patients, 39% prevalence in patients undergoing renal transplants on immunosuppressive therapy and 11.2% prevalence on patients with haematological malignancies undergoing chemotherapy [7]. All of these patients were suffering from gastrointestinal symptoms such as abdominal pain and diarrhoea, causing some to believe that *Blastocystis* is pathogenic only in immunocompromised individuals. However, despite the increased prevalence in immunocompromised individuals and links with IBS and IBD, the overwhelming majority of individuals who test positive for Blatocystis are asymptomatic [8],[9].

Blastocystis has also been isolated from many animal hosts. Of the 17 different STs that exist, STs 1-9 can be found in humans, with 90% of human cases involving STs 1-4. Most of the other subtypes can be found in other mammalian species with some found in reptiles. However, most subtypes have been found in a varied range of hosts which helps support the hypothesis that zoonotic infection occurs [10],[4].

Many phylogenetic studies have been performed on *Blastocystis* and the results of these studies have been the identification of many clades. Each clade represents a subtype and different isolates could be added to each clade as they were identified. As they were processed many isolates from different mammalian species were grouped into the same clades as each other with human isolates included, however reptile isolates diverged slightly. Other mammalian hosts included monkeys, pigs, cattle, horses, rats and Guinea pigs. This lack of host specificity suggests *Blastocystis* cross-infection between different animal hosts [3]. A study of 30 isolates, 24 from patients from one health facility (facility A) and 6 from another health facility (facility B) concluded that human-human transmission occurs. [11]. Food handlers and people who work at abattoirs and zoos have also demonstrated a higher risk of infection from Blastocystis, as well as increased prevalence amongst animals in zoological gardens and circuses [12],[13],[14]. In summary all of this data implies that *Blastocystis* infection can be transmitted via an animal-animal, animal-human and human-animal to route.

Genotypic analyses in both developing and developed countries have concluded that ST3 is the most prevalent subtype in *Blastocystis* positive individuals worldwide. However, some geographical subtype variance in specific countries has been observed [10]. ST3 has been shown to have the highest prevalence in Turkey [15], Singapore [16], France [17], Egypt [18], Japan, Pakistan, Bangladesh, Germany [19], the U.K and Liberia, with ST1 the most common in Libya and Nigeria [10].

A PCR based genotype classification method was used to identify and classify 102 *Blastocystis Hominis* isolates, 50 from Japan, 26 from Bangladesh, 10 from Pakistan, 12 from Germany and 4 from Thailand. The results concluded that ST3 was the most prevalent genotype in all the populations apart from in Thailand. ST1 and ST4 showed the second highest prevalence's. ST2 was only detected in Japan, ST5 in Germany and ST7 in Japan and Germany and ST6 was not detected. There was also a study done on 15 symptomatic and 11 asymptomatic patients from Bangladesh but it produced no statistically significant results [19].

Overtime an ever growing record of *Blastocystis* distribution continues to be compiled (**Figure 2**). This data set was further expanded on as part of a study using gene sequencing to determine the genotypes of 356 *Blastocystis* isolates. Of these 271 were isolated from samples in the United Kingdom, 38 from Libya, 25 from Liberia and 22 from Nigeria. Of the 9 subtypes that reside in humans 8 were identified but in varying frequencies between countries. Distribution in Libya and Nigeria showed a diversion away from normal consensus with ST1 being the most common subtype, whereas in the United Kingdom and Liberia like most countries ST3 dominated. No ST4 was present in Libya and no ST2 in Nigeria and all African populations were free of ST5, ST6, ST8 and ST9. The 271 U.K samples which included all subtypes from 1-8 were also analysed based on their origin of either IBS patients or unselected individuals to assess whether they Caused IBS. No significant correlation was produced [10].

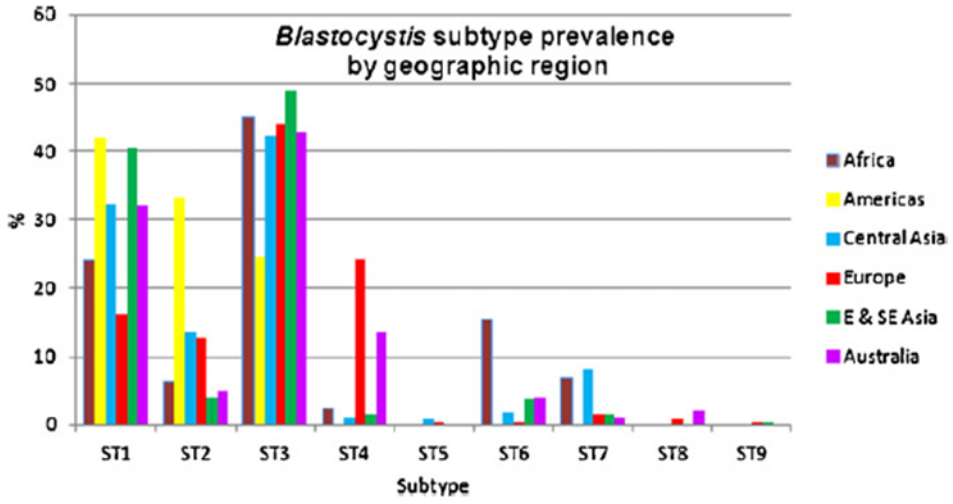

Figure 2 Subtype distribution by across various major geographic regions [10]

As shown above in **Figure 2** *Blastocystis* distribution of Subtypes 1-4 shows some consistency between different regions. For example, Africa, Central Asia and South East Asia ST3 is the most prevalent subtype followed by ST1, with ST2 in third and ST4 in fourth. In some of these regions there are subtypes amongst ST5-ST9 which show higher prevalence's than ST4. Subtypes 5-9 are less consistent in their distribution. The Americas show the most unusual distribution with ST1 being the

most prevalent subtype. However USA shows a more European distribution [10]. This data combined with the higher ST1 distribution rate in Asia and Africa and the fact that ST1 appears to be the subtype most correlated with pathogenicity, could be evidence that ST1 is a pathogenic subtype and is more prevalent in developing countries because of poor sanitation.

In summary, *Blastocystis* shows a reasonably consistent subtype distribution rate throughout various regions. Westernised cultures distributions appear to correlate with each other and developing countries also show some correlation with each other. Increased prevalence in certain subtypes amongst humans who work in close proximity with animals, as well as low prevalence in some urban areas provides evidence of zoonotic transmission. ST1 appears to show an increased distribution in developing countries and there is some evidence that supports its pathogenicity. However, the potential pathogenic mechanism of *Blastocystis* is hard to establish.

1.3 *Blastocystis* pathogenicity

Blastocystis's potential pathogenicity has been extremely difficult to determine and a matter for much dispute amongst researchers. *Blastocystis's* lack of pathogenic mechanisms such as flagella to provide movement resulting in its non-motility, as well lectins or rhoptries has led some researchers to believe that it is part of a healthy gut microbiota [20]. Also, *Blastocystis's* wide distribution as well as the fact that the overwhelming majority of cases are non-symptomatic supports this hypothesis. There have also been no outbreaks of *Blastocystis* infections in the form of epidemics or pandemics like for example *ebola* or SARS. However, increased prevalence of certain subtypes as well as an increase in an IgG2 *Blastocystis* specific antibody in symptomatic individuals, have led many to still believe a disease-causing effect of *Blastocystis* exists. Also, increased prevalence in immunosuppressed individuals with IBS symptoms provides evidence that *Blastocystis* could be pathogenic but only when the patient is immunosuppressed [7]. Data exists to support the two conflicting hypothesis. However, recent studies on how *Blastocystis* may be involved in dysbiosis [21] have garnered much support and could reveal *Blastocystis*' pathogenic mechanism. This mechanism involves colonisation of the gut and has resulted in research taking a public health approach as opposed to a clinical approach.

Eme et al identified approximately seven laterally acquired genes with potential pathogenic, immune response and evasion roles [22]. Amongst these genes is beta-1 3-galactosyltransferase (β1,3GalT) acquired from animals and is responsible for the biosynthesis of Lewis blood group antigens and their corresponding Antidiuretic Hormone determinants, which are expressed in the epithelial cells of the gastrointestinal tract. This suggests that *Blastocystis* can perform molecular mimicry to evade immune response [23], which will help in its colonisation of the gut as in mucosal bacteria [24]. Another LGT acquired gene which helps evade immune response is a cholesterol-alpha-glycosyltransferase. *Helicobacter pylori* possesses

this gene and it utilizes it by α-glucosylating cholesterol which results in it evading phagocytosis, T-cell activation and bacterial clearance. As *Blastocystis* has acquired this gene it is believed that it performs the same function [25].

There are also five gene families in *Blastocystis* which are thought to be involved in oxidative stress responses as *Blastocystis* can tolerate oxidative bursts. These bursts could be generated by host immune responses so these gene families could be involved in immune system evasion [26].

As *Blastocystis* possess a lack of orthodox pathogenic mechanisms a substantial amount of research has moved towards the effects of its colonisation. The most fundamental of *Blastocystis's* colonising effects is its influence on the healthy gut microbiota. A faecal DNA metagenomics study suggested a correlation between *Blastocystis* and specific enterotypes [27]. The enterotype classification used categorised all individuals gut microbial communities into the either *Bacteroides*, *Ruminococcus* or *Prevotella* [28]. *Blastocystis* appeared to be significantly more prevalent in individuals with the *Ruminococcus* and *Prevotella* enterotypes than in individuals with the *Bacteroides* enterotype. There also appeared to be a positive correlation between *Blastocystis,* lean individuals and microbial diversity. However, there was no correlation between just lean individuals and microbial diversity suggesting that for lean individuals to have a diverse and in which case healthy gut microbiome *Blastocystis* must be present [27]. This data implies that *Blastocystis* is good for a healthy gut. However, other studies have suggested that *Blastocystis* colonisation has negative effects.

Some of those negative effects could be partly facilitated by the positive impact *Blastocytis* has. *Blastocystis* having a positive impact on the gut microbiota would help sustain it in its ability to survive and thrive and eventually colonise. However, there are some members of the gut microbiome which appear to decrease in the presence of *Blastocystis* and amongst these is *Bifidobacterium longum* [21],[27],[29].

Nourrisson et al first provided evidence of the decrease of *Bifidobacterium sp* in the presence of Blastocystis, from a metagenomics study of faecal samples from *Blastocystis* positive patients [29]. *Bifidobacterium* is known to form a protective layer along the gut lining and is therefore important for gastrointestinal health. Co-incubation experiments of *Blastocystis* with many members of the gut microbiota by Yason et al concluded that a strain of ST7 helped facilitate the increase of many members of the gut microbiota. However, they also concluded that *Bifidobacterium longum* decreased in numbers in the presence of this strain. They then performed histopathological experiments on experimentally infected mice and concluded that the *Blastocystis* facilitated decrease in *B. longum* resulted in oxidative damage to the gut lining causing inflammation [21].

As a pathogenic mechanism of *Blastocystis* appears to be its impact on the gut microbiota, it is molecules produced by *Blastocystis* which are important to this.

Whether it produces important nutrients for microbiome species that thrive in its presence, toxic molecules for *B. longum* or causes oxidative damage to the intestinal lining, studying *Blastocystis* metabolism is highly important. The mitochondrion is integral to the metabolism of all eukaryotic organisms and analysis of *Blastocystis's* unique mitochondrial related organelle (MRO) may help provide answers to its pathogenicity.

1.4 *Blastocystis* metabolism

1.4.1 *Blastocystis* MRO

What is currently known about *Blastocystis* metabolism has been resolved by analysis of its MRO. Isolation by centrifugation and biochemical assays [30], as well as gene sequencing assays followed by tests for activity have been utilised to map *Blastocystis's* metabolic pathways [31]. Adaptation to anaerobic environments like many parasitic protists, along with many mechanisms acquired by LGT, has resulted in *Blastocystis's* MRO being a hugely unique and diverse organelle. It is this uniqueness which has resulted in the inability to properly categorise it.

Table 1

Class		ATP production	H_2 generation	Electron transport chain	O_2 utilization as the terminal electron acceptor
1	Aerobic mitochondria	O	X	O	O
2	Anaerobic mitochondria	O	X	O	X
3	H_2-producing mitochondria	O	O	O	X
4	Hydrogenosomes	O	O	X	X
5	Mitosomes	X	X	X	–

MRO classification devised by Muller et al [32]. Aerobic mitochondria in class 1 are canonical mitochondria. Classes 2 – 5 are all anaerobic adaptations of canonical mitochondria. O = Present in this class. X = Not present in this class - = Currently unknown.

MROs are classified using a system devised by Muller et al [33] (**table 1**). Class 1 covers all canonical aerobic mitochondria as found in most eukaryotes. Classes 2-5 consist of anaerobic adaptations of aerobic mitochondria mostly found in protozoan parasites, who are believed to have acquired their phenotypes through adaptation to microaerophilic environments [33].

The *Blastocystis* MRO possesses phenotypes characteristic of Aerobic mitochondria and Hydrogenosomes. For example, it contains cristae and has an organellar genome like aerobic mitochondria. However, like hydrogenosomes it produces H_2 and produces ATP via acetate : succinate CoA transferase (ASCT) and succinyl-coA synthetase (SCS). For this reason the *Blastocystis* MRO is not given a specific classification and is generally referred to as the *Blastocystis* MRO [31].

1.4.2 *Blastocystis* Krebs cycle

A largely unique feature of the *Blastocystis* MRO is its incomplete Krebs cycle (**figure 3 b**). In canonical mitochondria a full cycle of reactions involving 8 organic compounds takes place releasing electron carriers such as NADH and $FADH_2$ and energy storing molecules such as GTP (**figure 3a**). The Krebs cycle begins with the conversion of oxaloacetate to citrate by the addition of an acetate molecule to oxaloacetate catalysed by the high energy molecule acetyl-CoA. However, in *Blastocystis* the fate of acetyl-CoA is quite different, and Oxaloacetate is converted to malate sending the Krebs cycle in the opposite direction. Rather than completing a full cycle *Blastocystis's* Krebs cycle ends with the reduction of Fumarate to succinate facilitated by Fumarate Reductase (FRD), which is Succinate Dehydrogenase working in the opposite direction to its function in the canonical Krebs cycle [34]. A similar mechanism to this has been described in procyclic *Trypanosoma brucei*. During its insect stage the *T. brucei* Krebs cycle, appears to split into chunks, each operating for a different purpose, such as transportation of acetyl-CoA from the mitochondrion to the cytosol [35],[36].

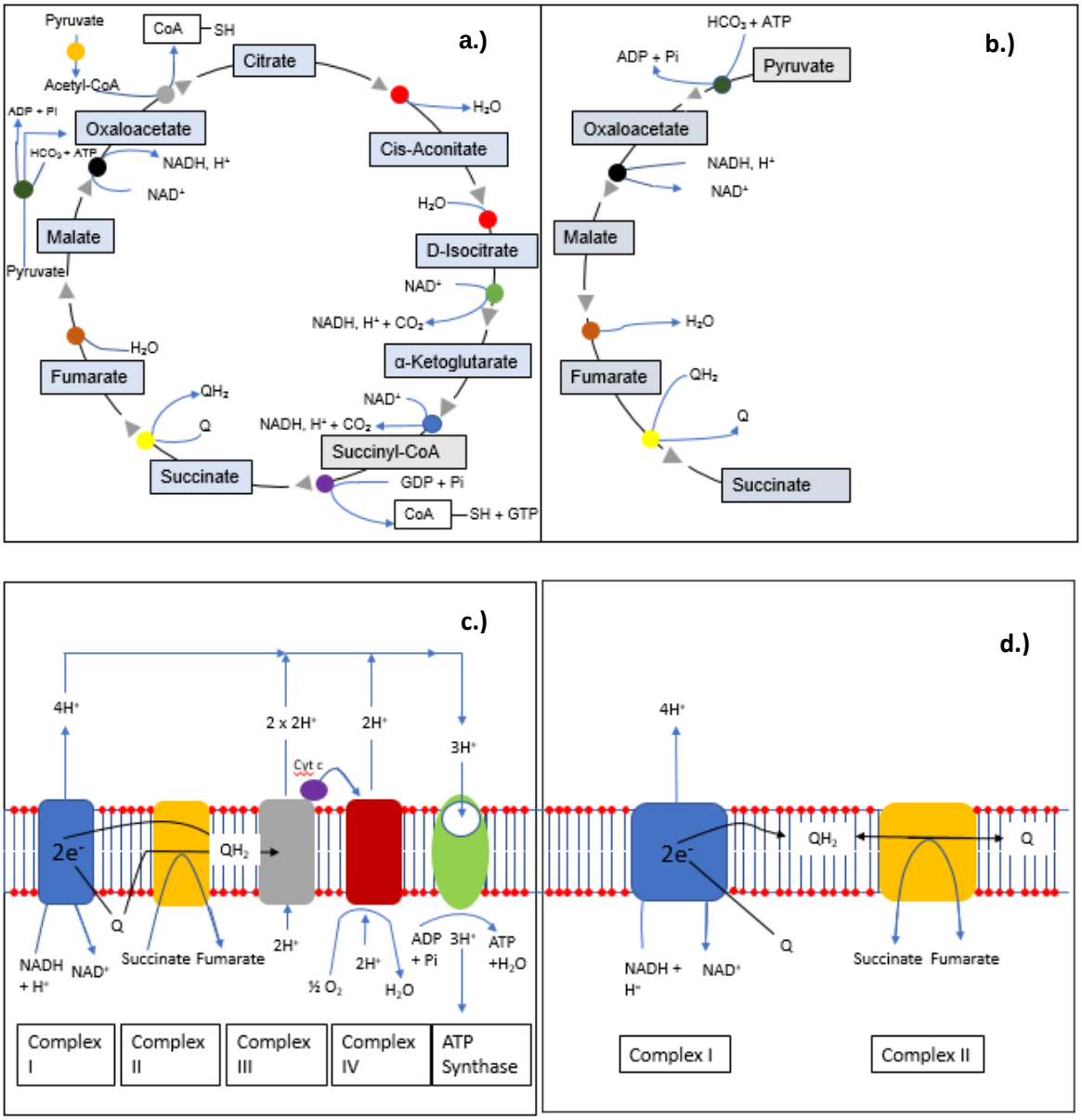

Figure-3 a. Krebs cycle in canonical mitochondria. **b.** Krebs cycle in Blastocystis. = Aconitase =Isocitrate dehydrogenase = α-Ketoglutarate dehydrogenase = Succinyl-CoA synthase = Succinate dehydrogenase / Fumarate reductase = Fumarase = Malate dehydrogenase = Citrate synthase = Pyruvate dehydrogenase = Pyruvate carboxylase **c**. Electron transport chain (ETC) in canonical mitochondria. **d.** Electron transport chain in *Blastocystis.*

1.4.3 *Blastocystis* electron transport chain

The Succinate Dehydrogenase catalysed reaction is involved in the electron transport chain (ETC) in canonical mitochondria as well as the Krebs Cycle (**figure 3c**). It oxidises Succinate to Fumarate and donates electrons to complex II of the ETC in the process, and the residual protons are transported across the inner mitochondrial membrane. The electrons are transferred from complex II to complex III, then to complex IV each complex pumping more protons across the inner mitochondrial membrane in the process. This mechanism generates an electrochemical proton gradient across the inner mitochondrial membrane with a

partial negative charge on the inside. The protons move down the electrochemical gradient from the inter-membrane space to the mitochondrial matrix through a channel in ATP synthase. The energy from this mechanism is harnessed to synthesise ATP facilitated by ATP synthase. In the *Blastocystis* ETC (**figure 3d**) Fumarate reductase (Complex II) reduces Fumarate to succinate and the process works in the opposite direction. In canonical mitochondria the electrons are transferred from Succinate Dehydrogenase (Complex II) to complex III by Ubiquinone which has a higher reduction potential than complex II so steals the electrons away. In the ciliate *Nyctotherus ovalis* rhodoquinone which has a lower reduction potential than complex II transfers electrons from complex I to fumarate reductase (Complex II) which then transfers them to Fumarate which acts as a terminal electron acceptor [39]. This same process appears to take place in *Blastocystis. Nyctotherus Ovalis* possesses a Hydrogenosome with some aerobic mitochondrial features and is the most similar known organelle to the *Blastocystis* MRO. The *N. ovalis* hydrogenosome is thought to be the missing link between aerobic mitochondria and the hydrogenosome [39]. It is thought that it convergently evolved with the *Blastocystis* MRO acquiring anaerobic phenotypes to adapt to a microaerophilic environment. Both *Blastocystis* and N. *ovalis* only possess complex I and complex II. As their ETC's are incomplete they have a different ATP synthesising mechanism and their ETC's just produce a membrane potential which is used for other purposes[39],[31].

1.4.4 *Blastocystis* glycolysis

Like most eukaryotes with canonical mitochondria Blastocystis's initial step in glucose metabolism is glycolysis. A unique property that has recently been discovered with regards to stramenopiles is mitochondrial glycolysis. The glycolytic steps of eukaryotic metabolism are believed to be bacterial in origin, and almost universally amongst mitochondrion and MRO baring organisms take place in the cytoplasm. However recent tests using sedimentation through centrifugal force to isolate the MROs of three stramenopiles, followed by gene sequencing and enzyme analysis suggest that stramenopiles do not reflect the universal consensus (**figure 4**). These tests suggested that Blastocystis was quite unique even amongst stramenopiles. Of the three stramenopiles tested two of them *Phaeodactylum tricornutum* and *Phytophthora infestans* both utilised cytosolic and mitochondrial glycolysis for the payoff phase and the final step of preparatory phase. The first four steps of the preparatory phase only took place in the cytoplasm. This also appeared to be the case in *Blastocystis,* except the payoff phase only takes place in the mitochondria with the final step of the preparatory phase taking place in both the mitochondria and the cytoplasm [40].

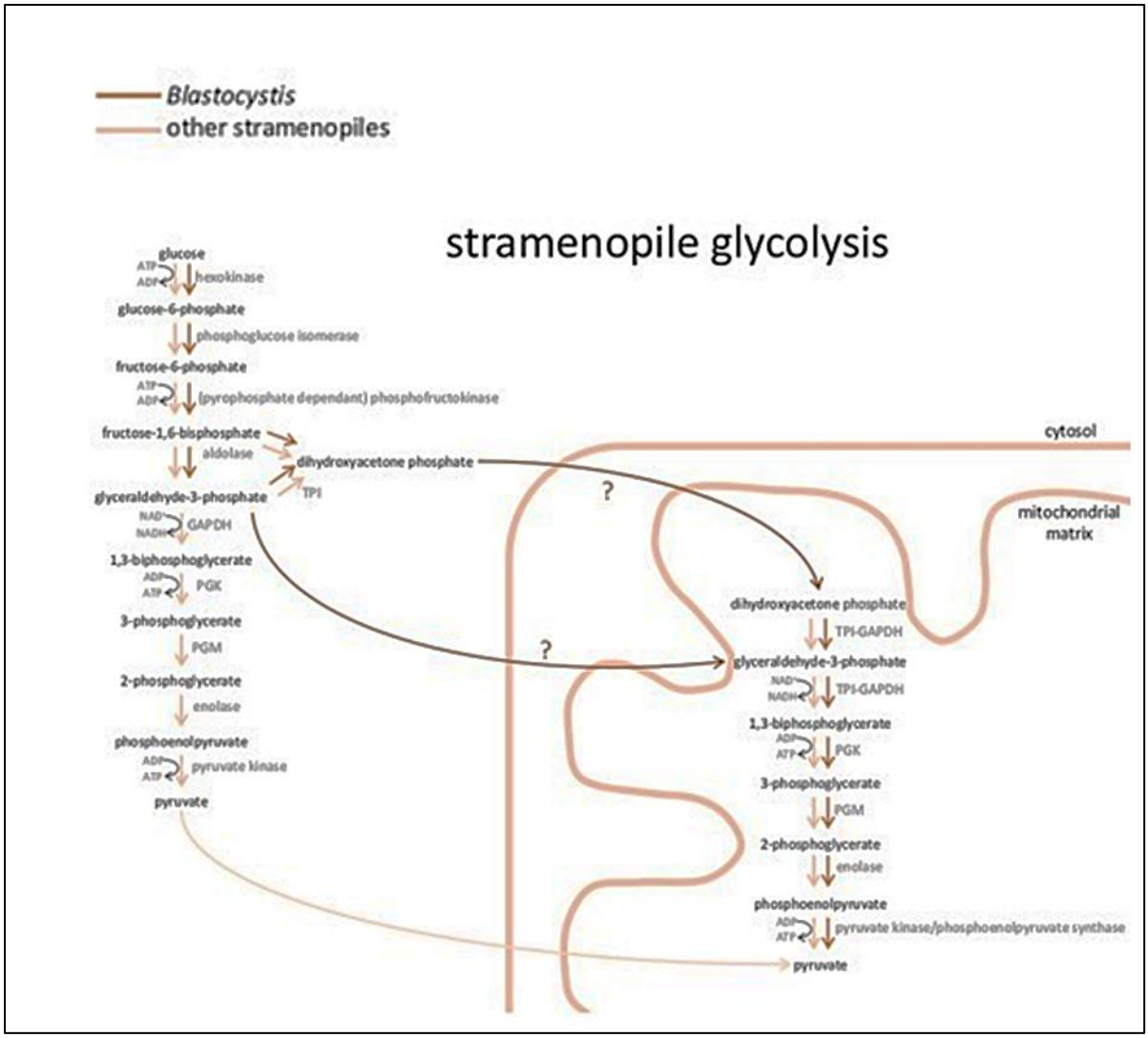

Figure 4 Stramenopile Glycolysis. Glycolytic payoff phase enzymes as well as triose phosphate isomerase are located in both the cytosol and the mitochondria, with the exception of *Blastocystis* were all the payoff enzymes are in the mitochondria[40]

1.4.5 *Blastocystis* and lateral gene transfer (LGT)

Gene acquisition by lateral gene transfer (LGT) has been shown to play an important role in Blastocystis' attaining a vast amount of genetic diversity. A phylogenic analysis of a strain of Blastocystis ST1 found that 167 genes which pervades 2.5% of its protein coding genome and belong to 74 gene families were acquired by LGT [5]. Most LGT acquired genes are from prokaryotes with many acquired from the enterotypes firmicutes, proteobacteria and bacteriodetes which are all abundant in the gut. This data implies that LGT was important for Blastocystis adaptation to the gut [5],[6]. Blastocystis is an obligate anaerobe, however it can tolerate oxidative bursts. These are both phenotypes which were acquired by LGT and help facilitate Blastocystis's adaptation to the gut environment. LGT played a role in the evolution of *Blastocystis's* metabolism and amongst the phenotypes acquired are mechanisms involved in carbohydrate scavenging. These mechanisms help provide *Blastocystis*

with a sustainable food source whilst it survives and thrives in the gut environment. Eme et al identified 17 laterally acquired genes involved in carbohydrate metabolism, five of which are involved in the metabolism and import of fucose [22]. Gut bacteria release fucosidases to breakdown glycans into fucose monomers for a food source and to present on their surface [41]. Also, mucosal fucosylated glycans are important for adherence of some bacteria to the gut lining [42]. So *Blastocystis* scavenging for fucose may result in a depleted fucose volume in the gut, which could result in the loss of a food source for many members of the gut microbiome. It could also result in the loss of adhesion molecules for some members of the gut microbiome. These two factors could result in the loss of bacteria in the gut and the loss of protection to the gut lining, leaving it more exposed to oxidative damage.

The five LGT acquired genes involved in L-fucose scavenging are alpha-L-fucosidase FUCA, L-fucose permease fucP and L-fuculose-phosphate aldolase fucA which are thought to be acquired from *Bacteriodes thetaiotaomicron* [43] and L-fucose Dehyrogenase and L-fuconolactase are proposed to be acquired from *C. jejuni* [44] as they belong to a metabolic pathway that it possesses. The pathways of these enzymes and the metabolic processes are shown in **figure 5**. FUCA is the enzyme which is released to degrade glycans in the gut and fucP is the permease which internalises the fucose monomers for metabolic use by the cells. The L-fucose is phosphorylated by an unknown mechanism then fucA converts L-fucose 1-phosphate to lactaldehyde which is subsequently added to dihydroacetone phosphate and joins the glycolytic pathway [22]. The end product of the glycolytic pathway is pyruvate which either generates ATP via ASCT and SCS, or takes the route into the *Blastocystis* Krebs cycle and goes on to be the terminal electron acceptor for the ETC.

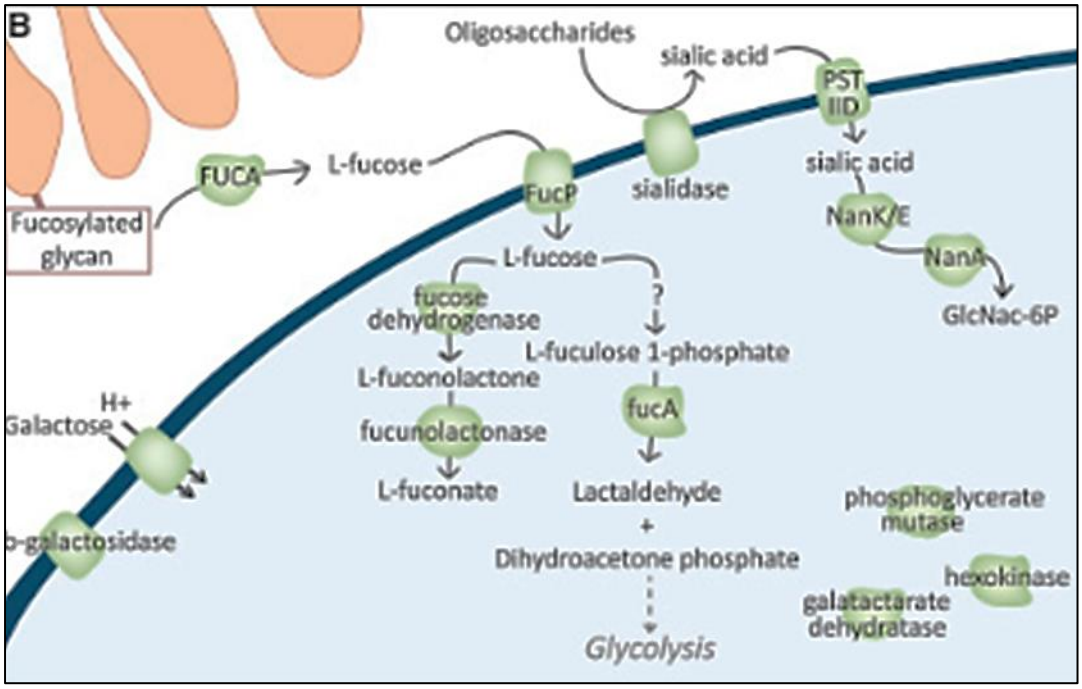

Figure 5 Enzymes involved in carbohydrate scavenging acquired by LGT [22]

1.4.6 *Blastocystis,* LGT and pyruvate metabolism

Significant components of *Blastocystis's* anaerobic ATP generating pathway appear to be acquired by LGT (**figure 6**). The intermediate step between glycolysis and the Krebs cycle in canonical mitochondria is the conversion of pyruvate to acetyl-CoA by pyruvate dehyrogenase (PDH). *Blastocystis* possess three pyruvate metabolising enzymes. PDH, Pyruvate ; ferredoxin oxidoreductase (PFO) and Pyruvate ; NADPH oxidoreductase (PNO). Both PFO and PNO appear to be acquired by LGT. Acetyl-CoA is generated from pyruvate by these enzymes, which is then converted to acetate and succinyl-CoA by ASCT which is also of LGT origin. Succinyl-CoA synthetase (SCS) which is of canonical mitochondrial origin then utilises Succinyl-CoA as a cofactor to generate ATP [22]. Also an RQUA gene with an MRO localisation signal was identified as being laterally acquired. RQUA codes for an enzyme that biosynthesises rhodoquinone, which transfers electrons from complex II to fumarate. Therefore, rhodoquinone may have played a role in adapting a reverse Krebs cycle and therefore adaptation to an anaerobic environment [45].

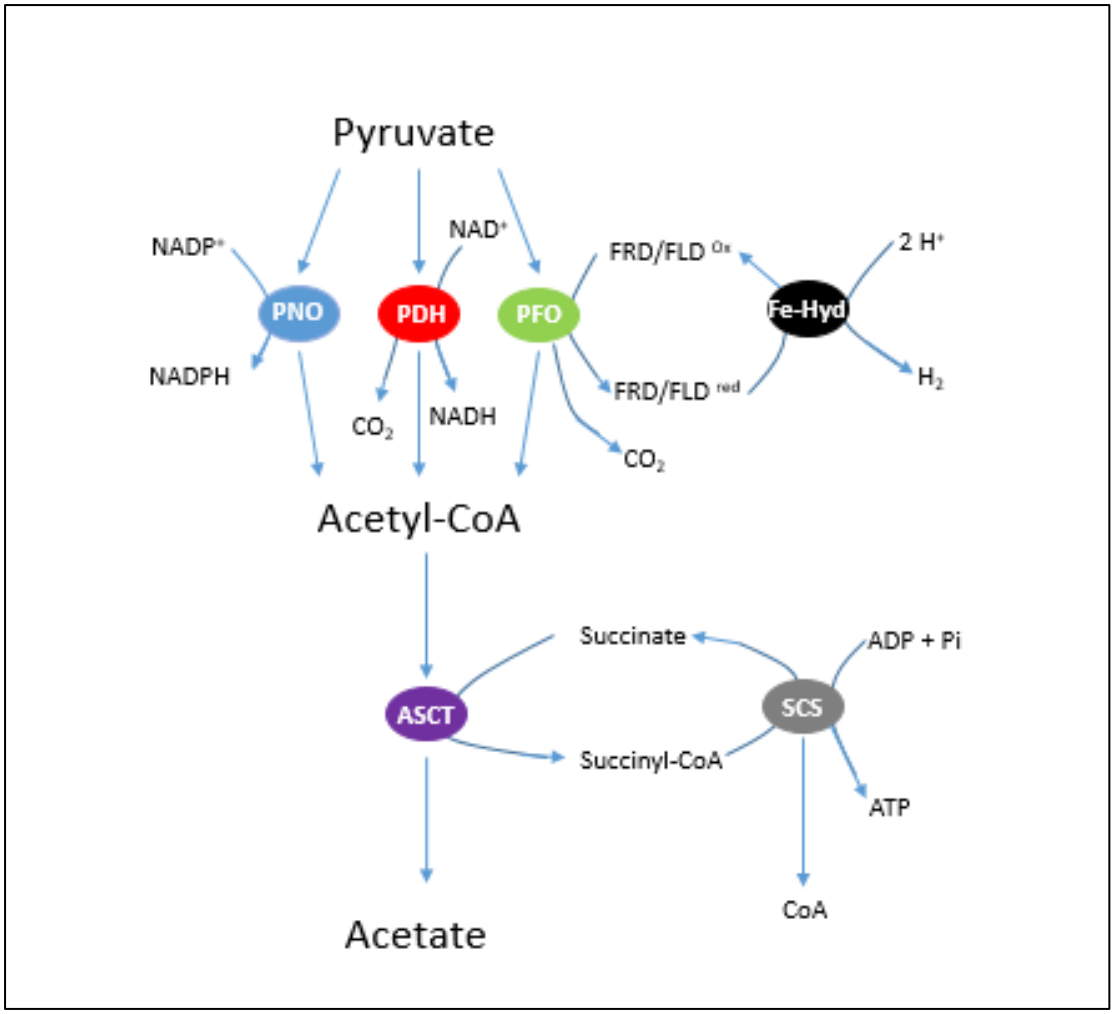

Figure 6 *Blastocystis's* anaerobic pyruvate metabolism and ATP production. PFO, PNO and ASCT are all likely to be acquired by LGT [34].

PFO and PNO are oxygen sensitive homoloques of PDH and play its same role in many anaerobic protists. PFO uses ferrodoxin and Flavodoxin as cofactors and works in tandem with an iron-iron-hydrogenase (Fefe-Hyd) which produces these cofactors (**figure 6**). Fefe-Hyd also produces hydrogen (H_2) in this process and is the source of H_2 in Hydrogenosomes. However, although the PFO gene has been detected in *Blastocystis* no PFO or Fefe-Hyd activity has been detected. PFO is present in *Trichomonas vaginalis* and is upregulated by the presence of iron. It is expressed on *T. vaginalis* cell surface and involved in adhesion to the vaginal epithelial cells[46]..

The flagellate *Euglena gracilis* has a similar pyruvate metabolising mechanism to *Blastocystis* as its mitochondria possess the oxygen tolerant PDH and the oxygen sensitive PFO. The *Euglena gracilis* mitochondria also possesses both a full ETC and the functionality to produce ATP using oxygen as a terminal electron acceptor as part of this mechanism. *Euglena gracillis* also possesses the mechanisms to produce ATP anaerobically. The *Euglena gracilis* mitochondria also possess both ubiquinone and rhodoquinone. All of these mechanisms sustain *E. gracilis* in both oxygen rich

and oxygen poor environments, and the presence of PFO and PDH, are believed to help facilitate its ability to survive and thrive in these environments [47]. This to a much lesser extent could be the case in *Blastocystis*. *Blastocystis* is an obligate anaerobe and does not possess the aerobic functions that *E. gracilis* does. However, it does possess reactive oxygen detoxifying mechanisms such as Superoxide Dismutase (SOD) and can tolerate oxidative bursts [34].

Acanthamoeba castellanii is another protist which has the means to survive in both aerobic and anaerobic environments [48],[49]. Its MRO has also been proposed as a possible intermediate between the Aerobic Mitochondria and the Hydrogenosome. *Acanthamoeba* is a habitual aerobic organism [48]. However, it regularly encounters microaerophilic environments. Therefore it has acquired the means to adapt to these environments [49]. *Acanthamoeba* possesses PFO however it also possesses PDH [50],[48]. Nitazoxanide is an inhibitor of PFO which is only effective at killing Acanthamoeba in microaerophilic conditions suggesting PFO is only active under microaerophilic conditions. So, like *E. gracilis, Acanthamoeba* uses this mechanism to facilitate its adaptation to aerobic and anaerobic environments. However Acanthamoeba is a habitual anaerobe [49]. This once again supports the hypothesis that the *Blastocystis* mechanism helps it tolerate oxidative bursts.

PNO is a homoloque of PFO, which is fused to an NADPH-haemoprotein reductase domain at its C-terminus. PNO uses NADP+ as a cofactor rather than ferredoxin or flavodoxin [47]. Unlike PFO, PNO activity has been detected in Blastocystis. PNO is present in the intestinal anaerobe Cryptosporidium parvum, as an orthodox pyruvate metabolising enzyme [49]. However, it is present in the cytosol rather than the C. parvum mitosome [49],[50]. PNO plays an important role in the C. parvum metabolism as it survives and thrives in the gut. C. parvum causes diarrhoea in mammals and survives and thrives in a similar environment to Blastocystis [49].

So unlike *E. Gracilis* or *Acanthamoeba, Blastocystis* has demonstrated PNO activity but no PFO activity. All three protists have demonstrated PDH activity and as PNO and PFO are both oxygen sensitive, it is possible that *Blastocystis's* pyruvate metabolising mechanism is for a similar purpose as *E. Gracilis* or *Acanthamoeba.* However, *Blastocystis* does not have the mechanisms to perform aerobic metabolism like *E. Gracilis* or *Acanthamoeba* do. So it is likely that it just tolerates oxidative bursts. Also as the PFO gene is also present it is possible that PFO is only upregulated in certain circumstances in Blastocystis like in *T. vaginalis.*

1.5 Project Aim

Here we optimise a method to study the metabolome of *Blastocystis* ST7 using NMR spectroscopy and subsequently utilise this method to analyse its pyruvate metabolism. We use ST7 because its whole genome has been sequenced in past studies and it is one of the subtypes that has been demonstrated to be pathogenic in past studies. The presence of the three different pyruvate metabolising enzymes and

their functions in other organisms, raise many questions about pyruvate metabolism in *Blastocystis*. The fate of pyruvate could provide important clues into the general metabolism of *Blastocystis*, its pathogenicity and its ability to survive and thrive. However, in order to understand this, it is necessary to look at the whole metabolome. It is important to study the metabolome because the end products of *Blastocystis* metabolism could be released by the cell and could affect its external environment. This could be an important factor with regards to *Blastocystis's* pathogenicity, its effect on the gut microbiota or both.

Chapter 2 – Establishing a method for metabolite extraction on *Blastocystis*

2.1 Introduction

Blastocystis is a protozoan anaerobe which resides in the gastrointestinal tract infecting approximately one billion people worldwide. It is an extremely genetically diverse organism encompassing 17 different subtypes (ST's). ST's 1 to 9 infect humans and have become a potential health concern being linked with irritable bowel syndrome (IBS) and inflammatory bowel disease (IBD). *Blastocystis*' pathogenicity has however been much disputed and their extreme diversity further complicates the understanding of their pathogenic mechanism [51],[52]. This has resulted in some researchers believing that *Blastocystis* is part of a healthy gut microbiota and could possibly even be beneficial to gastrointestinal health [53]. *Blastocystis's* effect on gastrointestinal health has been proposed to be its impact on the gut microbiome. Past studies have suggested that Blastocystis can have both positive and negative effects on the diversity of the gut microbiome. These effects could be caused by competition for nutrients or production of catabolites making metabolomics studies highly important [21]. *Blastocystis* could produce probiotic molecules which would be beneficial to the diversity of the gut microbiome, but could also produce molecules which are toxic to these bacterial communities. A metabolic analysis to study *Blastocystis* metabolism requires a protocol to lyse the cells and extract its metabolites and an analysation method to detect the metabolites.

Nuclear magnetic resonance (NMR) spectroscopy has proven to be a useful tool for metabolomics research. Liquid and gas chromatography coupled to mass spectrometry (LC/MS, GC/MS) are techniques which are commonly used as metabolite detection methods [54]. The chromatography step is useful when detecting specific molecules, but for many metabolomics studies all the molecules extracted need to be analysed. Mass spectrometry (MS) has been hugely successful in performing metabolomics studies as it is extremely sensitive and can detect molecules at Nanomolar to picomolar concentrations. However, the arduous sample preparation involving many steps such as ionisation can result in loss of sample and the integrity of the sample being affected. For this reason, accurate quantitative analysis and good reproducibility can prove difficult. Data analysis for mass spectrometry coupled to a chromatography step can involve three-dimensional analysis and includes values for time, intensity and mass/charge (m/z) [54].

However, 1D ^{1}H-NMR can be used for qualitative and quantitative analysis and although it is less sensitive than mass spectrometry, it yields more reproducible and quantitatively accurate results from less arduous sample preparation. The only sample preparation required for metabolomics NMR analysis is an extraction of the metabolites [55],[56]. Once extracted unlike mass spectrometry their concentration

and composition remains the same between the extraction and NMR acquisition, providing they are adequately stored. This is also advantageous to studies limited by time. 1D ^{1}H-NMR data analysis and annotation of metabolites involves interpretation of a series of chemical shifts to detect a metabolite and resonance intensities can be used to determine relative concentrations.

Many successful analyses of mammalian [55],[57],[58], plant [59], nematode [60] and bacterial cell [61] metabolomes, as well as metabolites in urine and plasma [62] have been conducted using NMR. Also many studies have been performed to find biomarkers to determine disease states and analyse general health in humans [63],[64] as well lipidomic analyses [56]. However, in protozoan parasites only the *Giardia lamblia* metabolome has been analysed this way [65].

In the only NMR facilitated metabolic analysis of a protozoan parasite to date the intestinal microbe *G. lamblia* was analysed by magic angle spinning (MAS). No lysis or extraction method was needed to perform this experiment and 1D-^{1}H NMR spectra and 2D ^{1}H^{1}H-TOCSY spectra were acquired. The *G. lamblia* metabolome was successfully analysed by this method [65]. However, in Blastocystis we will be looking to apply an extraction and lysis method and use a 1D ^{1}H- Noesy to generate spectra with adequate water suppression.

Here we analyse different steps of extraction methods to try and develop the optimum method to extract the metabolites of *Blastocystis spp,* so we can analyse the pyruvate metabolism of subtype 7. We develop a suitable method to analyse polar metabolites and produce reproducible comprehensive results to determine the optimum extraction solvent, lysis method and conclude that incubation temperature is not a significant factor in establishing the best method. We also annotated many compounds so their concentrations could be monitored individually and we could analyse the biological roles of the enzymes PDH, PFO and PNO and try to establish any differing functions they may have.

2.2 Materials and Method

Blastocystis culture

The *Blastocystis* S ST7 Cultures were grown axenically in 8 ml Iscove's Modified Dulbecco's Medium (IMDM) (Gibco - Catalogue no 12200069 Thermo Fisher scientific) 10% heat-inactivated Horse Serum (HIHS) (Gibco – Catalogue no 26050088 Thermo Fisher scientific). All cultures were transferred into fresh media every 3-4 days and expanded. All cultures were incubated at 37°C in an anaerobic chamber (Oxoid – Product code 10107992 Fisher scientific) maintained at an optimum environment by as gas pack (BD – Catalogue no 261205). Subsequently cell counts were done manually using a neubauer haemocytometer (Brand – Catalogue no 717810)

Establishing DSS/D2O Resolubalisation technique

4 ml 10% D2O 5% DSS was made resulting in a final concentration of 0.5% DSS (Sigma-Aldrich catalogue no 613150) and vortexed for 30 seconds. This was then aliquoted into 4 x 1ml samples.

4 x 1ml samples 10% D2O 5% DSS resulting in a final concentration of 0.5% DSS were made.

Cell lysis and metabolite extraction using cultured media

1 ml cultured IMDM was added to 1 ml H_2O + 2ml Methanol with a resulting solution concentration of M:W (1:1). 200 mg glass beads where then added and the cells were for vortexed for 30 seconds followed by a 3-minute incubation at room temperature (RT) then vortexed for a further 30 seconds. The solution was then divided into 4 x 1ml aliquots which were centrifuged for 15 minutes at 4°C at 10,000 g. The supernatants were then decanted into fresh tubes and lyophilised.

SDS-PAGE gel

To assess the cultured media for protein contamination a 10% SDS-PAGE gel was run for 1 hour at 180 volts. The gel was then visualised using coomasie brilliant blue on a shaker for 1 hour. The gel was de-stained in 10% Acetic acid, 50% Methanol on shaker for 2 hours with a solvent change after 1 hour.

Cell lysis and metabolite extraction using washed cells

The *Blastocystis* cultures were centrifuged at 1,000 g for 5 minutes at 4°C. The media was then removed and the pellets were re-suspended and given 2 x washes in 5 ml Locke's solution. The Locke's solution was then removed and the pellets were snap frozen in liquid nitrogen and stored at -80°C.

The *Blastocystis* cells were thawed then the lysis and metabolite extraction procedure was repeated trialling different steps with the washed cells. (**Table 2** for steps of extraction protocol trialled).

Table 2

Experiment no	Extraction solvent	Lysis	Incubation	Centrifugation	Drying
1	4 ml 75 % Ethanol	Sonication 3 x 30 seconds	3 minutes at -20°C	1,000 g 15 minutes at 4°C	lyophilization
1	4 ml 50% Methanol	Sonication 3 x 30 seconds	3 minutes at -20°C	1,000 g 15 minutes at 4°C	lyophilization
2	4 ml 50% Methanol	Sonication 3 x 30 seconds	3 minutes at -20°C	1,000 g 15 minutes at 4°C	lyophilization
2	4 ml 50% Methanol	Beads 200 mg beads vortex for 30 seconds	3 minutes at -20°C	1,000 g 15 minutes at 4°C	lyophilization
3	4 ml 50% Methanol	Sonication 3 x 30 seconds	3 minutes at -20°C	1,000 g 15 minutes at 4°C	lyophilization
3	4 ml 50% Methanol	Sonication 3 x 30 seconds	3 minutes at 60°C	1,000 g 15 minutes at 4°C	lyophilization
3	4 ml 50% Methanol	Sonication 3 x 30 seconds	3 minutes at RT	1,000 g 15 minutes at 4°C	lyophilization

The steps of the different extraction protocols trialled. Experiment-1 is to determine the best extraction solvent 75% Ethanol vs 50% Methanol, Experiment-2 is to determine the best lysis method Sonication vs bead bashing and experiment 3 is to determine the optimum incubation temperature RT vs -20°C vs 60°C

Preparation for NMR acquisition

The lyophilised desiccates were suspended in 330µl miliQ H_2O, vortexed for 30 seconds then centrifuged at 2,500 g for 10 minutes. The 4 supernatants of each sample where then recombined and 147 µl D_2O 5 mM DSS was added making the resultant sample 0.5mM DSS.

Analysis of aqueous extracts by ^1H NMR spectroscopy

The one-dimensional (1D) ^1H spectra were obtained using a 600 MHz NMR spectrometer (Bruker) at a temperature of 298K and a transmitter frequency of 600.05 MHz which was locked to D_2O, tuned and shimmed automatically and the 90° pulse measured using Icon NMR. The soft pulses were then set up and the receiver gain set to a maximum of 256. A NOESY was performed running 512 scans and 8 dummy scans with a spectral width of 12.02 ppm (7211 Hz), an acquisition time of 4.54 s and a relaxation delay of 1 s producing 65536 data points. The acquisition time was later reduced to 2.27 s and the relaxation delay increased to 3 s reducing the number of data points to 32768 to improve water suppression. An excitation sculpting experiment was performed running 256 scans and 8 dummy scans with a spectral width of 16.02 ppm (9615 Hz), an acquisition time of 1.704 seconds and a relaxation delay of 1 second producing 32768 data points.

Processing and analysation of ^1H NMR data

All NMR spectra were phased, baseline corrected and line-broadened to a 1Hz exponential window function using TOPSPIN 3.6.1(Bruker) software. The spectra were then imported into Chenomx 8.4. A shim correction of 1.2 Hz was applied and the region from 4.56 ppm to 4.97 ppm was deleted to eliminate water resonance peaks. Peak assignment was performed using the profiler tool fitting the spectral line to the proposed compounds in the chenomx library. The efficacies of the extraction solvents, lysis methods and incubation temperatures were then compared using a spectral comparison model in which the ratios of a selection of peaks were calculated in relation to the spectra they were being compared to (**equation 1** for the determination of the extraction solvent example).

Equation 1 n = I ethanol/I methanol

The median, standard deviation (stdev) and coefficient of variance (C.V) were all calculated to determine the reproducibility of the results. Any outliers were detected and removed from the analysis.

2.3 Results

To determine the optimal protocol to extract metabolites from the parasite *Blastocystis spp* ST7 for NMR analysis a series of extraction solvents, lysis techniques and incubation temperatures were analysed. The efficacy of each protocol was assessed using proton NMR and peak intensity compared using TOPSPIN 3.6.1 to determine which method extracted the highest concentrations of metabolites. Chenomx 8.4 was then used to determine which metabolites were extracted. We developed an efficient reproducible protocol to perform metabolomics studies on *Blastocystis spp* and found that the extraction solvent and lysis method were the most important factors for metabolite extraction.

DSS/D_2O addition to individual samples produced optimal accuracy of reference sample intensity

To establish the most the most efficient method of obtaining an accurate intensity of our reference sample DSS, the reproducibility of two different dilution methods were analysed. The optimal method would then be used to resolubilise our extracted metabolites after lyophilisation. A solution of 4 ml H_2O 10% D_2O 0.5% DSS was made and aliquoted into four 1 ml samples in the first method. In the second method four 100 µl samples of 10% D2O 0.5% DSS were added to four 900 µl aliquots H_2O individually. The addition of D_2O 5% DSS to each sample individually was determined to produce more consistent and reproducible results than making aliquots from one large sample (**table 3a and table 3b**) The C.V was calculated to determine the reproducibility of the two methods. The samples with 100 µl DSS/D_2O added to 900 µl H_2O individually produced a C.V of 0.01, whereas the 1 ml samples which were aliquoted from a 4 ml sample 10% D_2O 0.5 DSS produced a C.V of 0.04, so the individual samples were determined to be more reproducible. The aliquoted samples produced 3 peaks with intensities of 1, 0.98, 0.96 but one peak with an intensity of 0.9 (**figure 7a**). However, the individually mixed samples produced 3 peaks with intensities of 0.98 and 1 peak with an intensity of 1 (**figure 7b)**. Therefore, the addition of the DSS D_2O individually was determined to be the optimal method for obtaining an accurate DSS intensity.

Table 3a

Column1	Column2
Sample	**Relative intensity**
1	0.98
2	0.98
3	0.98
4	1
Median	0.99
stdev	0.01
C.V	0.01

Table 3b

Column1	Column2
Sample	**Relative intensity**
1	0.98
2	1.00
3	0.90
4	0.96
Median	0.96
stdev	0.04
C.V	0.04

Table-3 a. Relative intensities of the 4 x 1ml samples which had DSS added individually. **b.** Relative intensities of the 4 x 1 ml aliquots from a 4 ml sample.

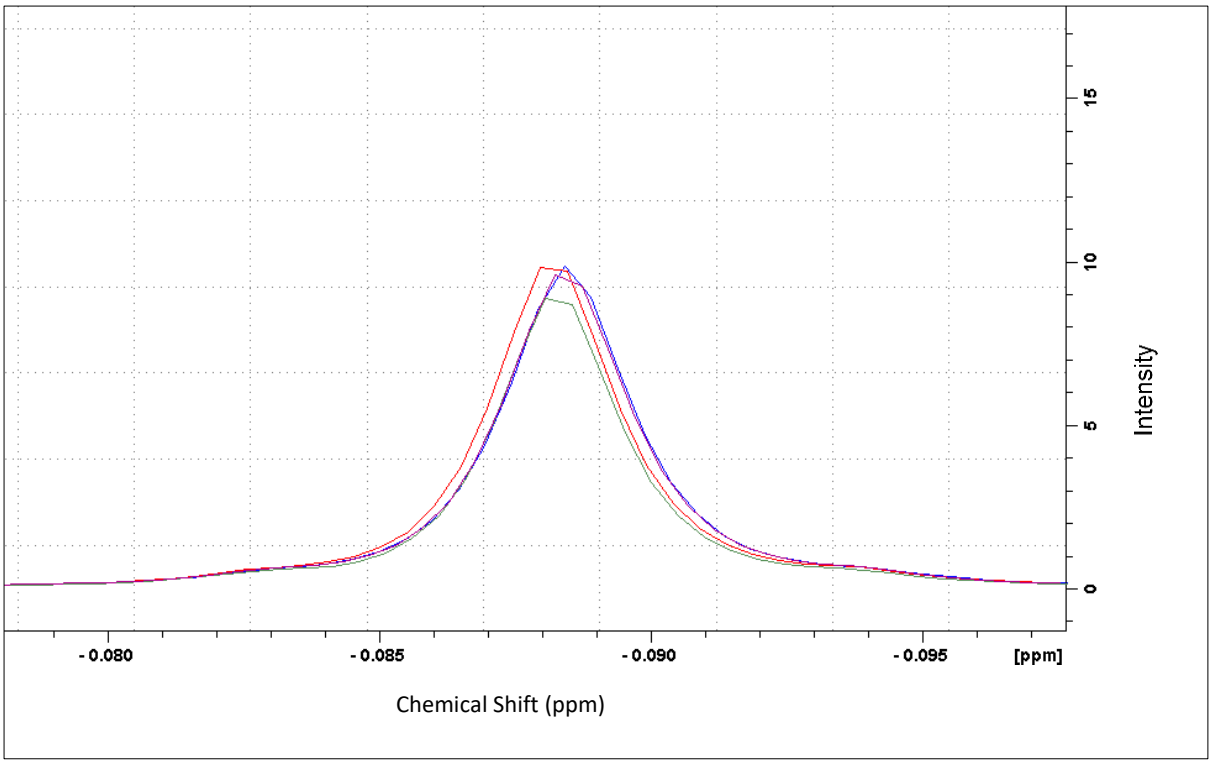

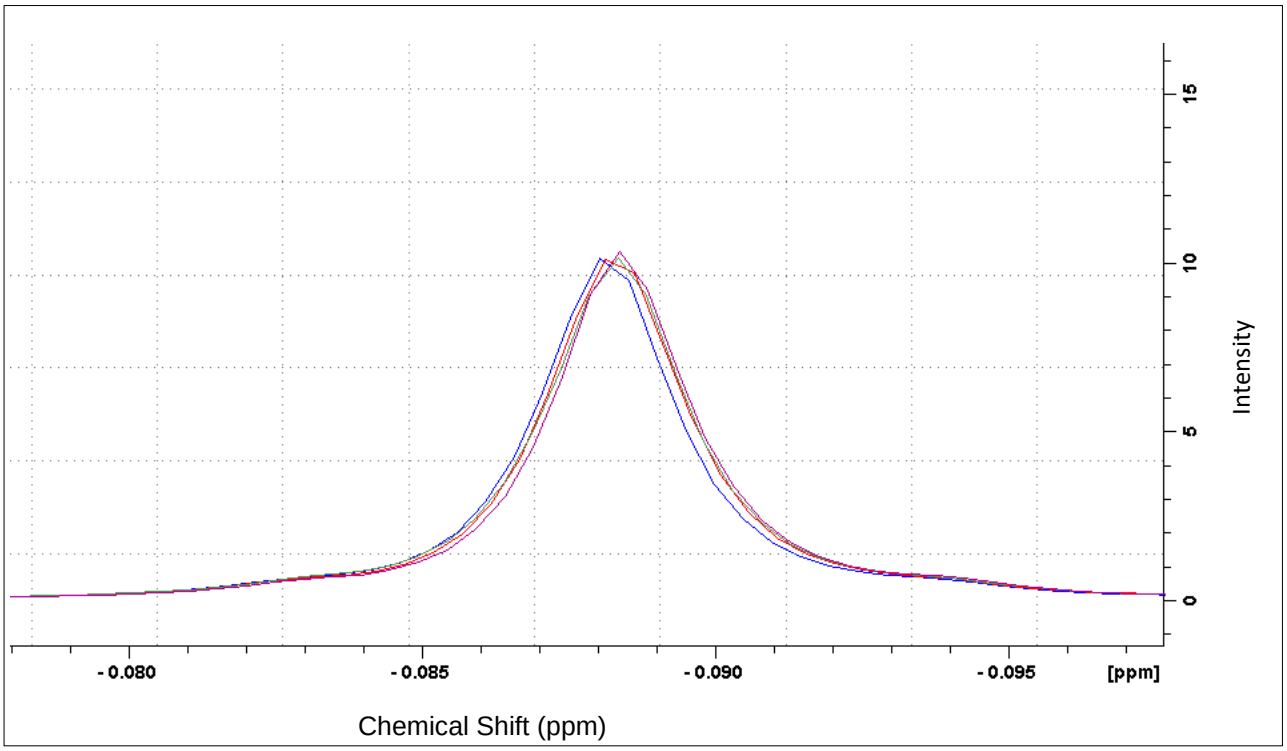

Figure 7a. DSS peaks produced from 4 x 1 ml aliquots from a 4 ml sample **b.** DSS peaks produced from 4 x ml samples which had DSS added individually.

Metabolite extraction from Blastocystis in culture media yielded protein contamination

The extraction of metabolites from *Blastocystis* whilst suspended in its culture media was trialled and produced a spectrum in which many metabolites were detected. However, between the spectral regions of 2.5 ppm and 3.7 ppm there was an extremely wide resonance which we believed to be protein contamination (**Figure 8**). Proteins often produce wide peaks on ^{1}H spectra because of the size and complexity of their structures. The media used was IMDM + Horse serum. Horse serum contains a large amount of protein. The wide resonance produced distorted the spectrum making phasing, baseline correction and metabolite detection extremely difficult. An SDS-PAGE gel confirmed that protein contamination was causing this (**Figure 9**). Bands were produced around 25 kDa on two of the replicates that were run, as well as some very faint bands around 70 kDa. Clear bands were produced around 70 kDa on one of the other replicates and the other replicate produced a very faint band around 70 kDa. This confirmed that protein contamination was distorting our data interpretation. Therefore, a wash step in Locke's solution was added to the procedure to remove the protein contamination. This step was performed at the start of the procedure to help perform small metabolite detection and devise the optimum extraction solvent, lysis method and incubation temperature.

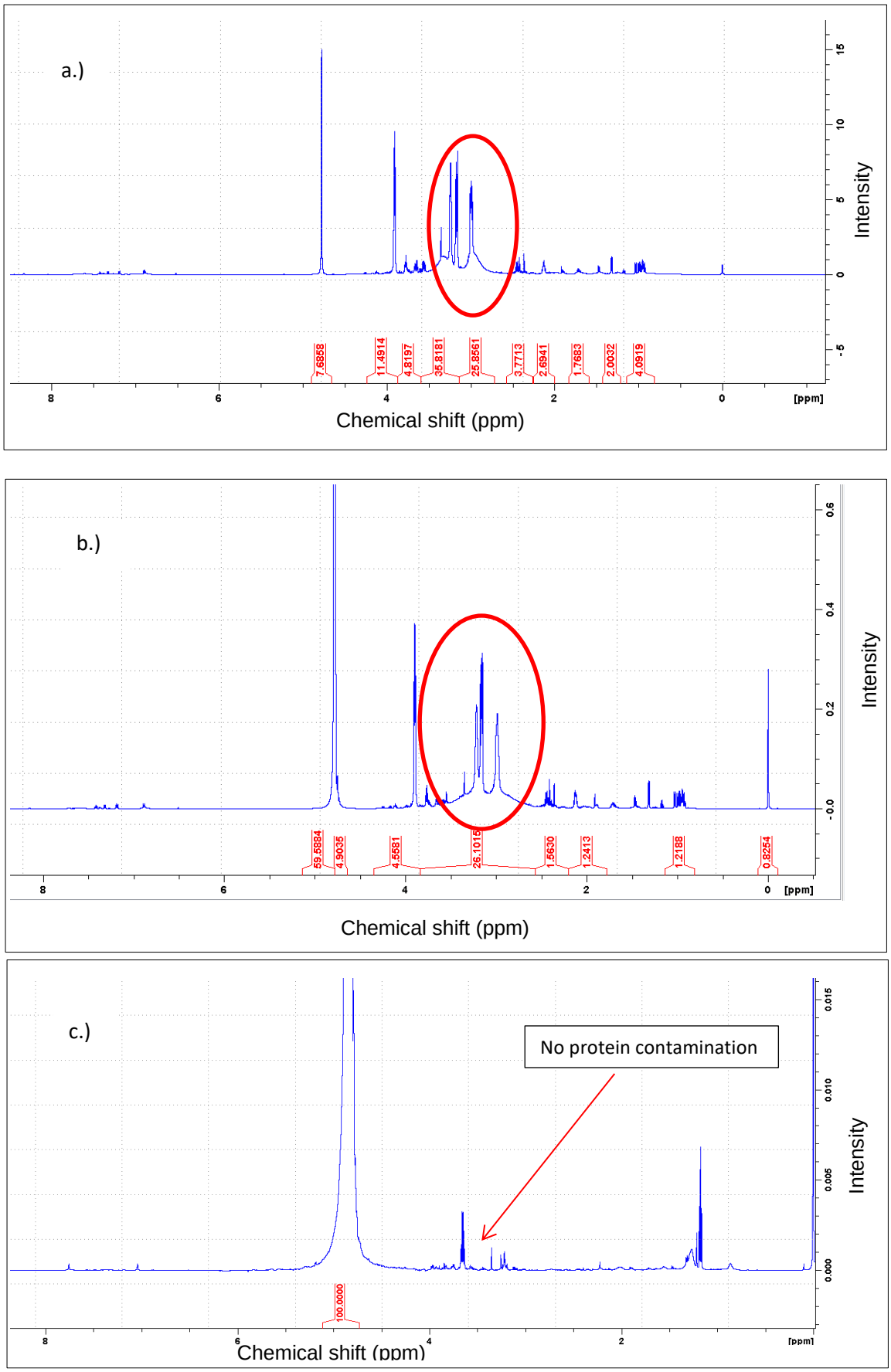

Figure 8 NMR spectra produced from the cell lysis using cultured media experiment. a.) Methanol was used as an extraction solvent. b.) Ethanol was used as an extraction solvent. c.) Spectrum after wash with lockes solution. = protein peaks

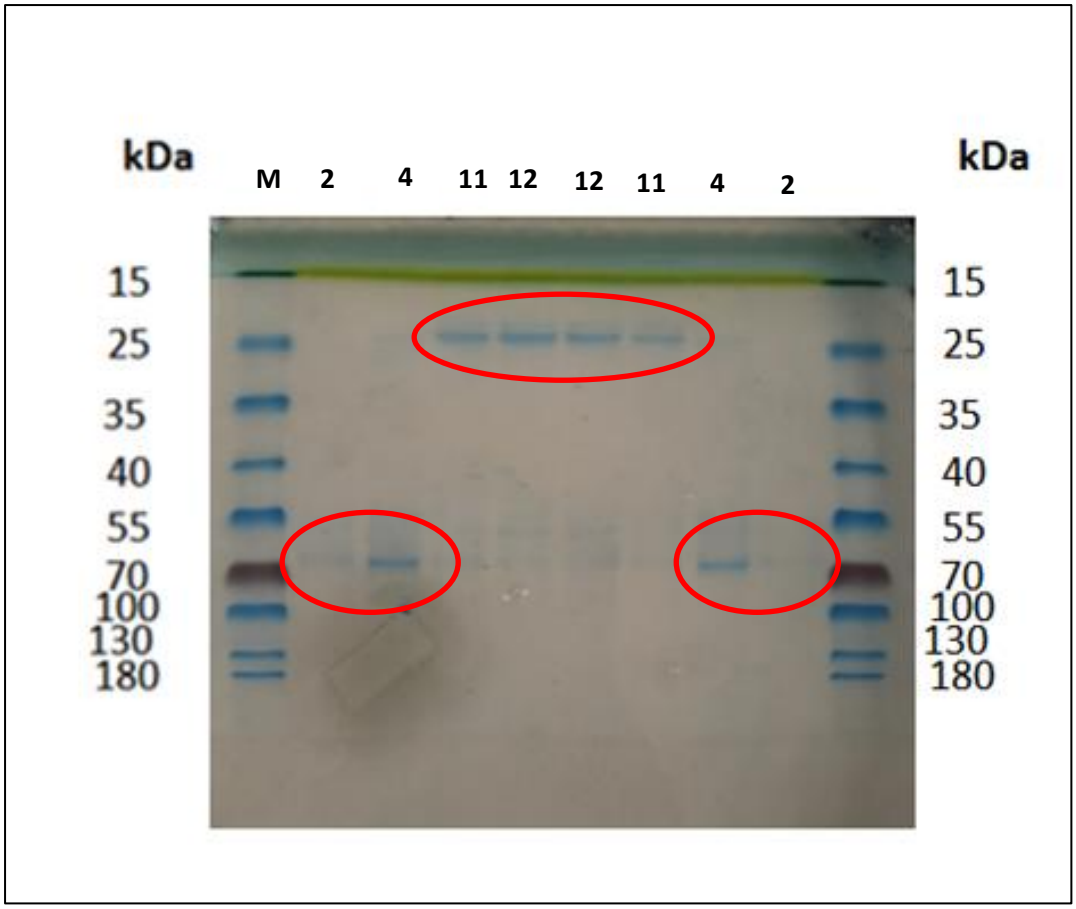

Figure 9 SDS-PAGE gel to confirm the presence of protein in the samples was what was distorting the NMR spectra. = protein band.

Optimisation of different steps of the extraction protocol

Following the determination of optimal method to obtain an accurate DSS reference signal and the identification and resolution of the protein contamination problem. We optimised each step of an extraction protocol, to lyse the Blastocystis cells and extract their metabolites. We analysed the efficacy of extraction solvents, lysis techniques and incubation temperatures. We used peak intensity rather than volume to compare different techniques, and establish which ones were most effective at extracting metabolites. The peak intensity is proportionate to the volume. We selected a series of peaks based on size (larger peaks will be less affected by noise as the noise consists of a smaller proportion of the peak), distance from the water peak (peaks further away from the water peak are less likely to be distorted by the water resonance) and position in the spectrum, so we could analyse a wider range of metabolites as molecules with different chemical properties produce resonances in different regions of the spectrum.

Methanol was determined to be the optimal extraction solvent

The first part of the extraction protocol we established was the optimal extraction solvent. Two sets of triplicates of Metabolite extractions from *Blastocystis* cells were

trialled using ethanol as an extraction solvent in one set and methanol in the other. Samples 36A, 36B and 36C are ethanol samples **(Table 4, Figure 10)** and samples 37A, 37B and 37C are methanol samples **(Table 4, Figure 10)** and the differences in the intensities produced is calculated using the formula I (intensity) ethanol/I methanol **(Table 4, Figure 10).** Therefore, all results above 1 suggest ethanol is a more efficient extraction solvent and results below 1 suggest methanol is more efficient. The triplicates produced from the methanol versus ethanol extractions produced consistent results. One sample set 36A v 37A was removed as an outlier except for the peak at 1.17 ppm and the peak at 3.66 ppm of sample set 36B v 37B was removed as an outlier (**figure 10**). The reproducibility of the triplicates was measured by the C.V (**table 4**) and the C.V improved as the outliers were removed (**figure 11**). All the reproducible results were below one with the exception of the peak at 1.17 ppm in the sample 36B v 37B experiment suggesting that methanol had worked better than ethanol and that methanol was the optimal extraction solvent (**figure 12** for a spectral overlay of sample 36C against sample 37C as an example of ethanol vs methanol).

Table 4

	36A v 37A	36B v 37B	36C v 37C	Median	stdvev	C.V	Median inc outliers	Stdev inc outliers	C.V Inc outliers
Peak 1.17	1.10	1.03	0.66	0.84	0.26	0.31	0.93	0.24	0.26
Peak 1.47	2.73	0.78	0.40	0.59	0.27	0.45	1.31	1.25	0.96
Peak 1.91	1.20	0.45	0.42	0.44	0.02	0.06	0.69	0.44	0.64
Peak 3.66	1.16	1.00	0.58	0.58	N/A	N/A	0.91	0.30	0.33
Peak 7.74	1.18	0.86	0.81	0.84	0.03	0.03	0.95	0.20	0.21
Peak 8.44	1.33	0.64	0.46	0.55	0.13	0.23	0.81	0.46	0.57

The differences in the intensities of a selection of peaks from the Ethanol vs Methanol experiment. 36A, 36B and 36C = Ethanol and 37A, 37B and 37C = Methanol. The data is displayed as an intensity ratio using the 'equation n = I ethanol/I methanol' so numbers above 1 represent a positive result for Ethanol and numbers below 1 represent a positive result for methanol. The median, standard deviation = stdev and coefficient of variance = C.V were all calculated with and without outliers. N/A = Not applicable.

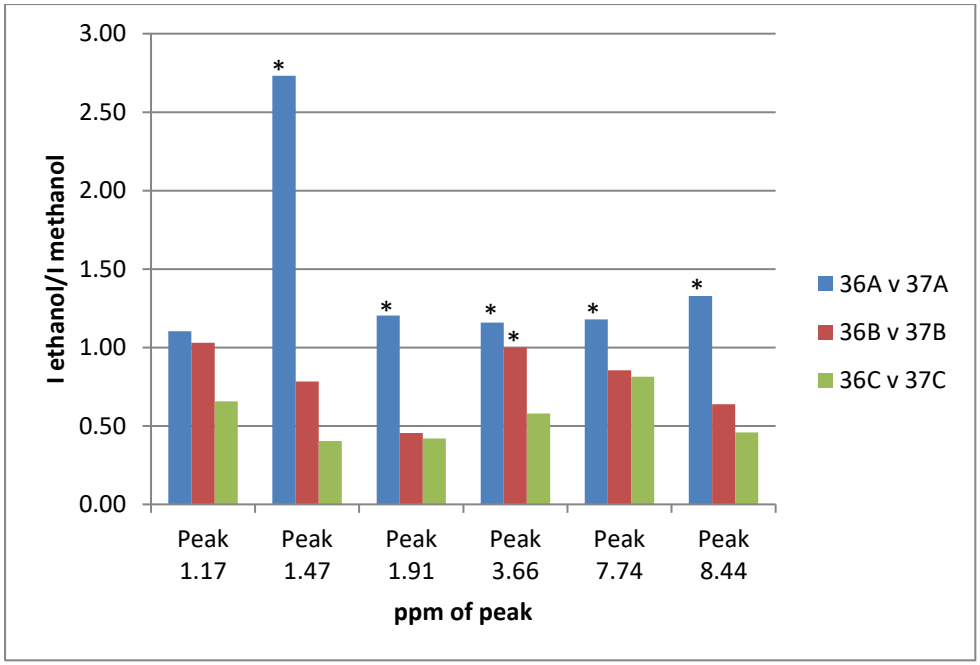

Figure 10 Difference in peak intensity between Methanol and Ethanol 36A 36B and 36C = Ethanol and 37A 37B and 37C = Methanol samples. I = Intensity. The data is displayed as an intensity ratio using the equation 'n = I ethanol/I methanol' so all numbers below 1 are a positive result for methanol and all numbers above 1 are positive result for ethanol. Positive results infer a better extraction solvent. * = outliers

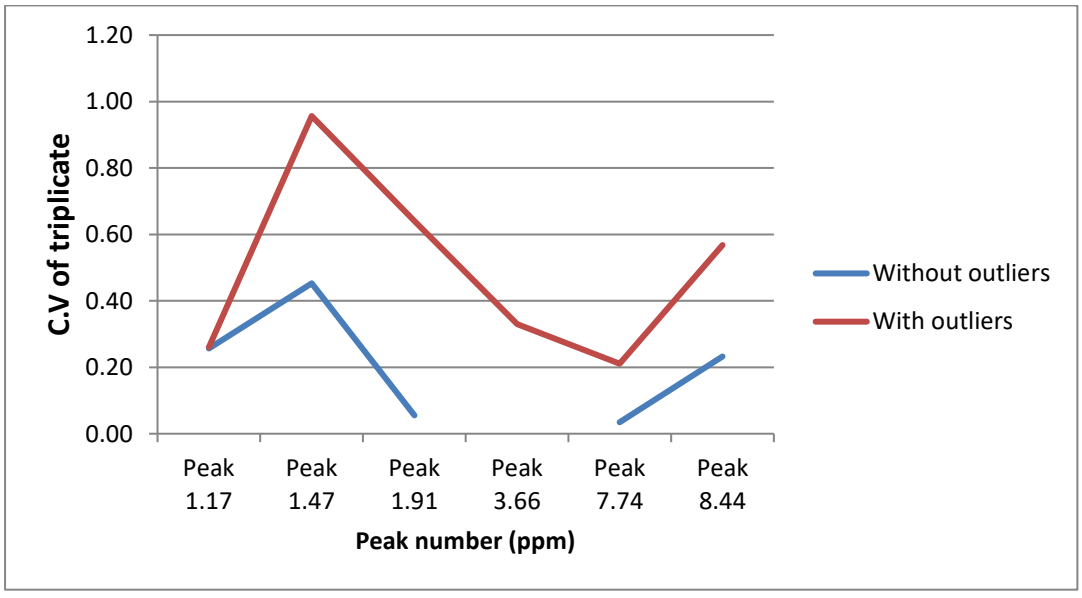

Figure 11 Reproducibility of the ethanol extractions against the methanol extractions - C.Vs of ethanol vs methanol peaks with outliers and without outliers.

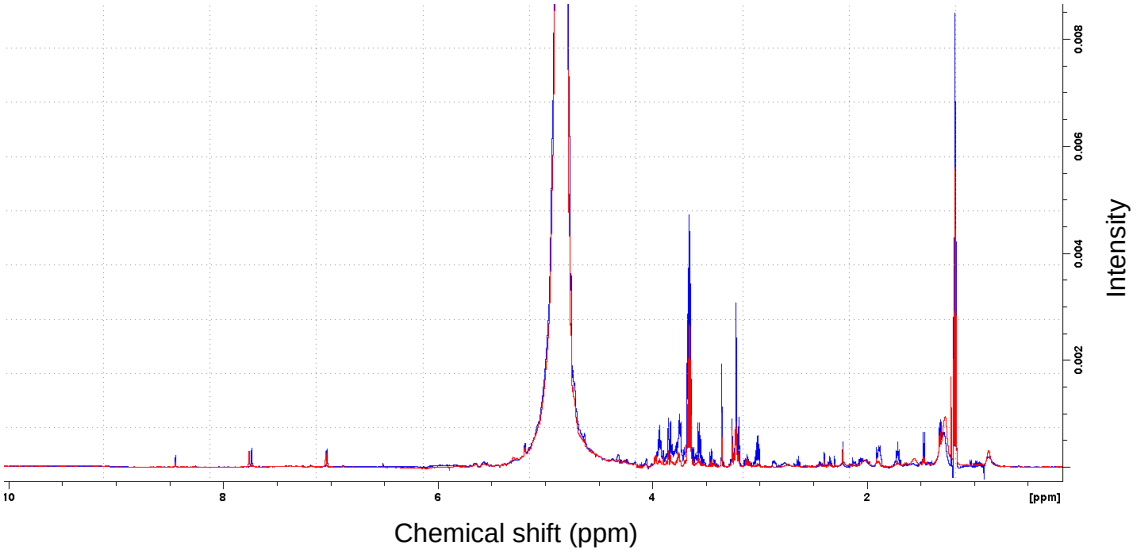

Figure 12 Spectral overlay of extraction 36C **(Ethanol)** over extraction 37C **(Methanol)** between 0 ppm and 10 ppm

Bead bashing was determined to be the Optimal lysis Method

The next part of the extraction protocol we established was the optimal lysis method. Two sets of triplicates of Metabolite extractions from *Blastocystis* cells were trialled using bead bashing as a lysis method in one set and sonication in the other. Samples 40A, 40B and 40C are samples in which sonication was used as a lysis method **(Table 5, Figure 13)** and samples 41A, 41B and 41C are samples in which bead bashing was used **(Table 5, Figure 13).** The differences in the intensities produced is calculated using the formula I sonication/I bead bashing **(Table 5, Figure 13).** Therefore, all results above 1 suggest sonication is a more efficient lysis method and results below 1 suggest bead bashing is more efficient. The C.V was calculated to measure the reproducibility of each sample comparison. The triplicates produced from the sonication and bead bashing lysis analysis produced consistent results and there were only 2 outliers which needed to be removed (**figure 13**). There were no selected peaks which were not applicable (**table 5**) as all peaks yielded at least 2 reproducible triplicates (**figure 13**). The peak at 1.32 ppm from the 40A v 41A sample comparison was removed as an outlier and the C.V dropped from 0.95 to 0.43 (**figure 14**). The peak at 8.44 ppm from the 40A v 41A sample comparison was also removed as an outlier and the C.V dropped from 0.88 to 0.24 (**figure 14**). All other peaks yielded 3 reproducible triplicates (**figure 13**). All reproducible sets of samples produced values below 1 suggesting that bead bashing had worked better than sonication. Therefore, bead bashing appears to be the optimal lysis method (**figure 15** for a spectral overlay of sample 40C bead bashing against sample 41C sonication).

Table 5

	40A v 41A	40B v 41B	40C v 41C	Median	stdvev	C.V	Median inc outliers	Stdev inc outliers	C.V Inc outliers
Peak 1.17	0.91	0.71	0.84	0.82	0.10	0.13	0.82	0.10	0.13
Peak 1.32	2.92	0.45	0.84	0.65	0.28	0.43	1.40	1.33	0.95
Peak 1.47	0.76	0.84	0.84	0.81	0.05	0.06	0.81	0.05	0.06
Peak 1.91	0.21	0.25	0.29	0.25	0.04	0.16	0.25	0.04	0.16
Peak 3.66	0.86	0.71	0.84	0.80	0.08	0.10	0.80	0.08	0.10
Peak 8.44	0.01	0.50	0.71	0.60	0.15	0.24	0.41	0.36	0.88

The differences in intensities of a selection of peaks from the Sonication vs Bead bashing experiment. 40A, 40B and 40C = Sonication and 41A, 41B and 41C = Bead bashing. The data is displayed as an intensity ratio using the equation 'n = I sonication/I bead bashing' so numbers above 1 represent a positive result for Sonication and numbers below 1 represent a positive result for Bead bashing. The median, standard deviation = stdev and coefficient of variance = C.V were all calculated with and without outliers.

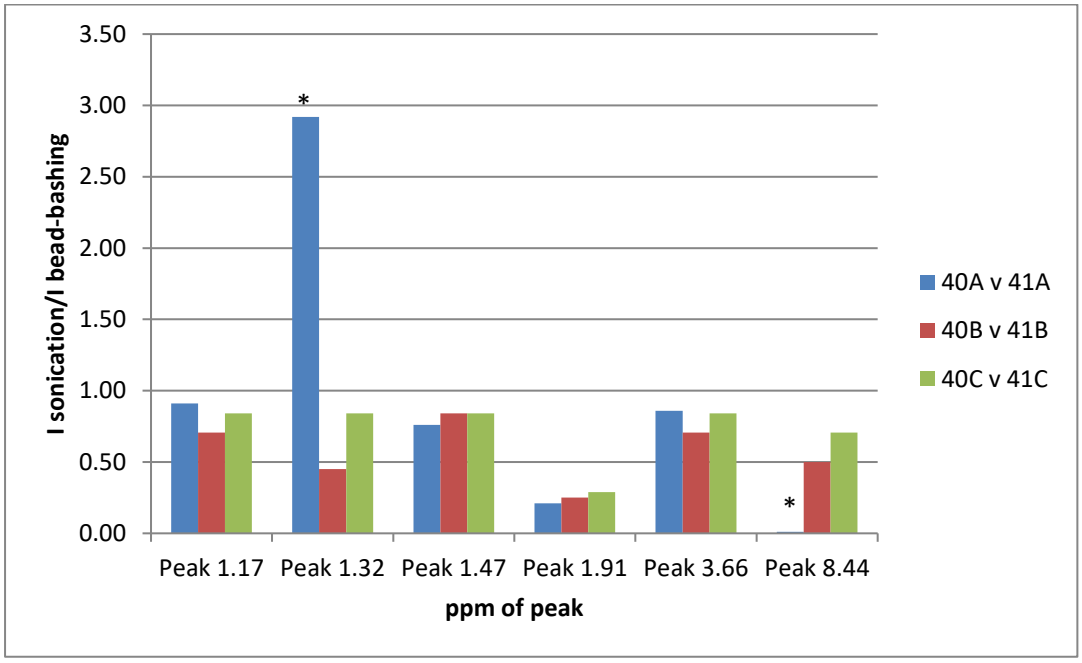

Figure 13 Difference in peak intensity between sonication and Bead bashing 40A, 40B and 40C = Sonication and 41A, 41B, 41C = Bead bashing samples. I = Intensity. The data is displayed as an intensity ratio using the equation 'n= I sonication/I bead bashing'. So all numbers below 1 are a positive result for Bead bashing and all numbers above 1 are a positive result for Sonication. Positive results infer a better lysis technique. * = outliers

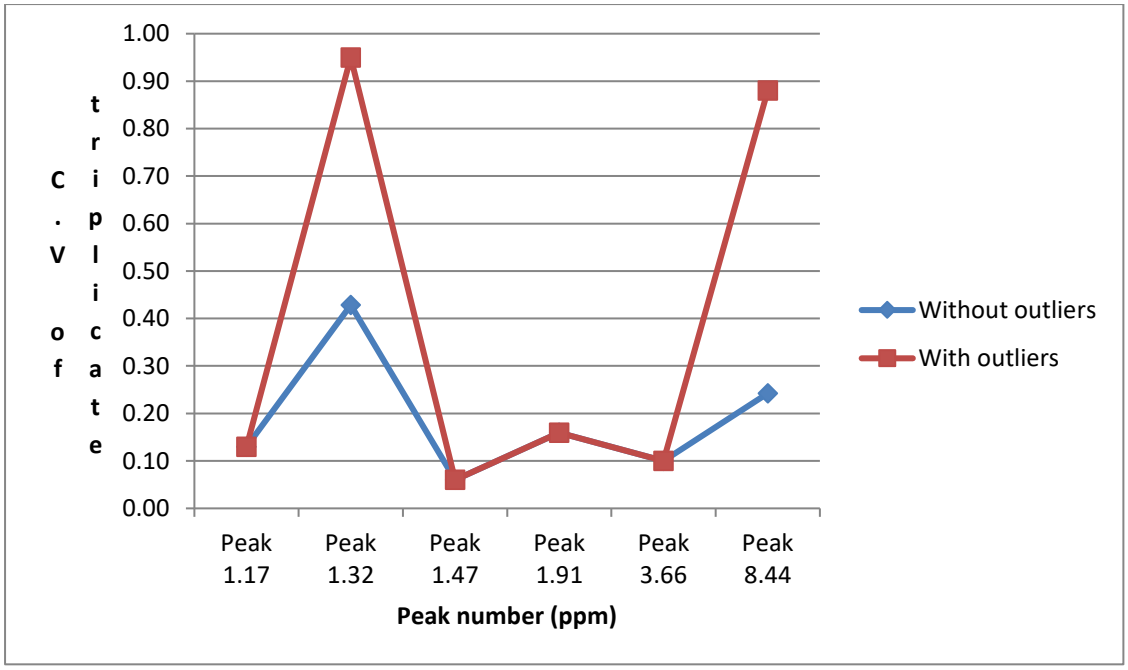

Figure 14 Reproducibility of sonication lysis against bead-bashing lysis C.Vs of sonication vs beadbashing peaks with outliers and without outliers.

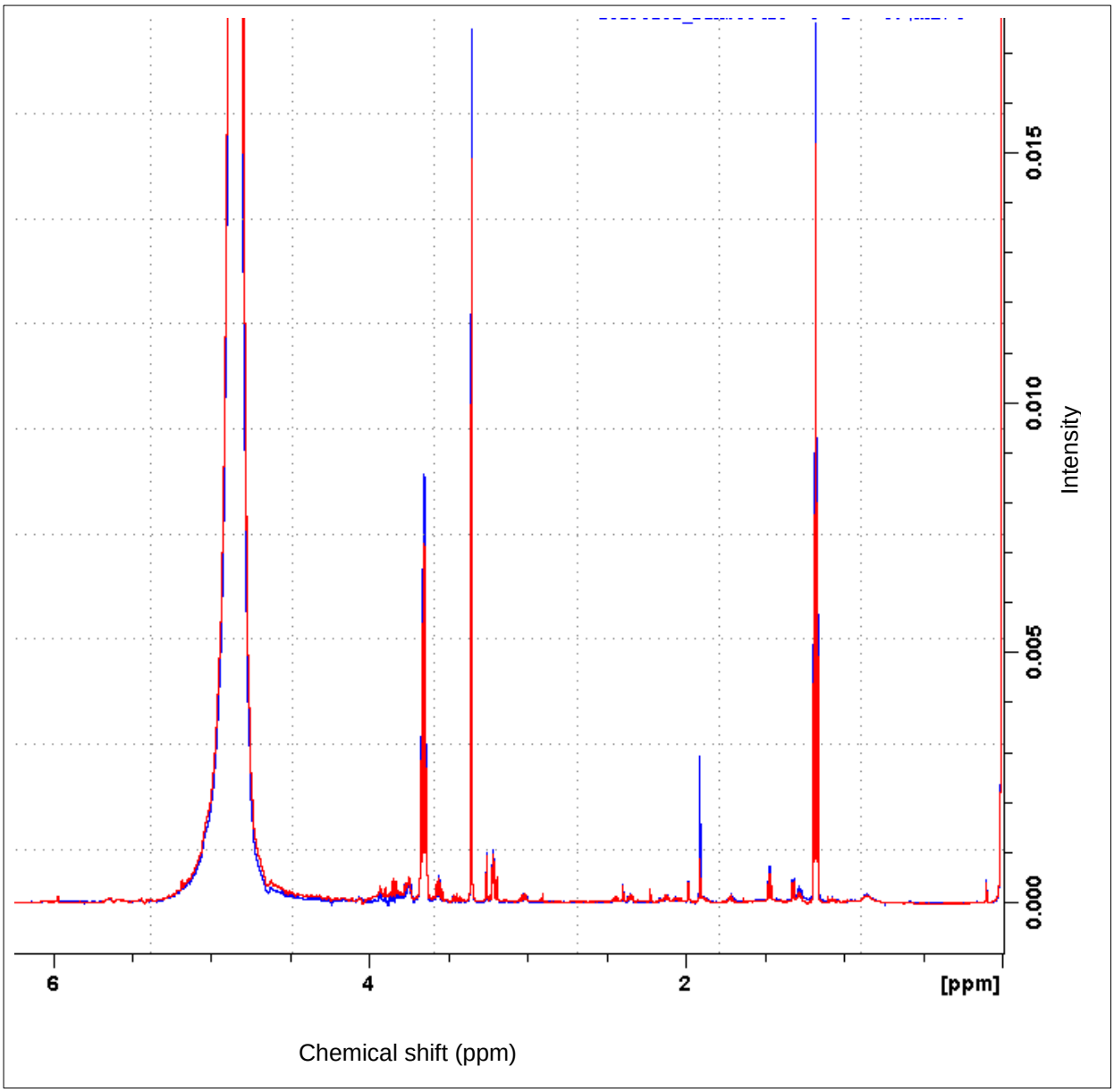

Figure 15 Spectral overlay of extraction 40C (**Sonication**) over extraction 41C **(bead bashing)** between 0 ppm and 8.25 ppm

Temperature was determined to not be an important factor in metabolite extraction

The third and final part of the extraction protocol we established was the optimal incubation temperature. Two sets of triplicates of Metabolite extractions from *Blastocystis* cells were trialled using -20°C as an incubation temperature in one set and room temperature (RT) in the other. Samples 54A, 54B and 54C are samples which were incubated at -20°C **(Table 6, Figure 16)** and samples 55A, 55B and 55C were incubated at RT **(Table 6, Figure 16).** The differences in the intensities produced is calculated using the formula I RT/I -20°C **(Table 6, Figure 16).** Therefore, all results above 1 suggest RT is a more efficient incubation temperature

and results below 1 suggest -20°C is more efficient. The C.V was calculated to measure the reproducibility of each sample comparison. The triplicates from the -20°C incubation and RT incubation produced consistent results and there was only one outlier to be removed (**figure 16**). All peaks except one produced 3 reproducible triplicates (**figure 16**). When the peak at 1.91 ppm from the sample comparison 54A v 55A was removed the C.V dropped from 0.19 to 0.12 (**table 6**). All but 2 of the medians were within 0.05 of 1 (**table 6**) so no significant results were produced. Therefore, neither RT nor -20°C appeared to be the more successful incubation temperature (**figure 17** for a spectral overlay of sample 54A -20°C incubation against 55A RT incubation).

Table 6

	54A v 55A	54B v 55B	54C v 55C	Median	Stdev	C.V	Median w/o outliers	stdev w/o outliers	C.V w/o outliers
Peak 1.17	0.95	1.00	1.10	1.02	0.08	0.08	1.02	0.08	0.08
Peak 1.91	0.68	1.00	0.84	0.84	0.16	0.19	0.92	0.11	0.12
Peak 2.39	1.00	0.96	1.07	1.01	0.06	0.05	1.01	0.06	0.05
Peak 3.22	1.06	0.97	1.10	1.04	0.07	0.06	1.04	0.07	0.06
Peak 3.25	1.10	1.02	1.11	1.08	0.05	0.05	1.08	0.05	0.05
Peak 3.66	0.96	1.03	1.09	1.03	0.07	0.06	1.03	0.07	0.06

The differences in intensities of a selection of peaks from the RT vs -20°C incubation experiment. 54A, 54B and 54C = -20°C incubation and 55A, 55B and 55C = RT incubation. The data is displayed as an intensity ratio using the equation 'n = I RT/I -20°C' so numbers above 1 represent a positive result for RT and numbers below 1 represent a positive result for -20°C. The median, standard deviation = stdev and coefficient of variance = C.V were all calculated with and without outliers.

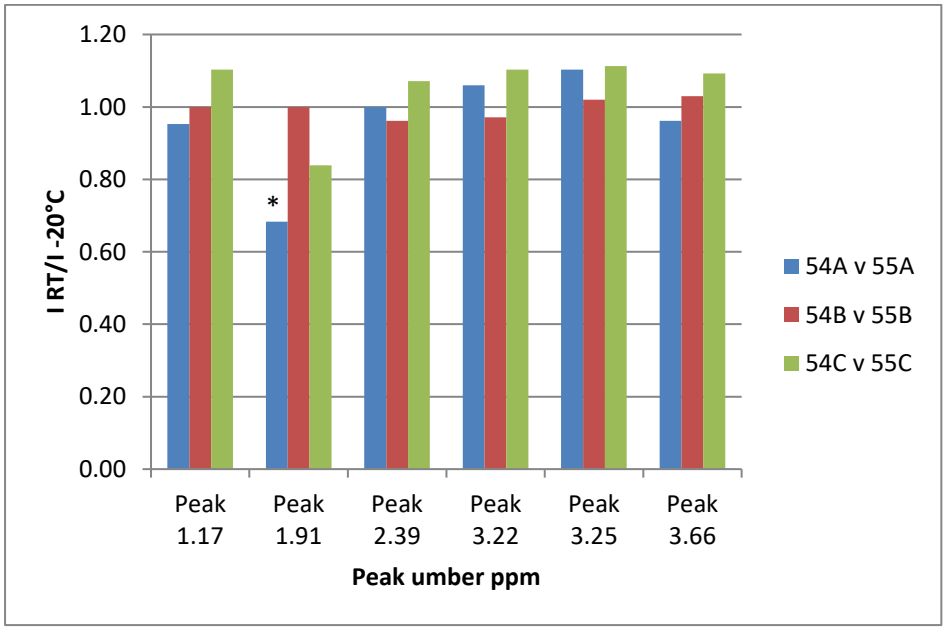

Figure 16 Difference in peak intensity between RT incubation and -20°C incubation 54A, 54B and 54C = -20°C incubation and 55A, 55B and 55C =RT incubation samples. I = Intensity. The data is displayed as an intensity ratio using the equation 'n = I RT/I -20°C' so all numbers below 1 are a positive result for -20°C incubation and all numbers above 1 are a positive result for RT. Positive results infer a more efficient incubation temperature * = outliers

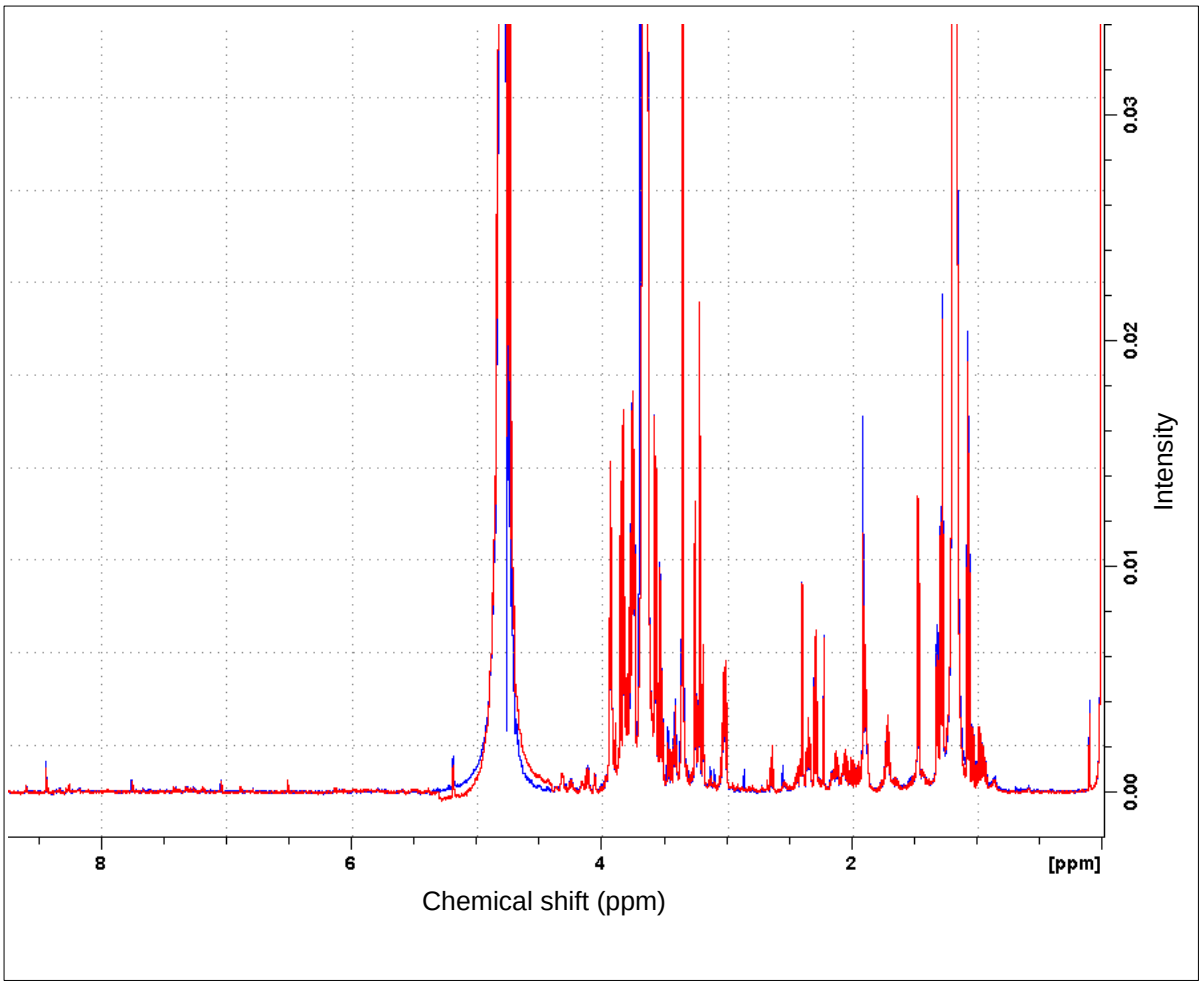

Figure 17 Spectral overlay of extraction 54A (-20°C incubation) over extraction 55A (RT incubation) between 0 ppm and 8.25 ppm

As well as RT and 60°C incubation temperatures a -20°C incubation was also trialled and compared to a 60°C incubation. Samples 48A and 48C are samples which were incubated at -20°C **(Table 7, Figure 18)** and samples 49A, and 49C were incubated at 60°C **(Table 7, Figure 18).** The differences in the intensities produced is calculated using the formula I 60°C/I -20°C **(Table 7, Figure 18).** Therefore, all results above 1 suggest 60°C is a more efficient incubation temperature and results below 1 suggest -20°C is more efficient. The C.V was calculated to measure the reproducibility of each sample comparison. Doubles were run for the 60°C incubation and -20°C incubation experiments as one of the samples did not work. However, the doubles produced consistent results and there were no outliers to be removed (**figure 18**). The C.V's all ranged between 0.03 and 0.12 suggesting that all results were reproducible (**table 7**). There were no significant results obtained from this experiment and therefore neither -20°C not 60°C appeared to be the more successful incubation temperature (**figure 19** for a spectral overlay of sample 48A -20°C incubation against 49A 60°C incubation). Temperature was determined to not be an important factor in metabolite extraction. Therefore, performing the experiment at RT would be sufficient to extract metabolites from *Blastocystis.*

Table 7

	48A v 49A	48C v 49C	Median	Stdev	C.V
Peak 1.17	1.17	1.03	1.10	0.10	0.09
Peak 1.91	1.19	1.00	1.10	0.14	0.12
Peak 2.39	1.03	1.00	1.02	0.02	0.02
Peak 3.22	1.04	0.95	1.00	0.06	0.06
Peak 3.25	1.04	0.96	1.00	0.06	0.06
Peak 3.66	1.11	1.00	1.06	0.08	0.08
Peak 8.44	1.57	1.51	1.54	0.04	0.03

The differences in intensities of a selection of peaks from the 60°C vs -20°C incubation experiment. 48A and 48C = -20°C incubation and 49A and 49C = 60°c incubation. The data is displayed as an intensity ratio using the equation 'n = I 60°C/I -20°C' so numbers above 1 represent a positive result for 60°C and numbers below 1 represent a positive result for -20°C. Standard deviation = stdev and coefficient of variance = C.V.

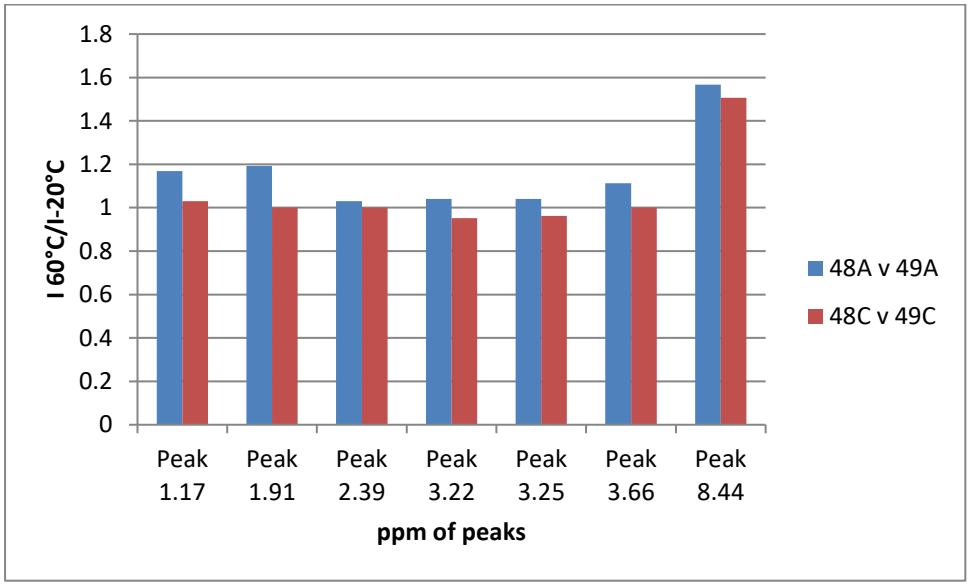

Figure 18 Difference in peak intensity between 60°C Incubation and -20°C Incubation 48A and 48C = -20°C incubation and 49A and 49C =60°C incubation samples. I = Intensity. The data is displayed as an intensity ratio using the equation 'n = I 60°C/I -20°C' so all numbers below 1 are a positive result for -20°C incubation and all numbers above 1 are a positive result for 60°C. Positive results infer a more efficient incubation temperature.

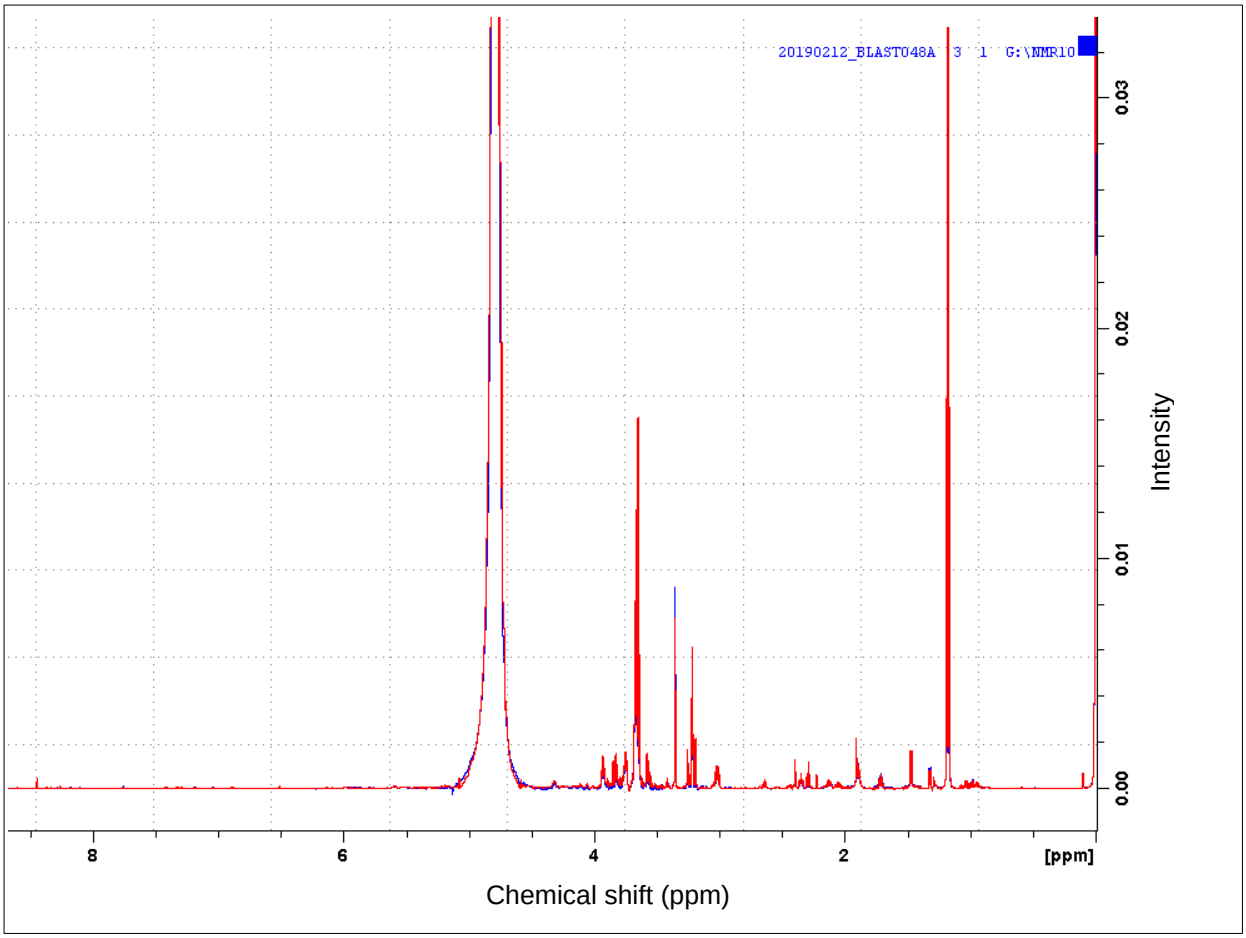

Figure 19 Spectral overlay of extraction 48A (-20°C incubation) over extraction 49A (60°C incubation) between 0 ppm and 8.25 ppm

Figure 20 is a 1D-^{1}H-NMR spectrum obtained from the final optimised extraction protocol. **Figure 21** is the region from the spectrum in **figure 20** between 0 ppm and 4 ppm and and **figure 22** is a region from the same spectrum between 6.5 ppm and 8.5 ppm. **Table 8** contains a list of the most abundant molecules extracted using this protocol. Ethanol and methanol were the most abundant molecules extracted. However amino acids such as alanine and glycine were also extracted as well as molecules involved in *Blastocystis* energy metabolism such as acetate, succinate and fumarate.

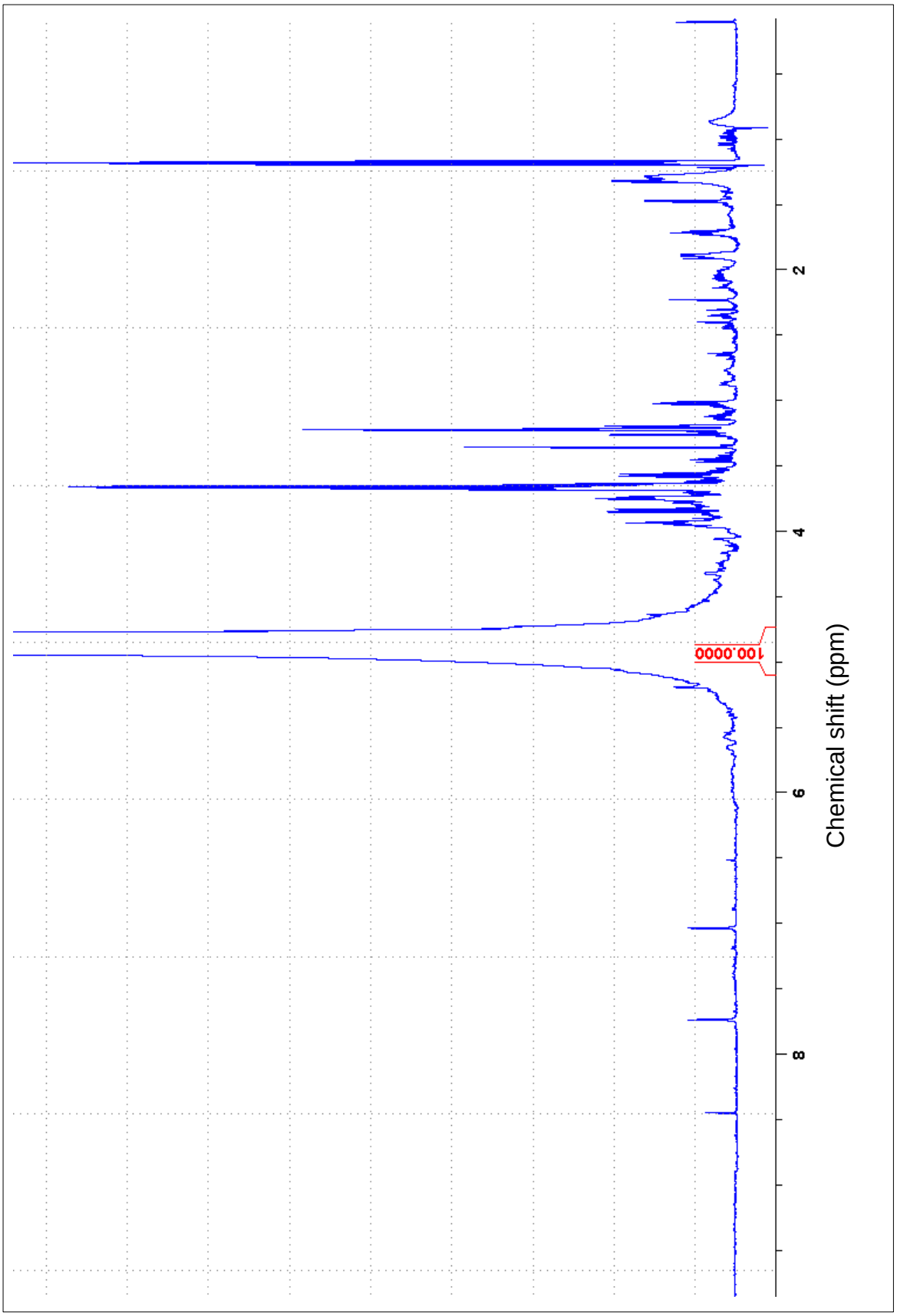

Figure 20 Spectrum obtained from the optimal extraction protocol deduced from this study. Using methanol as the extraction solvent, bead bashing as the lysis method and incubation at RT.

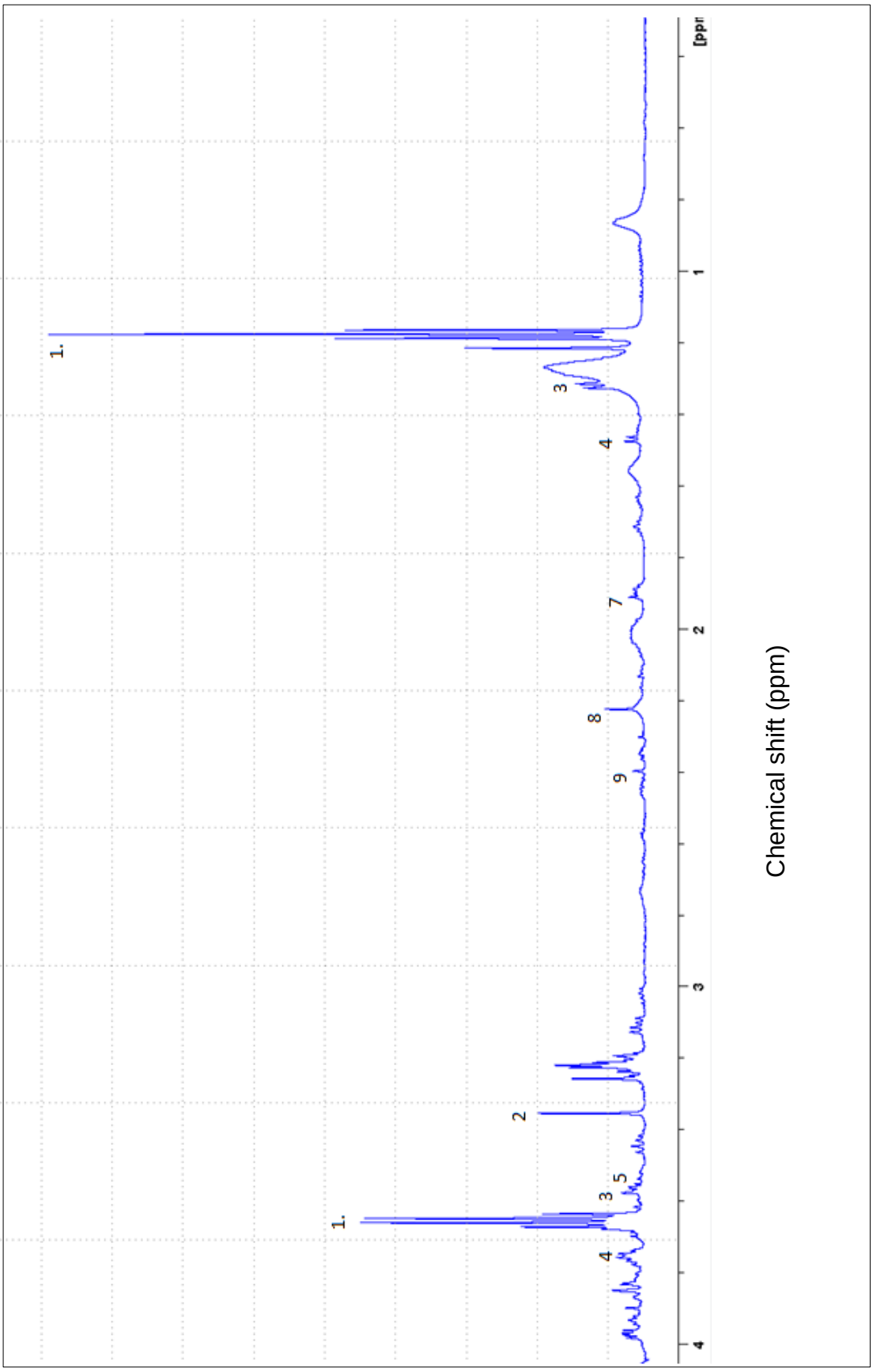

Figure 21 Region of spectrum (0 ppm to 4 ppm) obtained from the optimised extraction protocol. Numbers correspond to the molecules it table-7 for peak assignment

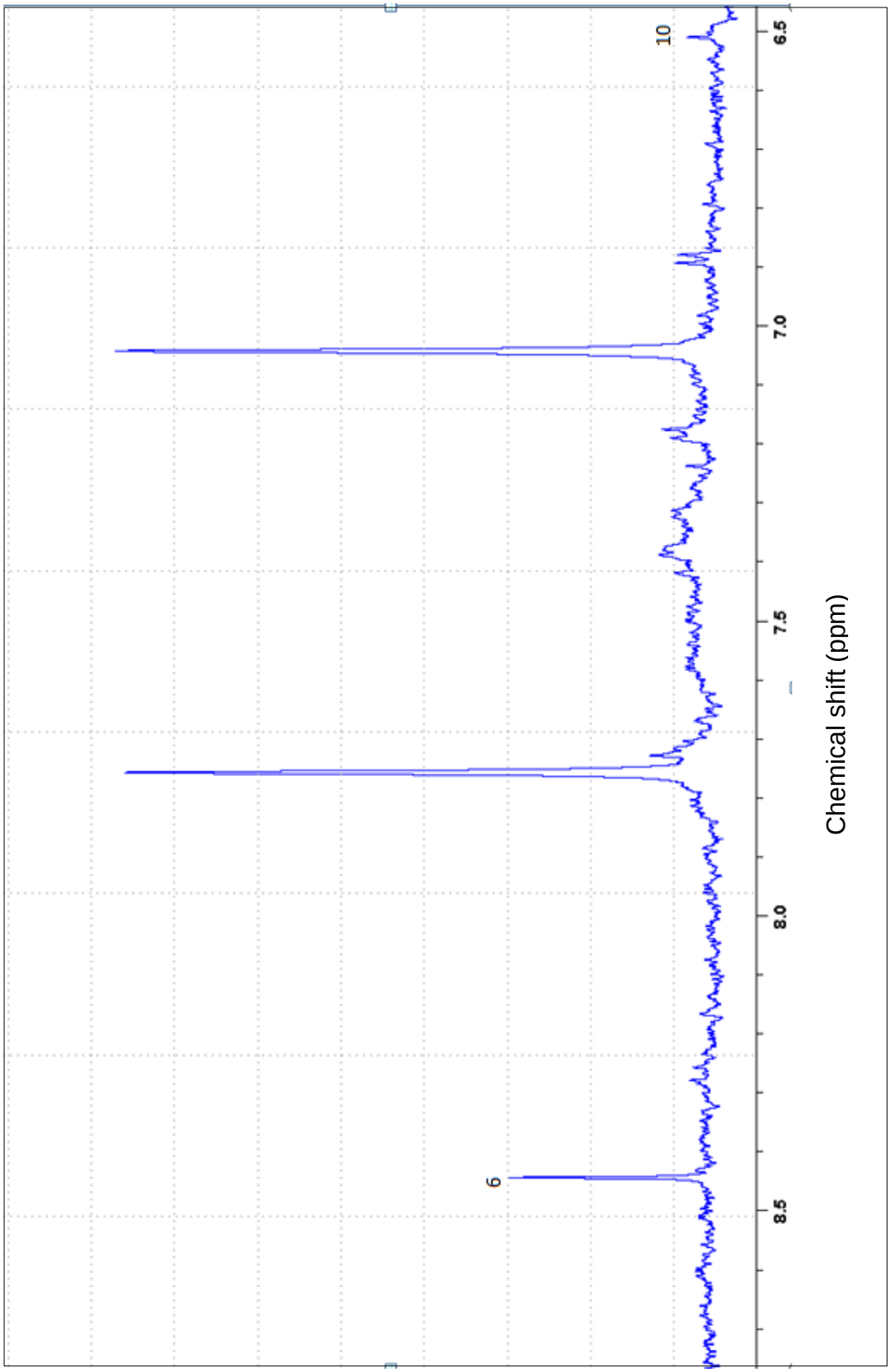

Figure 22 Region of spectrum (6.5 ppm to 8.5 ppm) obtained from the optimised extraction protocol. Numbers correspond to the molecules it table-7 for peak assignment

Table 8

Compound number	Metabolite	**Concentration (μM)**	**Shifts (ppm)**
1	**Ethanol**	363	1.2, 3.7
2	**Methanol**	39	3.4
3	**Threonine**	25	3.6, 1.3
4	**Alanine**	21	3.8, 1.5
5	**Glycine**	19	3.5
6	**Formate**	17	8.4
7	**Acetate**	7.5	1.9
8	**Acetone**	5.5	2.2
9	**Succinate**	3.4	2.4
10	**Fumarate**	2.4	6.5

Metabolites extracted by the optimal extraction method and their concentrations

2.4 Discussion

We devised a successful, reproducible and robust protocol to analyse the metabolome of *Blastocystis spp* ST7 by NMR analysis. We found that Methanol is a more effective extraction solvent than Ethanol, that bead bashing is a more effective lysis method than sonication and that incubation temperature is not a significant factor to perform metabolite extraction. This data was collated to produce a series of steps to form the optimal protocol to perform metabolite extraction on *Blastocystis*.

Two times washes involving resuspension of the cells in 5 ml Locke's solution followed by a 5-minute centrifugation at 1,000 g was determined to be an effective way of removing the protein contamination (**Figure 8)**. Therefore, this step was added at the start of the procedure to generate a more clear, pronounced and easily reproducible spectrum.

Methanol was determined to be a better extraction solvent than ethanol **(Figure 10)**. However, the peak analysis produced only three reproducible results. Each reproducible result was a pair with one outlier. The whole sample-A extraction was discarded as an outlier. This could have been caused by an error in aliquot division when mixing a culture of cells to aliquot them for comparative analysis. Good homogeneity may not have been successfully achieved. It could also have been due to pipetting errors or possible contamination caused by errors in cell culture. The inconsistent data would however be consistent with past research comparing these 2 extraction solvents where Methanol and Ethanol produced similar results [66].

Methanol was also determined to be more suitable than MTBE/Methanol and Chloroform/Methanol. Past research has found that when using Chloroform/Methanol extractions, it can be difficult to eliminate contaminants, as the Methanol sits on the top layer because of chloroforms high density. This results in a layer of debris between to two solvents rather than a pellet at the bottom [55],[57],[58]. This problem has been rectified by the introduction of an MTBE/Methanol extraction. MTBE has a lower density than methanol and the therefore methanol sits on the bottom layer with the pellet beneath it [67],[59]. However, when trialling this method we discovered that it was difficult to avoid MTBE and Methanol mixing which resulted in more contaminants being transferred to the methanol. This was because there was no clear formation of sediment or no clear boundary between the two solvents which is normally the case when performing phase separations.

Bead bashing was determined to be a more effective lysis technique than sonication **(Figure 13)**. These two techniques were selected as they are not as aggressive as other techniques and as *Blastocystis* does not possess a cell wall and is a single cellular organism so it does not possess extracellular matrix either. Different bead beating techniques were trialled by Geier et al on *Caenorhabditis elegans*, including some at cryogenic temperatures. Bead bashing produced successful results.

However, a tissue homogenizer proved to be the most effective method. *C. elegans* is however a multicellular organism and contains extracellular matrix and therefore a more aggressive lysis technique is necessary [60]. Cryopulveristation and tissue homogenisers were successful in many techniques to lyse mammalian cells [55],[57]. However, sonication had proved successful in *Arabidopsis thaliana* [59] which has a cell wall and is tougher to break than protozoan parasites which do not have a cell wall. As sonication and bead bashing had both proved successful in tougher cells than *Blastocystis* these two methods were selected. Bead bashing produced some very successful reproducible results **(Figure 14)** against sonication with only two selected peaks determined as outliers amongst all the samples. Differences in peak intensities ranged between 0.7 and 0.85 for most of the selected peaks with the exception of peak 1.91 whose differences in peak intensities ranged between 0.2073 and 0.25. So bead bashing was consistently more successful than sonication.

Incubation temperature was determined to not be a significant factor in successful metabolite extraction from *Blastocystis spp.* This is consistent with a past study by Beltran et al [58]. RT against -20°C **(Figure 16)** produced a range of scale differences between 0.95 and 1.10 with just one outlier of 0.68 in sample –A. There were therefore no consistent, significant results and this was reproducible suggesting that neither RT nor -20°C was more successful. In past studies on human vein tissue and *C. Elegans* incubation at RT has been successfully performed [68],[60] and it past studies on *Arabidopsis thaliana* successful extractions have been performed at -20°C.

In the 60°C incubation against the -20°C incubation **(Figure 18)** most of the results were between 0.95 and 1.04 with one peak with a 1.54 median which was disregarded as an outlier. Every other peak comparison was reasonably reproducible between the samples and there was no significant difference determined between the samples.

In summary, the optimal protocol determined by this study consists of the use of methanol at RT as an extraction solvent and bead bashing as a lysis technique, followed by a centrifugation step of 13,000 rpm (9447 g in a fixed 5 cm radius rotor) at 4°C for 20 minutes. Lyophilisation was used in each trial as a drying method and appeared to be a clean consistent and successful technique. Although many of the results were reproducible (**Figure 11** and **Figure 14**) there were many outliers and in some cases only two reproducible results were produced amongst triplicates (**Figure 10** and **Figure 18**). For this reason, more repeats are probably necessary and therefore for our final protocol quadruplets will be used and we can dismiss one outlier if necessary to have successful triplicates. Also, the metabolites extracted by this protocol included ethanol and methanol in quite a high abundance. However, they also included amino acids such as threonine, alanine and glycine and molecules involved in energy metabolism such as acetate, succinate and fumarate(**Table 8**). Although we were unable to analyse the wide range of molecules

Vermathen et al did in *Giardia lamblia* [65]. The protocol was determined to be a good procedure to use for the extraction step, as part of a metabolomics study on *Blastocystis*.

For future research, this procedure could be used to analyse the metabolomes of many other eukaryotic microorganisms, particularly protozoan parasites. So far *Giardia lamblia* is the only protozoan that has had its metabolome analysed by NMR which was done by MAS [65]. However, MAS is used for *in situ* analysis[65], and for the first time the organism could be broken up to analyse its metabolome from looking inside the cell. This could also be applied to other protozoans such as *Cryptosporidium Parvum, Entamoeba Histolytica or Acanthamoeba Castellanii. Acanthamoeba* can perform aerobic metabolism as well as anaerobic metabolism [49]. So some cultures could be grown aerobically and some could be grown anaerobically. This procedure could then be used to lyse both the aerobically grown cultures and the anaerobically grown cultures and then extract their metabolites. We could then use NMR to analyse their metabolomes to determine what different metabolites they produce under aerobic conditions compared to anaerobic conditions. This procedure would also be useful for identifying biomarkers to diagnose disease and drug targets to help treat disease.

The extraction protocol devised could also be further fine-tuned. For example, more repeats could be performed. As the reproducibility was not 100% consistent this could help further confirm the accuracy and significance of our results. There are also many other extraction solvents which could be trialled. Acetonitrile has in the past been successful at extracting polar and non- polar metabolites [58]. Devising a comprehensive protocol to extract non-polar hydrophobic metabolites such as membrane lipids would be beneficial for analysing the whole metabolome in even more detail. Also a chromatographic step could be added to isolate more metabolites specifically, as is often done in mass-spectrometry [57],[58],[59],[60],[68]. A tandem step would not be workable in NMR but as an extra step at the start of the procedure this could be trialled.

2.5 Conclusion

In this study we developed an efficient, robust and reproducible protocol to extract and analyse polar metabolites from *Blastocystis*. We generated many ^{1}H-NMR spectra to provide detail on the efficacy of each step of the protocol. This is the first extraction method described for NMR metabolomics analysis of *Blastocystis*. In future we look to improve on this procedure by optimising its reproducibility, its metabolite range and its specificity. We also look to apply this protocol or an adaptation of it to other parasites and possibly use it for disease diagnosis and to look for biomarkers.

Chapter 3 – ^{13}C labelling, metabolomics and the fate of pyruvate in *Blastocystis*

3.1 Introduction

Pyruvate metabolism is integral to energy metabolism in all eukaryotic organisms, as it is at a crossroads on the path from glucose consumption to ATP production. *Blastocystis* possess many genes involved in fucose scavenging in the gut for a carbohydrate source which will later be metabolised to pyruvate [22]. *Blastocystis* possesses three different pyruvate metabolising enzymes (**Figure 6**). Pyruvate Dehydrogenase (PDH) as found in canonical aerobic mitochondria [52],[34],[31], Pyruvate Ferredoxin Oxidoreductase (PFO) an oxygen sensitive enzyme mostly found in anaerobic mitochondrial related organelles (MRO's) [52],[34],[31] and Pyruvate NADPH Oxidoreductase (PNO) a homoloque of PFO [52],[34]. All three of these enzymes have been conserved in evolution and therefore may possess different mechanisms essential to *Blastocystis*' survival and ability to thrive. An analysis of each of these enzymes metabolites individually could provide essential information on *Blastocystis'* physiology, pathogenicity and ability to survive and thrive and therefore spread disease.

As pyruvate is an organic molecule its metabolic products contain carbon atoms making ^{13}C-NMR a suitable analysis method. To perform sensitive ^{13}C-NMR you must first achieve carbon labelling in the organism as the natural abundance of ^{13}C is only approximately 1%. This is achieved by incorporating ^{13}C into organism's metabolic products and has been approached in a number of different ways in different organisms.

For instance, the carbohydrate metabolic pathways and amino acid synthesis of the thermophilic anaerobic archaebacterium *Thermoproteus neutrophilis* was studied by adding ^{13}C-Acetate into its growth media. Acetate is assimilated by reductive carboxylation to acetyl-CoA which is then converted to pyruvate in a mechanism which works in reverse to *Blastocystis'* (**figure 6**). A number of amino acids are synthesised via subsidiaries of this pathway. The products of these pathways were all successfully analysed by 1D ^{13}C-NMR and *T. neutrophilis* amino acid synthesis pathways were elucidated [69].

In another study the carbohydrate metabolic pathways of *Actinobacillus succinogenes* has also been analysed using 1D ^{13}C-NMR. Succinate has a large speciality chemicals market and is used in many industries including food and pharmaceuticals [70]. To understand *A. succinogenes* metabolism 1D ^{13}C-NMR was used to map its metabolic pathways. The cultures were grown in ^{13}C-Glucose then the metabolites were analysed by 1D-^{13}C-NMR to develop a metabolic flux model.

As Glucose is the primary nutrient in many metabolic pathways, ^{13}C-Glucose is good for elucidating the energy metabolism of organisms [71].

^{13}C-Glucose was also used as a supplement in a fungal culture media when attempting to produce, label and detect cyclopiazonic acid. The strain used was *Aspergillus flavus* and a ^{13}C-^{13}C COSY was performed. Labelling was successfully achieved. [72].

Another assay in which ^{13}C-Glucose was used was to analyse the control of glycolysis and impact on citrate production in *Aspergillus niger* in different Glucose concentrations. This study showed that citric acid labelling was concentration specific and at lower glucose concentration switched from C2/C4 to C1/C5 labelling. It was also suggested from these results that in high glucose the orthodox glycolysis control step at phosphofructokinase is shifted to glyceraldehyde-3-phosphate-dehydrogenase [73].

Few studies have been conducted on microorganisms using ^{13}C-Pyruvate labelling. However, to analyse an organism's pyruvate metabolism this would be a hugely useful technique. Using both ^{13}C-Pyruvate and ^{13}C-Glucose to achieve ^{13}C-Labelling should be able to give clues on the fate of pyruvate in *Blastocystis.*

Pyruvate metabolism is central to many metabolic pathways and mechanisms in the *Blastocystis* MRO as it is in canonical mitochondria. Pyruvate is converted to acetyl-CoA by three different enzymes and each one utilises a different cofactor (**Figure 6**). Acetyl-CoA is then converted to acetate by the subsequent enzymes in *Blastocystis'* ATP producing pathway. An increase in PDH activity results in an increase in NADH concentration which could result in an increase in complex I activity as NADH reduces complex I. An increase in PNO activity results in an increase in NADPH concentration which could result in an increase in fatty acid synthesis as NADPH is a common cofactor in fatty acid synthesis pathways [52],[34],[74]. PFO uses ferredoxin and flavodoxin as cofactors. These 2 molecules operate in a cycle with PFO and Fe-Hyd the latter producing H_2 [46],[52],[34]. An increase in pyruvate metabolism in general will result in an increase in Acetyl:Succinate CoA-transferase 1B (ASCT 1B) activity which will result in acetate production but will also result in an increase in succinyl-CoA production (**Figure 6)**. This will result in an increase in ATP production by SCS which utilizes succinyl-CoA as a cofactor producing succinate. Succinyl-CoA is also used as a cofactor by a complex of 3 enzymes consisting of Methylmalonyl-CoA mutase, Methylmalonyl-CoA epimerase and propionyl-CoA carboxylase in another ATP producing mechanism. This complex works in a cycle with ASCT 1C, which uses succinate as a cofactor converting it to propionate [52]. So, pyruvate can affect many different metabolic pathways and the reason for the presence of the 3 pyruvate metabolising enzymes in Blastocystis' still requires elucidation. The analysis of the metabolites produced by pyruvate metabolism or changes in metabolites relative to pyruvate concentration could help further elucidate their function.

We must also consider the sensitivity of carbon nuclear spin in comparison to proton nuclear spin to acquire the clear spectra we obtained from the proton experiments. Because of differing gyromagnetic ratios 1D ^{13}C-NMR acquisitions, must be run for approximately 1000 times as long as 1D ^{1}H-NMR. This is because ^{1}H has a gyromagnetic ratio approximately four times larger than 1^{3}C [75]. This can be demonstrated in **equation 2** with a ^{1}H example in **equation 3** and a ^{13}C example in **equation 4**

Equation 2

$$S/N = \alpha n\, \gamma e \sqrt{\gamma^3 d\, B_0^3\, t}$$

Equation to solve for the differences the gyromagnetic ratio has on the signal to noise ratio of a specific atom. S/N = signal/noise αn = numberof nuclei γe = gyromagnetic ratio of the exciting nucleus γd = gyromagnetic ratio of the detectted nucleus B_0 = Size of the magnetic field.

Equation 3

$$2.83 = 1x1(\sqrt{1^3 x\ 2^3 x1\ })$$

Equation-2 applied to ^{1}H signal/noise in comparison to ^{13}C signal/noise

Equation 4

$$2.79 = 1x0.25(\sqrt{0.25^3\ x\ 2^3\ \ x1000})$$

Equation 2 applied to ^{13}C signal/noise in comparison ^{1}H signal/noise. The gyromagnetic ratio of ^{1}H is approximately four times higher than that of ^{13}C.

As well as sensitivity we must also consider the effect of carbon coupling. Because of the proximity and the size of the ^{13}C chemical shift, ^{13}C coupling can cause signals to be split between multiple peaks. Either homonuclear decoupling or a method of carbon dilution to prevent this happening may be necessary.

In this study we use ^{13}C-Glucose to try and achieve successful ^{13}C labelling in *Blastocystis* ST7 so we can analyse its pyruvate metabolism. We initially grew the *Blastocystis* cells with ^{13}C-Glucose added to the media and also try incubating them in their isotonic media lockes solution containing ^{13}C-Glucose to try and achieve successful labelling. We then applied an extraction protocol to lyse them and free the metabolites. Finally 1D-^{13}C NMR is what was used to assess the success of the labelling. We also analysed the growth media containing ^{13}C-Glucose before and after inoculation to analyse *Blastocystis'* metabolic footprint. Finally, we perform this experiment again using u^{13}C-Pyruvate. The data provided from these experiments could provide important clues to the fate of pyruvate in this protozoan parasite. As pyruvate is very central to *Blastocystis* energy metabolism it could affect a wide

range of important factors including its ability to survive and thrive in the gut environment. It could also provide important clues about *Blastocystis'* pathogenic mechanism and its ability to cause disease.

3.2 Materials and Method

^{13}C-Labelling Blastocystis culture

The *Blastocystis* ST7 Cultures were grown in 8 ml Iscove's Modified Dulbecco's Medium (IMDM) (Gibco - Catalogue no 12200069 Thermo Fisher scientific)10% heat-inactivated Horse Serum (HIHS)(Gibco – Catalogue no 26050088 Thermo Fisher scientific)12.5 mM ^{13}C-Glucose. All cultures were transferred into fresh media every 3-4 days and expanded. All cultures were incubated at 37°C in an anaerobic chamber (Oxoid – Product code 10107992 Fisher scientific) maintained at an optimum environment by as gas pack (BD – Catalogue no 261205). Subsequently cell counts were done manually using a neubauer haemocytometer (Brand – Catalogue no 717810). For the pyruvate experiment the same process was performed supplementing the media with ^{13}C-Pyruvate instead of ^{13}C-Glucose.

Incubation in Lockes solution + ^{13}C-Glucose

Homogenous cultures of *Blastocystis* cells containing a. 2.38 x 10^6 cells b. 1.94 x 10^6 cells c. 2.02 x 10^6 cells were separated into 4 equal aliquots. All aliquots were incubated in 8 ml Locke's solution (NaCl 8 g; $CaCl_2$ 0.2 g; KCl 0.2 g; $MgCl_2$ $6H_2O$ 0.01 g; Na_2HPO_4 2 g; $NaHCO_3$ 0.4 g; KH_2PO_4 0.3 g; dH_2O 1L) containing 50 mM ^{13}C-Glucose. Aliquots a. 1-4 were incubated for 1 hr, aliquots b. 1-4 were incubated for 2 hrs and aliquots c. 1-4 were incubated for 4hrs.

Cell lysis and metabolite extraction

The Blastocystis cultures were centrifuged at 1,000g for 5 minutes at 4°C. The media was then removed and the pellets were re-suspended and given 2 x washes in 5 ml lockes solution. The lockes solution was then removed and the pellets were snap frozen in liquid nitrogen and stored at -80°C.

The cells were added to 4 ml methanol:water at a concentration of M:W (1:1). 200mg glass beads where then added and the cells where for vortexed for 30 seconds followed by a 3-minute incubation at room temperature (RT) then vortexed for a further 30 seconds. The solution was then divided into 4 x 1ml aliquots which were centrifuged for 15 minutes at 4°C at 10,000 g. The supernatants were then decanted into fresh tubes and lyophilised.

Microscopic analysis

Blastocystis cells were analysed by light microscopy to confirm their alteration into cyst form.

Preparation for NMR acquisition – Labelled cells

The lyophilised desiccates were suspended in 330µl miliQ H_2O, vortexed for 30 seconds then centrifuged at 2,500 g for 10 minutes. The 4 supernatants of each sample where then recombined and 147 µl D2O 10 mM DSS was added making the resultant sample 1 mM DSS.

Preparation for NMR acquisition – Culture media

1 ml IMDM culture media was removed from the ^{13}C-Glucose culture and from the ^{13}C-Pyruvate culture before and after incubation. Then 111 µ1 D_2O 10 mM DSS was added making the resultant sample 1 mM DSS.

Analysis of aqueous extracts by NMR spectroscopy

The ^{13}C-spectra were obtained using a 600 MHz NMR spectrometer (Bruker) at a temperature of 298K and a transmitter frequency of 150.898 MHz which was locked to D_2O, tuned and shimmed automatically and the 90° pulse measured using Icon NMR. The soft pulses were then set up and the receiver gain set to a maximum of 256. A sucrose sample was run to qualify the spectrometer. A 1D experiment was performed running 2048 scans and 4 dummy scans with a spectral width of 238.95 ppm (36057 Hz), an acquisition time of 0.90876 s and a relaxation delay of 2 s producing 65536 data points. The number of scans was later increased to 4096 to achieve a better signal to noise. A ^{1}H^{13}C-HSQC was performed running 4096 scans and 0 dummy scans with an F2 spectral width of 16.0242 ppm (9615.385 MHz) for proton and an F1 spectral width of 165 ppm (24897.387) for ^{13}C, acquisition times of 0.1064960 seconds for proton and 0.0000201 seconds for ^{13}C and a relaxation delay of 1 second producing 2048 data points.

Processing and analysis of ^{13}C-NMR data

All NMR spectra were phased, baseline corrected and line-broadened to a 10 Hz window function to increase signal to noise ratio using TOPSPIN 3.6.1(Bruker) software. Peak assignment was performed using The Ohio State University Campus Chemical Instrument Centre (CCIC) customised Metabolomics Database for NMR analysis, the Biological magnetic resonance data bank (BMRB), the Human metabolome data base (HMDB) and the Madison metabolomics consortium database (MMCD)

3.3 Results

To analyse the pyruvate metabolism of the protozoan parasite *Blastocystis* ST7 we attempted to achieve ^{13}C-labelling so we could use ^{13}C-NMR to analyse its metabolome. We grew the *Blastocystis* cultures in media containing 12.5 mM ^{13}C-Glucose. We also incubated *Blastocystis* cultures in *Blastocystis'* isotonic media lockes solution containing 50 mM ^{13}C-Glucose to see if *Blastocystis* would scavenge the Glucose to achieve successful labelling. As well as this we analysed *Blastocystis*' growth media before and after incubation of cells to establish its metabolic footprint. We then repeated these experiments using ^{13}C-Pyruvate in the media instead of ^{13}C-Glucose. We found that concentrations of ^{13}C-Glucose and ^{13}C-Pyruvate had decreased after incubation and other molecules were detected providing clues about the metabolic fate of pyruvate.

IMDM media + ^{13}C-Glucose was ineffective as a ^{13}C labelling source in *Blastocystis*

First, we grew *Blastocystis* ST7 cells in IMDM media containing ^{13}C-Glucose, to achieve sufficient carbon-13 labelling to obtain a strong ^{13}C-NMR signal to analyse pyruvate metabolites. At each addition of fresh media an extraction was performed to analyse the efficacy of ^{13}C-Glucose as a carbon-13 labelling source. Two batches of cells underwent 5 passages of fresh media. **Figure 23a** is a 1D-^{13}C NMR spectrum of a sample obtained from an extraction performed on ST7 after one passage. Both ethanol and glycerol are present in this extraction. All other spectra can be seen in the supplementary information **(S1 – S3b). Figure 23b** shows the ^{13}C-NMR intensities/no cells x10^6 of ethanol and glycerol after 1, 3 and 5 passages for the two samples we analysed (Sample A and sample B). Intensity/no cells x 10^6 is proportional to concentration. Ethanol demonstrated an increase in concentration after each passage in sample B. However, a consistent and reproducible increase in concentration of molecules extracted at each passage was not demonstrated suggesting that successful carbon labelling was not being achieved.

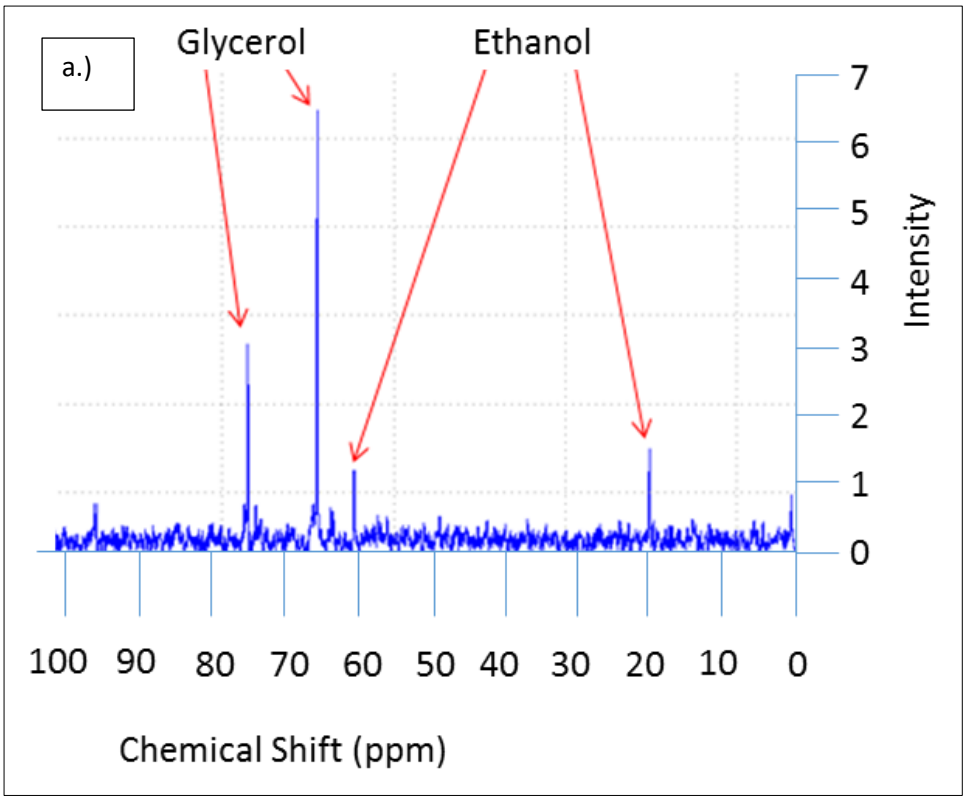

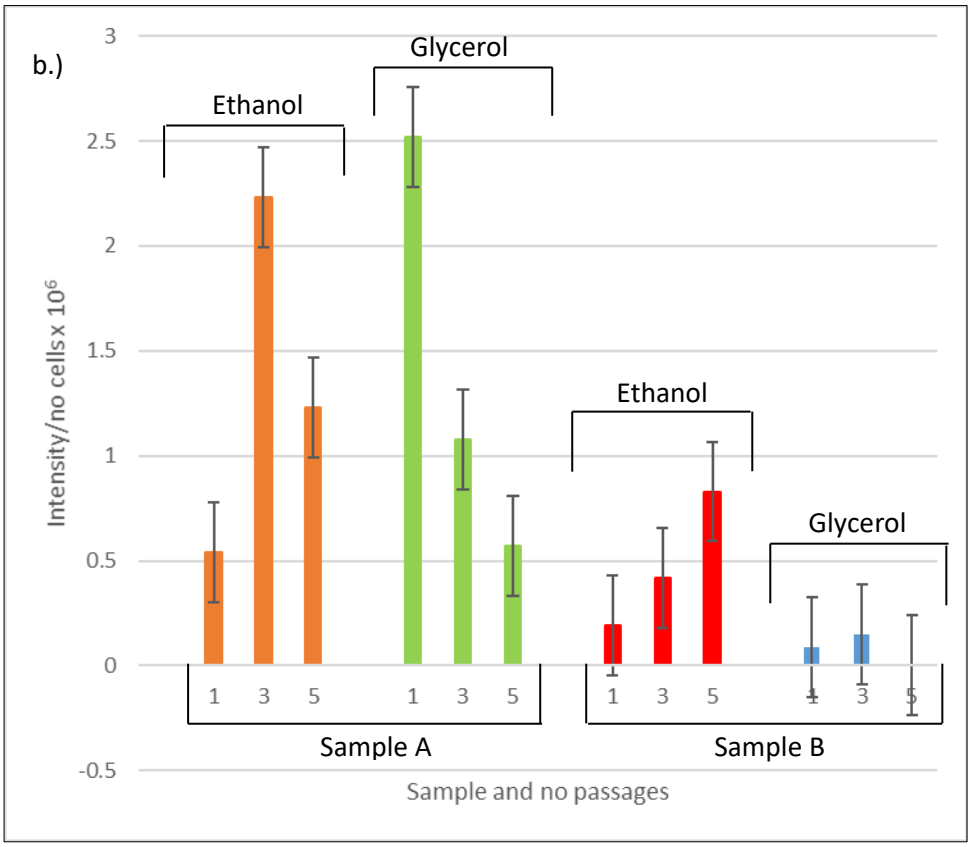

Figure 23 a. 1D ^{13}C NMR spectrum of a sample obtained from an extraction after 1 passage of *Blastocystis* ST7 using IMDM containing 13C-Glucose as a growth media to achieve carbon-13 labelling. **b.** The Intensities/no cells x 10^6 which is proportional to concentration of Ethanol in 2 samples (Ethanol A and Ethanol B) and Glycerol in 2 samples (Glycerol A and Glycerol B)

Table 9

	No Cells x (10^6)	
	A samples	**B samples**
Passage 1	2.58	2.11
Passage 3	4.71	10.75
Passage 5	1.22	1.81

Cell counts for each passage. Samples correspond to the samples analysed in figure-23b. Ethanol A and Glycerol A both correspond to sample A and ethanol B and Glycerol B both correspond to sample B.

lockes solution +^{13}C-Glucose was ineffective as a ^{13}C Labelling source in *Blastocystis*

As the ^{13}C-labelling appeared to only be effective on a small number of metabolites, from incubation in the culture media, two incubations of *Blastocystis* cells in lockes solution + 25 mM ^{13}C-Glucose were performed, to try and achieve successful labelling. Cells were incubated for one hour, two hours and three hours. **Figure 24a** is a 1D-^{13}C NMR spectral overlay comparing an ethanol resonance from a one hour incubation, a two hour incubation and a three hour incubation. **Figure 24b** is from the same spectral overlay but comparing a glucose resonance. Only ethanol was produced by these incubations with the 25 mM glucose as *Blastocystis'* food source. The full set of ethanol and glucose peaks from the two incubations can be seen in the supporting information (**Figure S4a** – **Figure S5b**). The concentration of ethanol appeared to decrease after three hours in both samples (**Figure 24c**). The concentration of Glucose showed a decrease after two hours in sample A followed by an increase after three hours. In sample B the concentration of glucose demonstrated a steady increase after two and three hours. Therefore, the concentration of glucose did not show a steady decrease as expected. As the concentration of ethanol decreases it appears that although lockes solution was effective at removing protein contamination it can also diminish the concentration of metabolites. As no steady decrease of Glucose or increase of ethanol is shown between one and three hours the ^{13}C-labelling has not been improving in relation to time.

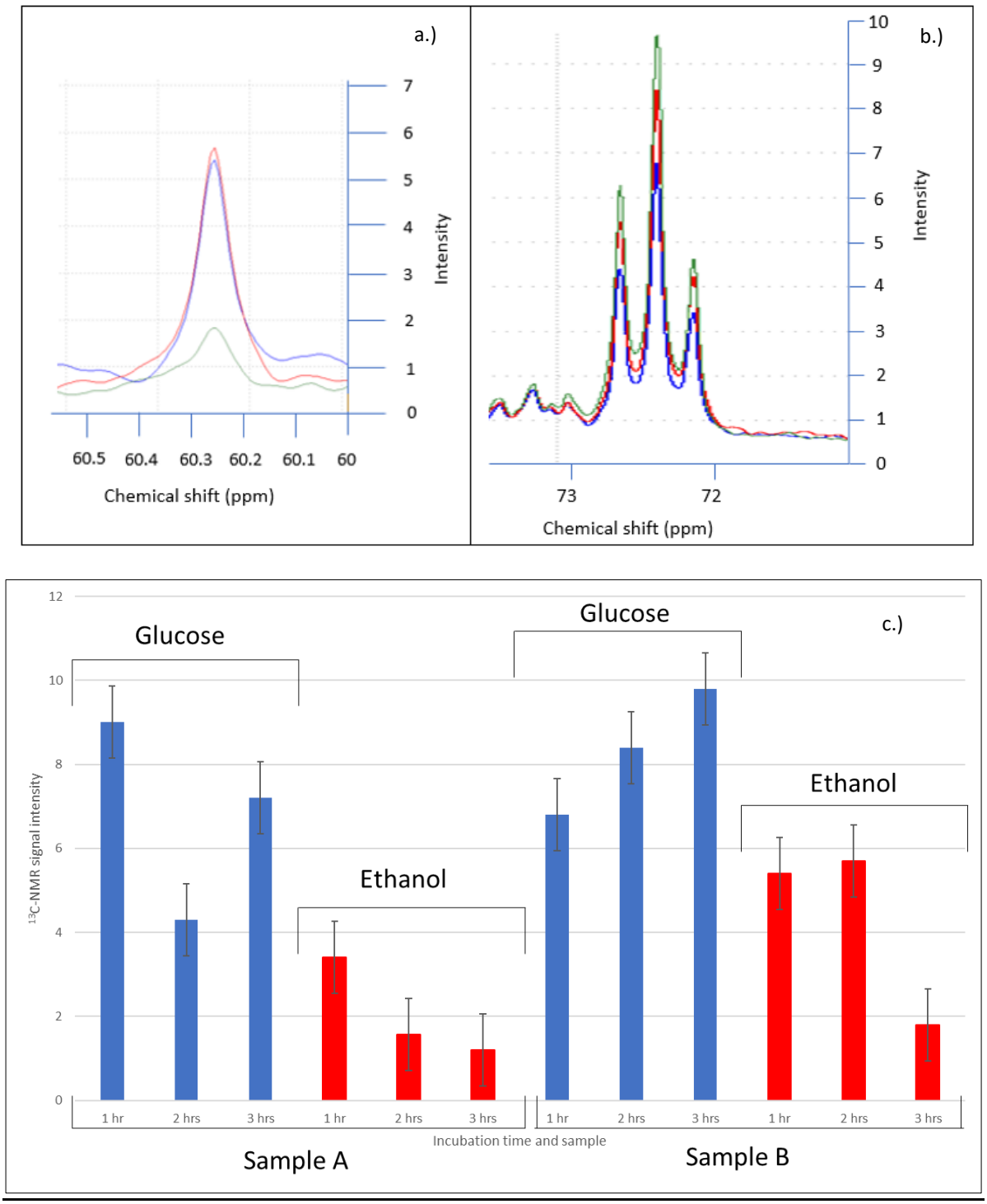

Figure 24 a. 1D-^{13}C NMR Spectral overlay showing Ethanol peaks from the one hour, two hour and three hour incubations of *Blastocytis* in lockes solution + 25mM ^{13}C-Glucose. **b.** 1D-^{13}C NMR spectral overlay of Glucose peaks from one hour, two hour and three hour incubations of *Blastocytis* in lockes solution + 25mM ^{13}C-Glucose. **c.** 1D-^{13}C NMR intensities of Glucose and Ethanol produced by 2 cultures of *Blastocystis* (sample A and sample B) following incubation for 1 hour, 2 hours and 3 hours in lockes solution + 25 mM ^{13}C-Glucose.

Microscopic analysis of Blastocystis confirmed that it was morphing into cyst form

Microscopic analysis of Blastocystis confirmed in was morphing into cyst form making metabolite extraction extremely difficult. **Figure 25a** is a microscopic image showing Blastocystis in cyst. **Figure-25b** shows Blastocystis in vacuolar form.

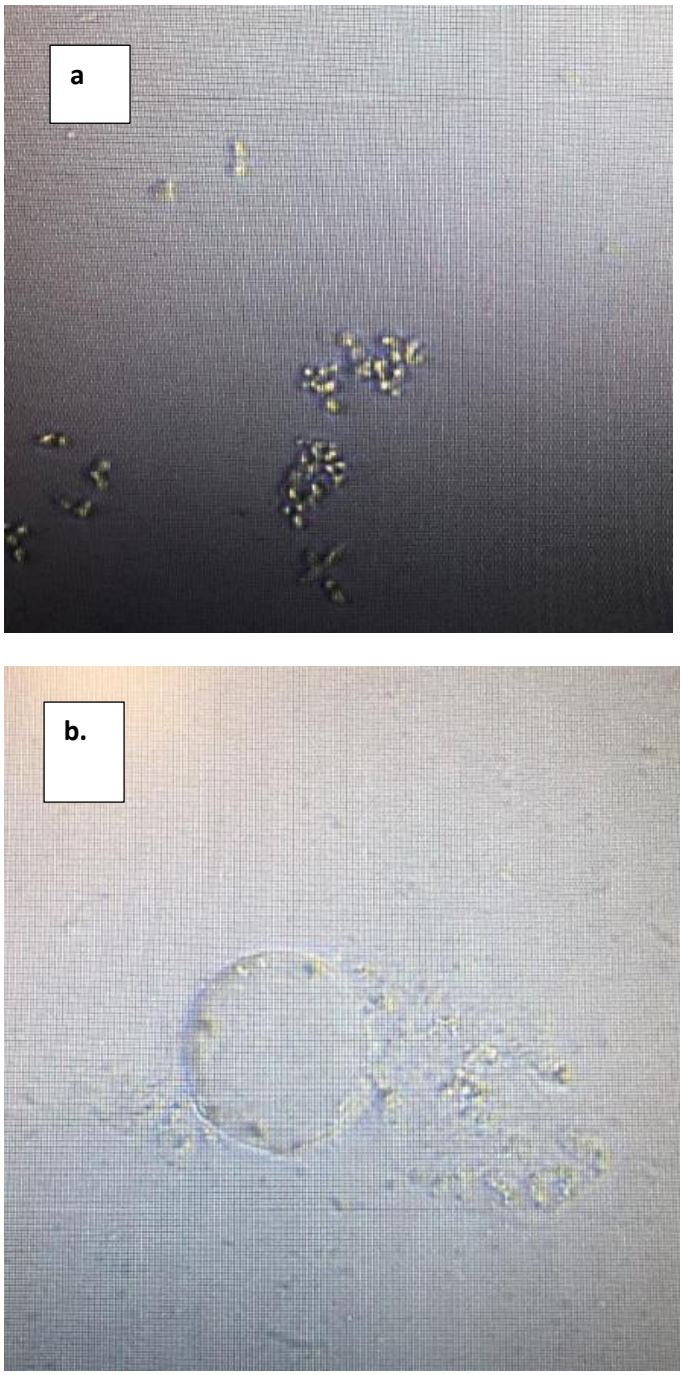

Figure 25 a. An image taken of Blastocystis useing light microscopy. *Blastocystis* appears to be in cyst form **b.** A past image taken of Blastocystis in vaculoar form showing different morphology to the image in **figure 25a**

^{13}C-Glucose NMR resonance peakes were identified in IMDM media

As the number of ^{13}C labelled metabolites extracted was limited because of the organism going into cyst form we measured *Blastocystis*' metabolic footprint. First the IMDM+HS media which was used to culture *Blastocystis* was analysed following the addition of ^{13}C-Glucose. The ^{13}C-Glucose was identified in the media by running a subsequent experiment in which the ^{13}C-Glucose concentration was doubled. **Figure 26a** is a 1D-^{13}C NMR spectrum of IMDM+HS+12.5 mM ^{13}C-Glucose. **Figure 26b** is an overlay of **figure 26a** of an experiment that was run in which the ^{13}C-Glucose concentration was doubled to 25 mM. The intensity at 25 mM showed a small increase suggesting that this could be Glucose that we are analysing. To confirm this the Glucose chemical shifts and intensities were identified using BMRB. **Table 10** shows these chemical shifts which closely match spectra in **figure 26a** and **figure 26b**. This also demonstrated that IMDM media does not affect the glucose chemical shift and that we are obtaining accurate results using this method.

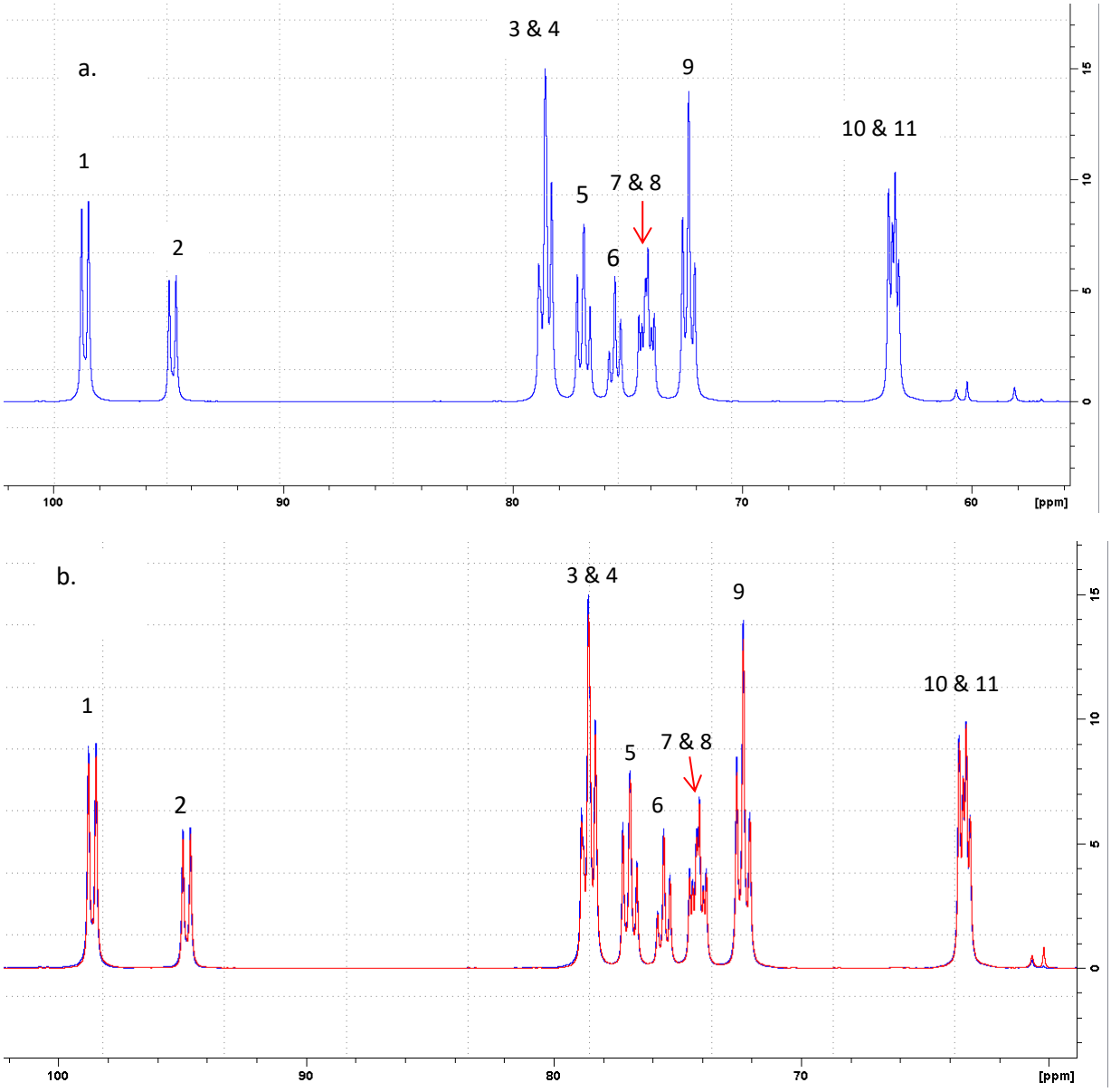

Figure 26 a. 1D ^{13}C NMR spectrum of ^{13}C-Glucose peaks detected in IMDM media 12.5 mM ^{13}C-Glucose. **b.** Spectral Overlay demonstrating the increase in resonance intensity of ^{13}C-Glucose peaks in 25 mM ^{13}C-Glucose compared to 12.5 mM 13C-Glucose. Numbers 1 – 11 correspond with chemical shifts in table-7

Table 10

Shift ID	Chemical shift BMRB (ppm)	Chemical shift from experiment (ppm)
1	98.643	98.61
2	94.826	94.78
3	78.69	78.565
4	78.474	78.517
5	76.854	76.884
6	75.48	75.523
7	74.202	74.185
8	74.166	74.089
9	72.352	72.313
10	63.454	63.443
11	63.284	63.316

Chemical shifts of ^{13}C-Glucose attained from analysis of IMDM+HS+^{13}C-Glucose media. These were matched to chemical shift data acquired from BMRB to confirm which molecule was detected.

Ethanol, xylitol and lactate are the end products of *Blastocystis'* Glucose metabolism

The IMDM+HS+^{13}C-Glucose media was analysed before and after incubation of the *Blastocystis* cells. This enabled us to detect which molecules were the end products of *Blastocystis'* glucose metabolism whilst morphing into cyst form and were being excreted by *Blastocystis* into the growth media. **Figure 27a** is a spectral overlay of the experiment run before the incubation (T1) against the experiment run after the incubation (T2), and **figure 27b** is taken from the region between 70 ppm and 80 ppm of the spectral overlay in **figure 27a**. The region of **figure 27a** between 155 ppm and 185 ppm can be seen in more detail in appendix **figure S6**. **Figure 27c** shows the ^{13}C-NMR intensities of ^{13}C Glucose and the end products *Blastocystis*' glucose metabolism before (T1) and after (T2) incubation in IMDM growth media. The intensity of Glucose shows a decrease at T2 compared to T1. The intensity is proportional to the concentration. Ethanol, xylitol and lactate are all absent at T1 and present at T2. These results suggest that ethanol, xylitol and lactate are all end products of Blastocystis' glucose metabolic pathways. The chemical shifts of ethanol, xylitol and lactate can be seen in **table 11.**

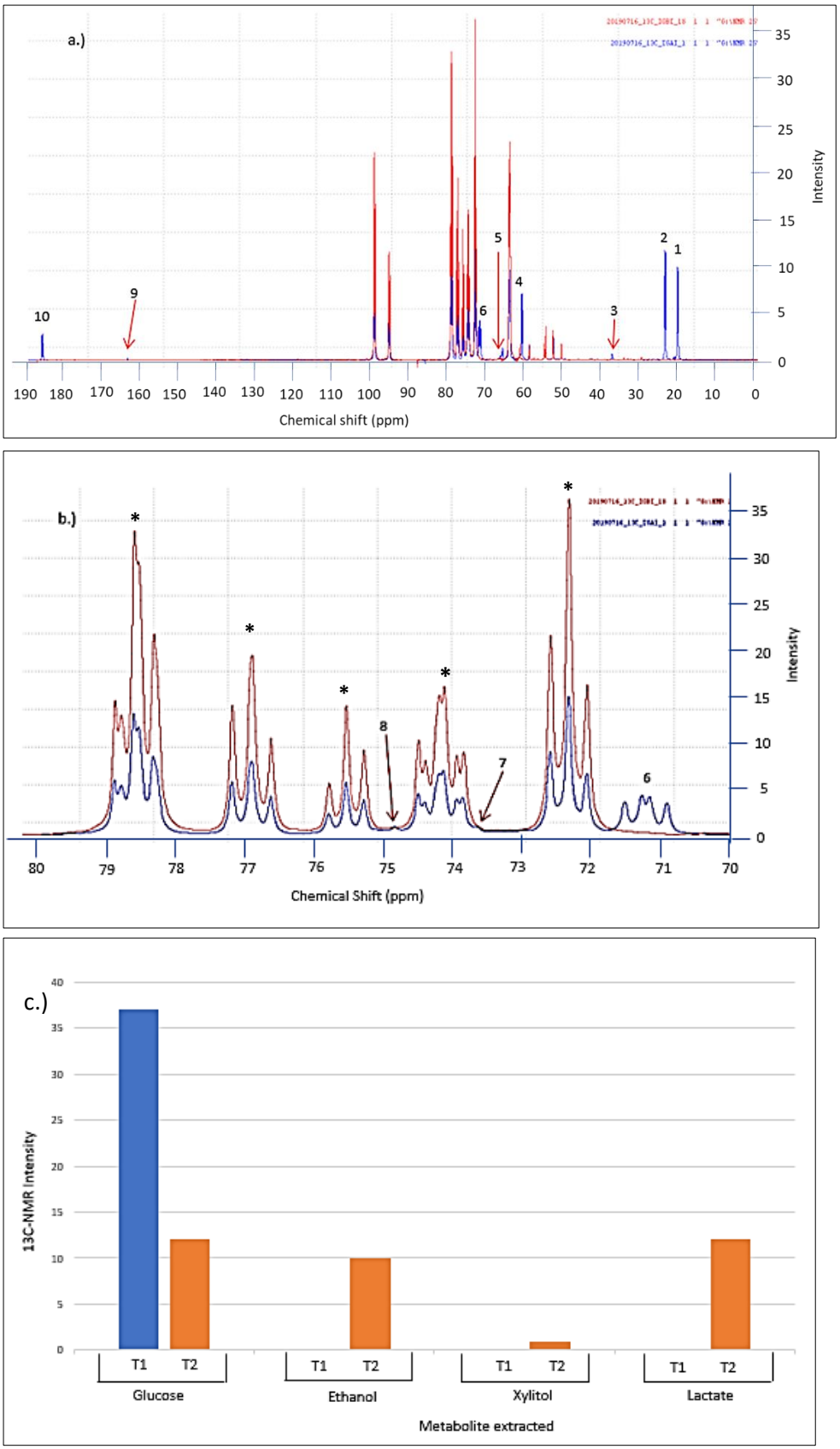

Figure 27 a. 1D-^{13}C NMR spectral overlay of IMDM+HS+^{13}C-Glucose before (T1) and after (T2) incubation of *Blastocytis.* **b.** Region of spectral overlay between 70 ppm and 80 ppm * = Glucose peak. Numbers 1-10 correspond with the peak assignments in **table 10** **c.** ^{13}C-NMR intensities of glucose and products of glucose metabolism before (T1) and after (T2) incubation

Table 11

Metabolite number	Chemical shift (ppm)	Metabolite
1	19.52	Ethanol
2	22.784	Lactate
3	36.71	Unassigned
4	60.179	Ethanol
5	65.258	Gluconic acid, xylitol. L-thrietol or Glycerol
6	71.196	Lactate
7	73.64	Xylitol
8	74.82	Xylitol, I-Threitol or Glycerol
9	162.916	Unassigned
10	185.157	Lactate

Metabolites detected in Glucose added media following incubation which were not present pre-incubation.

Ethanol and xylitol are the end products of *Blastocystis'* Pyruvate metabolism

The IMDM+HS+^{13}C-Pyruvate media was analysed before and after incubation of the *Blastocystis* cells. This enabled us to detect which molecules were the end products of *Blastocystis'* pyruvate metabolism whilst morphing into cyst form and were being excreted by *Blastocystis* into the growth media. **Figure 28a** and **figure 28b** are spectral overlays of the region between 20 ppm and 65 ppm and the region between 65 ppm and 80 ppm respectively obtained from the experiments run before (T1) the incubation against the experiments run after (T2) the incubation. A spectral overlay of the region between 100 ppm and 220 ppm can be seen in the appendix **figure S7.** **Figure 28c** shows the ^{13}C-NMR intensities of ^{13}C pyruvate and the end products of *Blastocystis*' pyruvate metabolism before (T1) and after (T2) incubation in IMDM growth media. The intensity of pyruvate shows a decrease at T2 compared to T1. The intensity is proportional to the concentration. Xylitol is absent at T1 and present at T2. Ethanol is at an extremely low concentration at T1 and shows a significant increase at T2. These results suggest that ethanol and xylitol are end products of Blastocystis' pyruvate metabolic pathways. The chemical shifts of ethanol and xylitol can be seen in **table 12.**

.

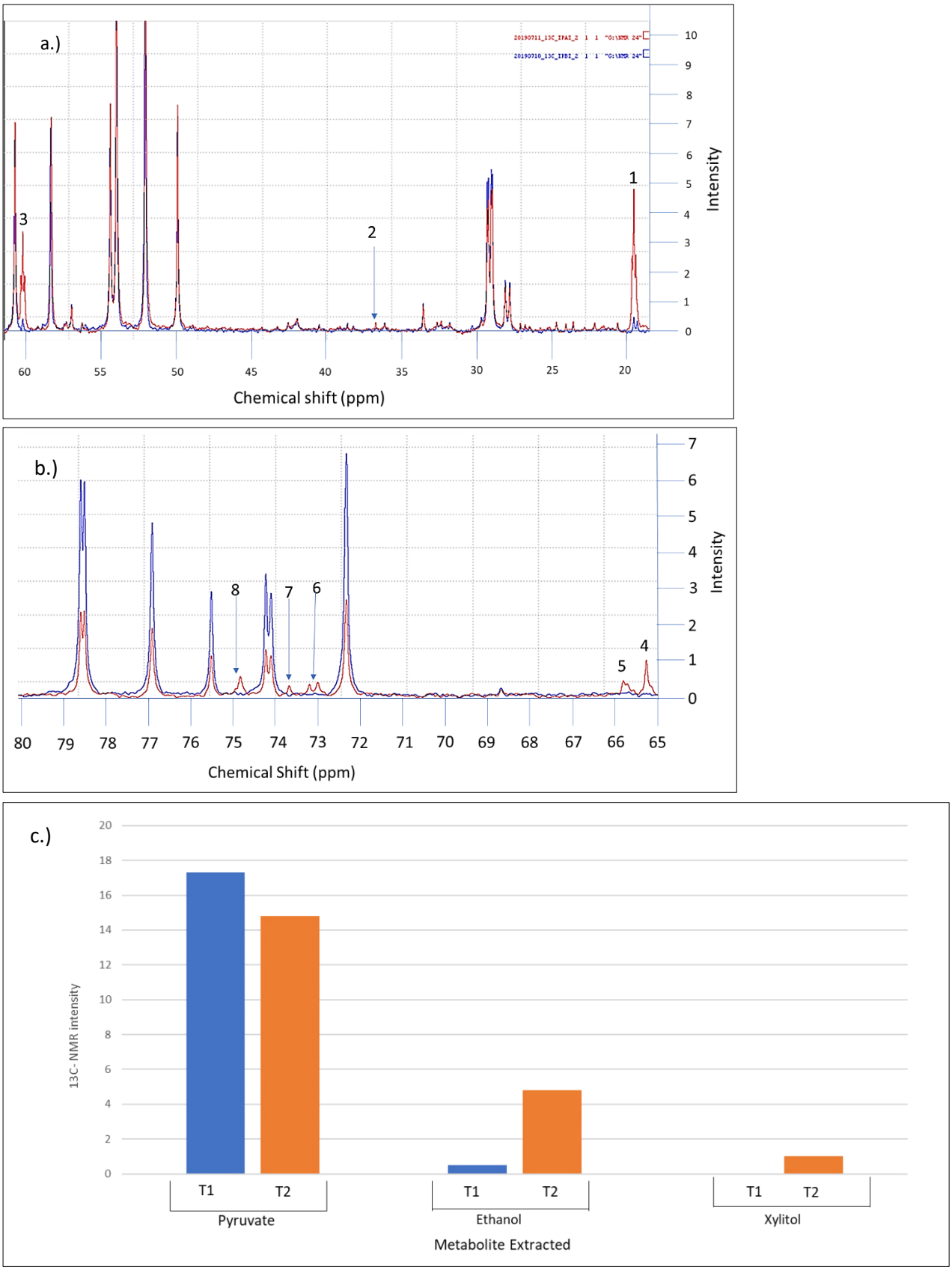

Figure 28. a and **b** Spectral overlays of 1D ^{13}C-NMR analysis of IMDM+HS+^{13}C-Pyruvate before (T1) and after (T2) incubation of *Blastocystis*. **a.** Region between 20 ppm and 65 ppm. **b.** Region between 65 ppm and 80 ppm. Numbers 1-8 correspond with peak assignments in **table 12. c.** ^{13}C-NMR intensities of pyruvate and products of pyruvate metabolism before (T1) and after (T2) incubation.

Table 12

Metabolite number	Chemical shift (ppm)	Metabolite
1	19.54	Ethanol
2	36.7	Unassigned
3	60.191	Ethanol
4	65.253	Xylitol
5	65.732	Unassigned
6	73.107	Unassigned
7	73.685	Xylitol
8	74.823	Xylitol
9	105.852	Unassigned
10	127.279	Unassigned
11	162.895	Unassigned

Metabolites detected in pyruvate added media following incubation which were not present pre-incubation.

3.4 Discussion

We used NMR spectroscopy to analyse the pyruvate metabolome of the protozoan stramenopile *Blastocystis* ST7*.* This study could provide data to help identify any possible disease causing mechanisms this potential parasite may have. We used ^{13}C-Glucose to try and achieve ^{13}C labelling of *Blastocystis'* metabolites by adding it to its growth media and also by incubation of *Blastocystis* in Locke's solution containing 50 mM ^{13}C-Glucose. We also analysed *Blastocystis's* growth media before and after incubation. The analysis of the growth media was performed on samples that had been supplemented with u^{13}C-Glucose and on samples which had been supplemented with u^{13}C-Pyruvate. We established a potential metabolic footprint for *Blastocystis* ST7 Glucose and pyruvate metabolism either in cyst form or during the process of morphing into cyst form.

The ^{13}C-Labelling using ^{13}C-Glucose in the culture media then extracting the metabolites by the extraction protocol demonstrated no successive increase in ^{13}C resonances **(Figure 23b)**. However, it was successful in labelling ethanol and glycerol **(Figure 23a).** Lysis methods have been successful in extracting the labelled metabolites in past studies[73]. The fungus *Aspergillus nigers* glycolytic metabolites were successfully labelled and extracted after lysis with a homogenizer [73]. Cyclopiazonic acid was successfully extracted from *Aspergillus flavus* to analyse its complex structure. This was done using 60% methanol as an extraction solvent and performing a fractionation procedure. The majority of the cyclopiazonic acid migrated towards the methanol phase and was then isolated using chromatography [72]. Therefore, methanol has been demonstrated to be a successful extraction solvent. ^{13}C-Labelling using glucose has also been demonstrated to be successful in other organisms such as *Actinobacillus succinogenes* for succinate production [70].

Other ^{13}C-organic molecules have been used to induce labelling in past studies. Such as ^{13}C-Acetate in *Thermoproteus neutrophilis* to study the organism's amino acid synthesis and carbohydrate metabolic pathways [69] and ^{13}C-glycerol in *Pichia pastoris* to study its protein production. Methanol was also used as an inducer in this study to increase gene expression and by extension increase protein production [76]. Both ^{13}C-Acetate and ^{13}C-Glycerol were successfully incorporated however studies using ^{13}C-Pyruvate have been difficult to come by.

As the labelling only had limited success no ^{13}C dilution method or homoculear decoupling method was needed. However, to resolve the low carbon sensitivity problem the total of scans was doubled from 2048 to 4096.

The novel idea of incubating *Blastocystis* in its isotonic media lockes solution + 50 mM ^{13}C-Glucose also produced no successive increase in ^{13}C resonance. However, the three-hour incubation demonstrated a decrease in ethanol intensity against the one-hour incubation (**Figure-24c**), suggesting that lockes solution may diminish the concentration of metabolites. However, an extremely low concentration of cells was

used for this experiment. One, two and three hours are also quite short incubation times and it is possible that a longer incubation is necessary.

Although both the IMDM media incubation and the Locke's solution incubation followed by an extraction being performed were not producing successful results to extract many ^{13}C labelled metabolites. Ethanol was being successfully extracted. It was later confirmed by the microscopy results that during incubation *Blastocystis* was very quickly morphing into cyst form **(Figure 25a)**.

Blastocystis is thought to be metabolically inactive and dormant in its cyst form and encased by a hard fibrillar shell [5]. Therefore, lysis and extraction methods would have been limited because of the cyst being harder to break up and a lack of metabolites to extract once the lysis has been performed. However, ethanol was still consistently isolated by the extraction methods and in some cases Glycerol was also isolated.

As the *Blastocystis* were quickly morphing into cyst form making the analysis of their metabolome difficult by the above methods the analysis of their metabolic footprint was trialled. This involved the analysis of their culture media before and after incubation. This was performed on the ^{13}C-Glucose supplemented IMDM+HS as well as the ^{13}C-Pyruvate supplemented IMDM+HS. Although the entire metabolome of *Blastocystis* could not be analysed this way we could detect which metabolites it excretes. Analysations of metabolic footprints have been performed on many other organisms [65],[77],[78].

For example in one past study, single and mixed yeast cultures were analysed using *Saccharomyces cerevisiae* and *Lachancea thermotolerans,* to determine what different metabolites they produced during alcoholic fermentation. Both the single and mixed cultures were analysed at their death phase initiation (T1) and their death phase termination (T2) to determine which different metabolites they produced. They produced evidence of different metabolites what were produced between single and mixed cultures [77].

This method of analysis has also been used to analyse faecal and urinary samples to find a biomarker for ageing in mice. Analysis of young and old mouse faecal samples suggested that differences in amino acid metabolism, TCA cycle metabolism, tryptophan-nicotinamide adenine dinucleotide pathway and the host-microbiota metabolic axis all applied in relation to ageing [78].

As part of the only NMR metabolomics study of a protozoan parasite so far, Vermathen et al analysed the metabolic footprint of *Giardia lamblia*. The spectra of the samples were taken before (t_0) and after (t_{3d}) and the $C\Delta = (t_0 - t_{3d})$ was calculated and converted into a concentration. This demonstrated that 24 molecules including leucine valine, ethanol, acetate and glucose were higher in cultured media than in the fresh media and ten molecules including arginine, aspartate and trehalose were higher the fresh media[65].

The analysis of the *Blastocystis* metabolic foot print did not produce the wide range of metabolites demonstrated in the above studies. However, analysis of *Blastocystis'* Glucose metabolic footprint did show the emergence of ethanol, lactate and another molecule which is most likely to be either glycerol or xylitol after incubation **(Table 11)**. The analysis of *Blastocystis'* pyruvate metabolic footprint produced similar results confirming the production of ethanol and more clearly demonstrating the production of xylitol **(Table 12)**. However no lactate was detected. Lactate dehydrogenase (LDH) activity production and release of lactate has been demonstrated in *Blastocystis* in past studies [30]. Lactate has been demonstrated to have probiotic effects and therefore lactate production could have a positive effect on the gut microbiome. One of lactates probiotic effects is that it enhances the production of butyrate by other members of the gut microbiome.

However, in past studies ethanol has demonstrated a negative effect on the diversity of the gut microbiome [79],[80]. High alcoholic drink consumption has demonstrated a negative correlation of microbial diversity of the gut compared to those who don't drink [79],[80]. Ethanol production has never before been demonstrated in *Blastocystis*. However, anaerobic fermentation and the production of ethanol have been demonstrated in *N. Ovalis.* It has therefore been proposed that N. Ovalis possesses the pyruvate decarboxylase (PDC) and alcohol dehydrogenase enzymes (ADH) [39]. The *N. Ovalis* hydrogenosome is thought to be the most closely related organelle to the *Blastocystis* MRO and therefore *N. Ovalis* is likely to be a closely related organism. The production of ethanol in this study therefore suggests that *Blastocystis* may possess the PDC and ADH mechanism as another route pyruvate takes in *Blastocytis'* metabolism (**figure 29**). However, as *Blastocystis* was morphing into cyst form early in its incubation it could well be the case that it undergoes the cytosolic fermentation whilst it is encysting and the ATP produced from glycolysis is used by the cell to provide energy for its encysting mechanisms. The lack of other metabolites detected helps confirm that the fermentation was taking place whilst in cyst form or whilst morphing into cyst form. As another pathway could have been detected that pyruvate takes in Blastocystis and this affects the flow of pyruvate through its usual route. Pyruvate is most commonly converted to acetyl-CoA by PDH, PFO or PNO. Acetyl-CoA then progresses to being converted to acetate in a process that facilitates ATP production (**figure 29**) [52],[31],[34]. Pyruvate can also be directed down a reverse Krebs cycle by Pyruvate Carboxylase (PyrC) [34]. As *Blastocystis* is metabolically inactive whilst in cyst form it is possible that the mitochondria becomes inactive the cytosolic metabolism continues. The data from this study supports that.

Although xylitol was detected in both the pyruvate and glucose metabolic footprint analyses, some ^{13}C-Glucose was detected in the pyruvate supplemented media at natural abundance. After analysis of the KEGG pathways it is more likely xylitol is produced from Glucose via the pentose and glucoronate interconversion pathways (**figure 29**). As *Blastocystis* morphs into cyst form and starts to become

metabolically inactive and dormant, the residual glucose may take an alternative pathway as well as glycolysis. The pentose and glucoronate interconversion pathways are alternative routes glucose could take which result in xylitol production. The cytosolic xylitol producing pathway in **figure 29** is a common route which is part of the pentose and glucoronate interconversion pathways and is fitting with the KEGG pathways (https://www.genome.jp/kegg-bin/show_pathway?map00010) – For glycolysis (https://www.genome.jp/kegg-bin/show_pathway?map00040+C00379) – For the pentose and glucoronate interconversion pathways.

In past studies xylitol has demonstrated anti-adhesion effects. This could have an effect on the gut microbiome as there are both members of the gut microbiota and pathogenic organisms that like to bind to gastrointestinal epithelial cells [81],[82].

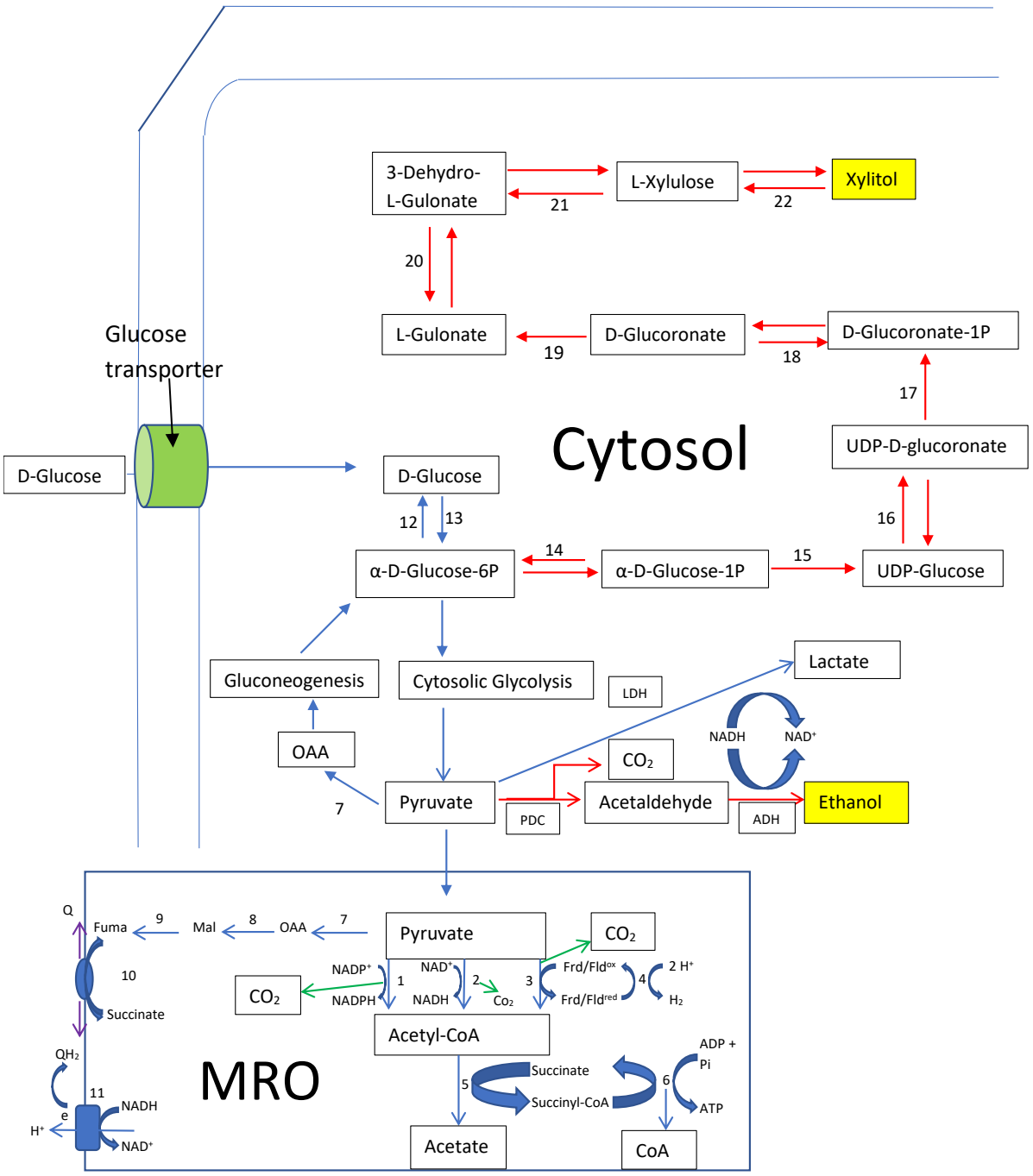

Figure 29 . Diagram of proposed new Blastocystis Glucose and pyruvate metabolism pathways possibly whilst morphing into cyst form. New pathways are denoted by the red arrows and new products detected are highlighted in yellow. 1 = Pyruvate ; NADPH Oxidoreductase (PNO) 2 = Pyruvate Dehydrogenase (PDH) 3 = Pyruvate ; Ferredoxin Oxidoreductase (PFO) 4 = Iron;Iron Hydrogenase (FeFeHyd) 5 = Acetate:Succinate CoA Transferase(ASCT) 6 = Succinyl-CoA Synthase (SCS) 7 = Pyruvate carboxylase (PyrC) 8 = Malate Dehydrogenase (MDH) 9 = Fumarase (FUM) 10 = Fumarate Reductase (FRD) 11 = Complex I. OAA = Oxaloacetate Mal = Malate Fuma = Fumarate. 12 = Glucose 6-phosphatase 13 = Hexokinase 14 = Phosphoglucomutase 15 = UTP-Glucose-1-phosphate uridylyltransferase 16 = UDP-Glucose 6-dehydrogenase 17 = Glucuronate-1-phosphate uridylyltransferase 18 = Glucoronokinase 19 = Glucuronate reductase 20 = L-Gulonate 3-dehydrogenase 21 = dehydro-L-gulonate decarboxylase 22 = L-xylulose reductase

Further studies that could be conducted on this include repeating the lockes solution incubation procedure but for much longer with much larger cell cultures. The incubation could be conducted over a period of days rather than hours. To learn more about the three pyruvate metabolising enzymes use of potential inducers could be used to conduct over expression assays. Also NMR procedures commonly produce many outliers and many repeats are often needed. Therefore conducting the experiments using ten to twenty repeats may also improve our data set. Using cultures which don't so easily go into cyst form we could also perform assays selectively inhibiting two of the three pyruvate metabolising enzymes so we could analyser them individually.

There are also many applications this data could be used for. If the anaerobic fermentation process is an essential part of the encystation process of *Blastocystis.* The enzymes that facilitate anaerobic fermentation could be a useful drug target. If you could block *Blastocystis* from going into cyst form it might not be able to survive outside of the host and could be prevented from thriving and therefore spreading. Also, if *Blastocystis* takes part in the fermentation process, the mechanism that facilitates this could be a used as part of the brewing process, and be used to produce alcoholic beverages. However, *Blastocystis* grows extremely slowly, so the use of *Blastocystis* to produce alcoholic beverages would not be a highly productive process. However, the yeast *Saccharomyces cerevisiae* has been determined to be a highly productive organism for carrying out the anaerobic fermentation process [83]. Therefore, cloning the PDC and ADH genes from *Blastocystis* into *S. cerevisiae* could potentially improve its efficiency in producing alcoholic beverages.

3.5 Conclusion

We conducted a ^{13}C-1D NMR study to analyse the pyruvate metabolism of the protozoan stramenopile *Blastocystis*. We were unable to analyse *Blastocystis's* entire metabolome due the organism going into cyst form making extraction of metabolites difficult. However, we were able to analyse its glucose and pyruvate metabolic footprint. We discovered a potentially novel pathway that pyruvate metabolism may take and that *Blastocystis* could possibly perform anaerobic fermentation. We also discovered a potentially novel pathway that glucose metabolism may take. This could help provide data about *Blastocystis's* potential pathogenic mechanism and should it be parasitic provide clues about how to treat it.

Chapter 4 – Discussion

We established the first metabolomics method to study the whole metabolome of *Blastocystis* and applied it to analyse its pyruvate metabolism using NMR spectroscopy. All past studies to analyse *Blastocystis's* metabolism have involved isolation of its mitochondria, cytosol and lysosome followed by biochemical analysis or characterisation [30]. In the first study of this project we devised a suitable protocol to extract *Blastocystis'* metabolites so that its metabolome could be analysed. We determined that methanol was a more efficient extraction solvent than ethanol and that bead beating was a better lysis technique than sonication. Temperature had no effect on metabolite extraction efficiency. Therefore, to extract the metabolites we added the *Blastocystis* cells to 50% methanol, lysed the cells with glass beads, incubated them for 3 minutes at room temperature and then centrifuged the lysate so that the polar metabolites would migrate towards the supernatant.

We also used ^{13}C-Glucose and ^{13}C-Pyruvate to label the metabolites to perform ^{13}C-NMR which help facilitate the detection of organic molecules, some of which were products of *Blastocystis'* pyruvate metabolism. The protocol devised in the first study was used to extract the metabolites from the cells following the ^{13}C labelling. The whole metabolome study proved to be difficult because of *Blastocystis* morphing into cyst form. However, we were able to analyse *Blastocystis's* metabolic footprint and determine which breakdown products it excretes after taking up glucose or pyruvate. The metabolic footprint provided evidence of which metabolic pathways glucose and pyruvate follow and we extracted information regarding a potential novel metabolic pathway pyruvate may take in *Blastocystis*. The three most abundant metabolites detected from *Blastocystis'* metabolic footprint were lactate, ethanol and xylitol and all three of these could have a significant impact on the gut microbiome and gastrointestinal health.

4.1 Lactate

The lactate that was detected following incubation in the media containing ^{13}C-Glucose suggests the functional activity of the enzyme lactate dehydrogenase (LDH) (**figure 29**). LDH is canonically cytosolic and past studies have also detected LDH activity in the cytosol of *Blastocystis* [84]. In past studies lactate has demonstrated probiotic effects [85],[86]. Lactate is fermented to butyrate in many gut microfloras and butyrate is important for mucosal homeostasis [85]. Lactate can also be important for generating various nutrients from food stuffs, which cannot be broken down by the human digestive system alone [86]. Many probiotic strains of bacteria are lactic acid bacteria belonging to the genus *Lactobacillus*. However lactate is acidic and can also have detrimental effects on the human gut. For example, in patients with short bowel syndrome (SBS) the reduced size of the gastrointestinal tract can result in a higher flow of carbohydrates into the colon. A higher carbohydrate volume results in higher activity in colonic bacteria producing organic acids. Therefore acid-resistant colonic bacteria thrive while other members of the gut

microbiome decline. The increase in acid-resistant D-lactate producing bacteria such as *Lactobacillus acidophilus* and *Lactobacillus fermentum* results in an increase in D-lactate absorption. The increase in absorption can result in D-lactic acidosis which is associated with neurological effects ataxia, slurred speech and confusion [87].

Past studies have suggested that *Blastocystis* has probiotic effects and its presence results in an increase in numbers of many members of the gut microbiome [27]. However, some important members of the gut microbiome have shown a decline in *Blastocystis's* presence resulting in inflammation of the gut lining and gastrointestinal symptoms being experienced [21]. The lack of orthodox pathogenic characteristics demonstrated in *Blastocystis* has resulted in research being more focussed on colonisation than infection [88]. Long term colonisation and continuous production of lactate would better explain both the probiotic effects and the detrimental effects on the gut microbiome than short term infection. A combination of these effects causes dysbiosis which has been proposed to be the mechanism in which *Blastocystis* causes gastrointestinal symptoms [21].

4.2 Ethanol

The ethanol detected following incubation in media containing ^{13}C-Glucose and media containing ^{13}C-Pyruvate suggests the presence of an anaerobic ethanol fermentation pathway (**figure 29** Ethanol producing pathway). Activity of an ethanol fermentation pathway has never been detected in *Blastocystis* before.

Consumption of alcoholic drinks has been demonstrated to have a significant effect on the gut microbiota and cause dysbiosis [89],[90]. As 95% of the ethanol consumed is expelled from the body by detoxification to H_2O and CO_2 in the liver it is likely to be the small amount that evades absorption in the small intestine that causes the dysbiosis. Therefore, the production of ethanol in the small or large intestine by a microbe potentially could also cause dysbiosis. As with lactate the long term colonisation of the gut and continuous production of ethanol is more likely to cause dysbiosis than short term infection [79].

4.3 Xylitol

The xylitol detected following the incubation in media containing ^{13}C-Glucose suggests the presence of the xylitol producing pathway shown in **figure 29.** As glucose enters the cell and is converted to glucose-6-phosphate to ensure it stays in the cell, the metabolic route it takes is always likely to be that of glycolysis. However, in irregular circumstances such as morphing into cyst form, inactive mitochondria could cause a build-up of glucose, resulting in the residual molecules taking an alternative pathway such as the xylitol producing pathway shown in **figure 29.**

In past studies xylitol has demonstrated anti-adhesion effects and effects that disrupt biofilms. Many examples of these effects are anti-cariogenic [91],[82]. Xylitol has therefore been used to treat dental infections, however xylitol has demonstrated anti-

adhesion effects against many species of bacteria including gut infecting microbes [92].The pathogenic mechanisms of disease causing microbes in the gastrointestinal tract, often include attachment to the gastrointestinal epithelial cells. Therefore, preventing this adhesion could be a beneficial mechanism that xylitol could provide for gastrointestinal health. Whilst in the past, protozoa in the gut have been considered to be parasitic, it is now known than many eukaryotic microbes are symbiotic, and their diversity in the gut is as important as bacterial diversity [93]. Our results support previous studies conducted, where *Blastocystis* has shown a lower prevalence in the gut in symptomatic individuals than healthy individuals [94].

Another positive impact *Blastocystis* has demonstrated in the gut is its positive correlation with the diversity of the gut microbiome [27],[21]. However *B. longum* a member of the gut microbiome which is involved in protecting the gut lining demonstrates a decrease in numbers in the presence of *Blastocystis*. Histopathological analyses of mouse gastrointestinal tract demonstrated damage of the gastrointestinal epithelial cells following infection with *Blastocystis* [21]. As xylitol has anti-adhesion effects it could be the production of xylitol by *Blastocystis* which is causing a decrease in *B. longum* protecting the gut lining, leaving it exposed [21]. Xylitol has been demonstrated to effect gene expression with regards to bacterial capsule, extracellular matrix and the expression of various receptors possibly rendering the bacterium unable to bind to their regular target [95],[81],[96],[97]. *B. longum* being unable to bind to the gut epithelial cells could leave the gastrointestinal tract exposed to oxidative damage. This could be possibly caused by *Blastocystis*, or caused by host immune responses in response to *Blastocystis* [21].

4.4 Future research

Further studies of *Blastocystis's* relationship with the gut microbiome and its potential pathogenic mechanism, could involve a combination of a metabolomics and a metagenomics study. This could involve analysation of faecal samples from individuals who tested positive for *Blastocystis,* with and without gastrointestinal symptoms. These could be compared to faecal samples from individuals who tested negative for *Blastocystis*. By extracting and sequencing the metagenome of each faecal sample, we will be able to detect which bacterium are present and in what numbers. This data will provide us with information on the impact *Blastocystis* has on different members of the gut microbiome, and how this impact could either cause symptoms or be beneficial. The metabolomics study on the same cohorts faecal samples, could provide more data on molecules in the gut, which *Blastocystis* may produce which could affect the gut microbiome and impact gastrointestinal health in general. These studies could be expanded to animals and different subtypes of *Blastocystis* could be analysed to provide us with a wider knowledge of the spread of *Blastocystis* and potential zoonotic infection. This would also help identify which subtypes are pathogenic.

Understanding *Blastocystis* relationship with the gut microbiome could be highly important for the future of gastrointestinal health in general. As *Blastocystis* has some positive effects and the overwhelming majority of subtypes and colonisations do not cause symptoms it is likely that the non-symptomatic subtypes are actually symbiotic. As these would be beneficial to gastrointestinal health it is important that these are identified and not targeted by therapeutics. It is important to identify the subtypes that could be detrimental to health and find any unique characteristics they may have as these could be potential drug targets.

4.5 Conclusion

We identified three molecules lactate, ethanol and xylitol which are excreted by the protozoan anaerobe *Blastocystis,* possibly whilst morphing into cyst form. We tried to establish what their impact could be on gastrointestinal health. Lactate has in past studies demonstrated probiotic properties. Lactate is a precursor for butyrate which has an important impact on the homeostasis of the gut. However, as lactate is an acidic molecule a high concentration of it or certain circumstances can result in lactic acidosis. Ethanol has in past studies demonstrated detrimental effects on gastrointestinal health, as consumption of alcoholic beverages has demonstrated a negative correlation with the diversity of the gut microbiota. Xylitol has anti-adhesion properties, which could be beneficial or detrimental to the health of the gut. Xylitol could prevent pathogenic microbe binding to the epithelial cells. However it could also prevent *B. longum* from doing the same. *B. longum* is highly important for protecting the epithelial cells of the gut. Many of the effects that these molecules inflict have been demonstrated in individuals who tested positive for *Blastocystis* in past studies. This data could be used and expanded on in future studies to elucidate what beneficial and detrimental effects different *Blastocystis* subtypes may have on gastrointestinal health.

Appendix

Supporting information

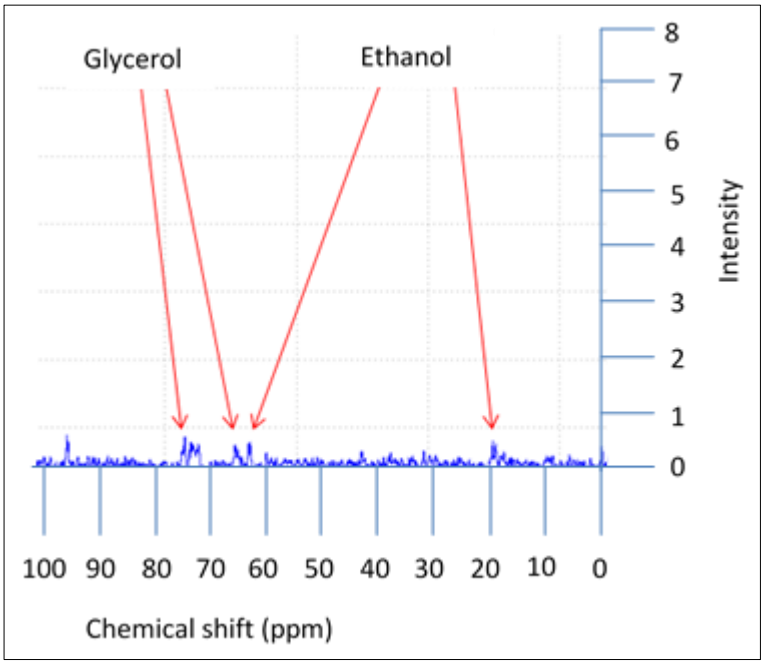

Figure S1. 1D ^{13}C NMR spectrum obtained from an extraction after 1 passage of *Blastocystis* ST7 using IMDM as a growth media and ^{13}C-Glucose to achieve carbon-13 labelling.

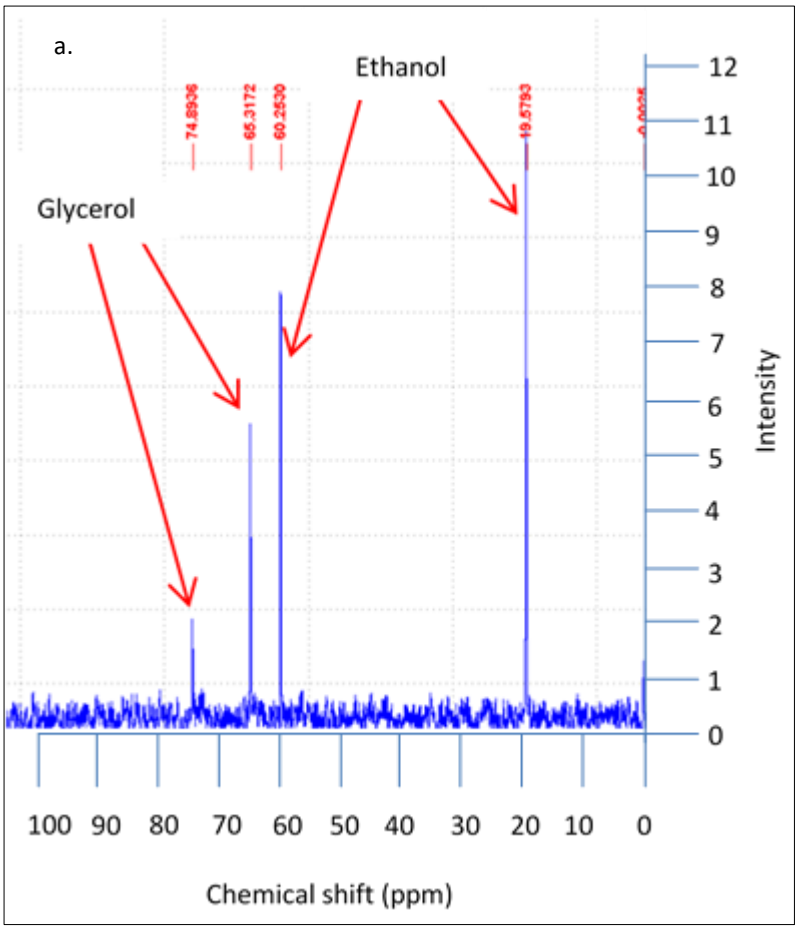

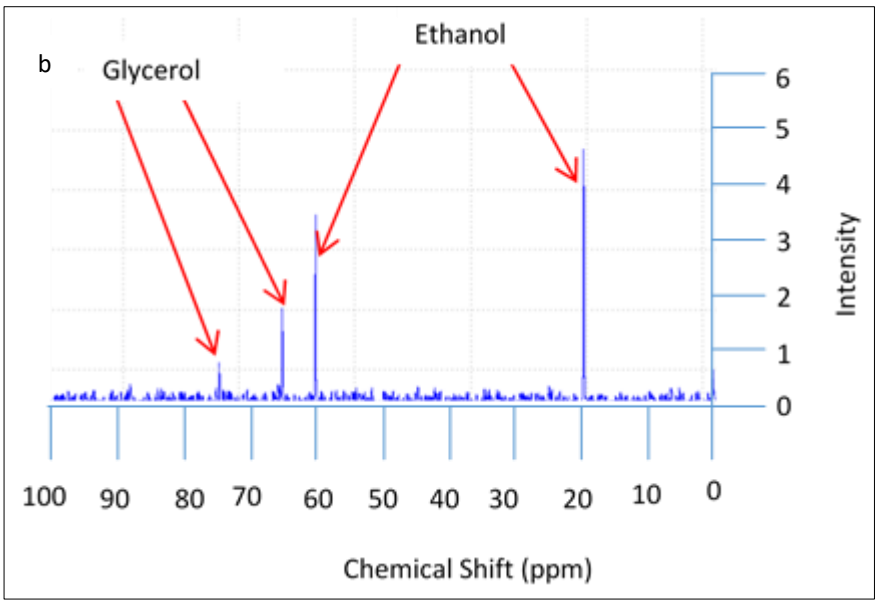

Figure S2 a. and b. 1D ^{13}C NMR spectra of replicates obtained from extractions after three passages of Blastocystis ST7 using IMDM as a growth media and 13C-Glucose to achieve carbon-13 labelling. The intensities of the spectra are set to the same scale for comparison.

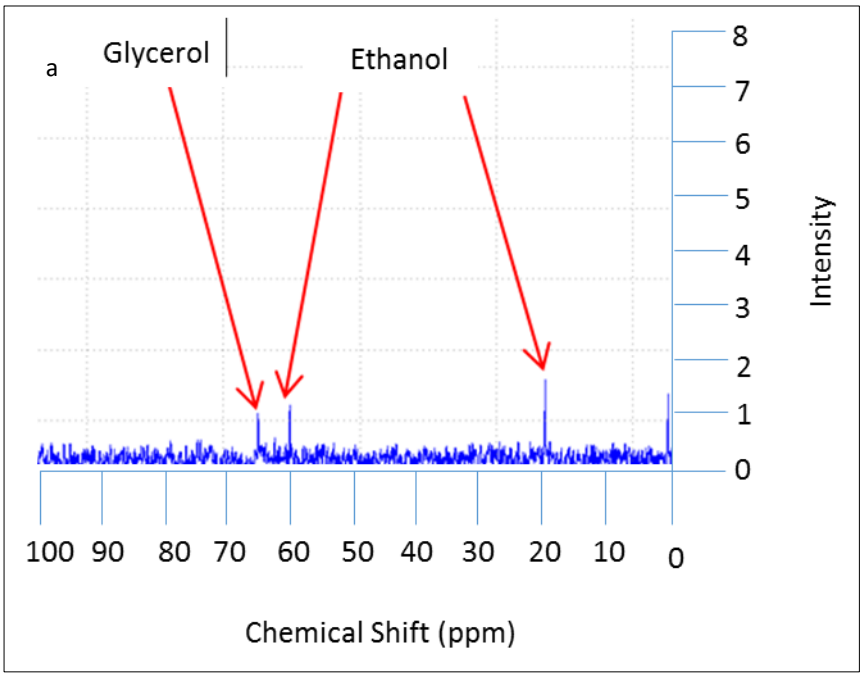

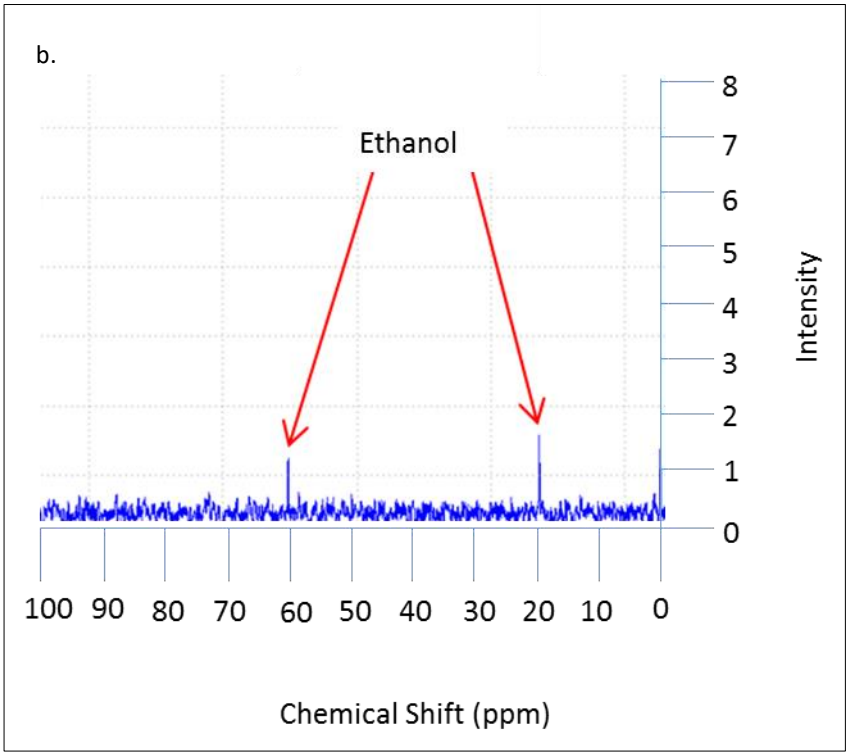

Figure S3 a. and b. 1D ^{13}C NMR spectra obtained from extractions after five passages of Blastocystis ST7 using IMDM as a growth media and ^{13}C-Glucose to achieve carbon-13 labelling. The intensities of the spectra are set to the same scale for comparison.

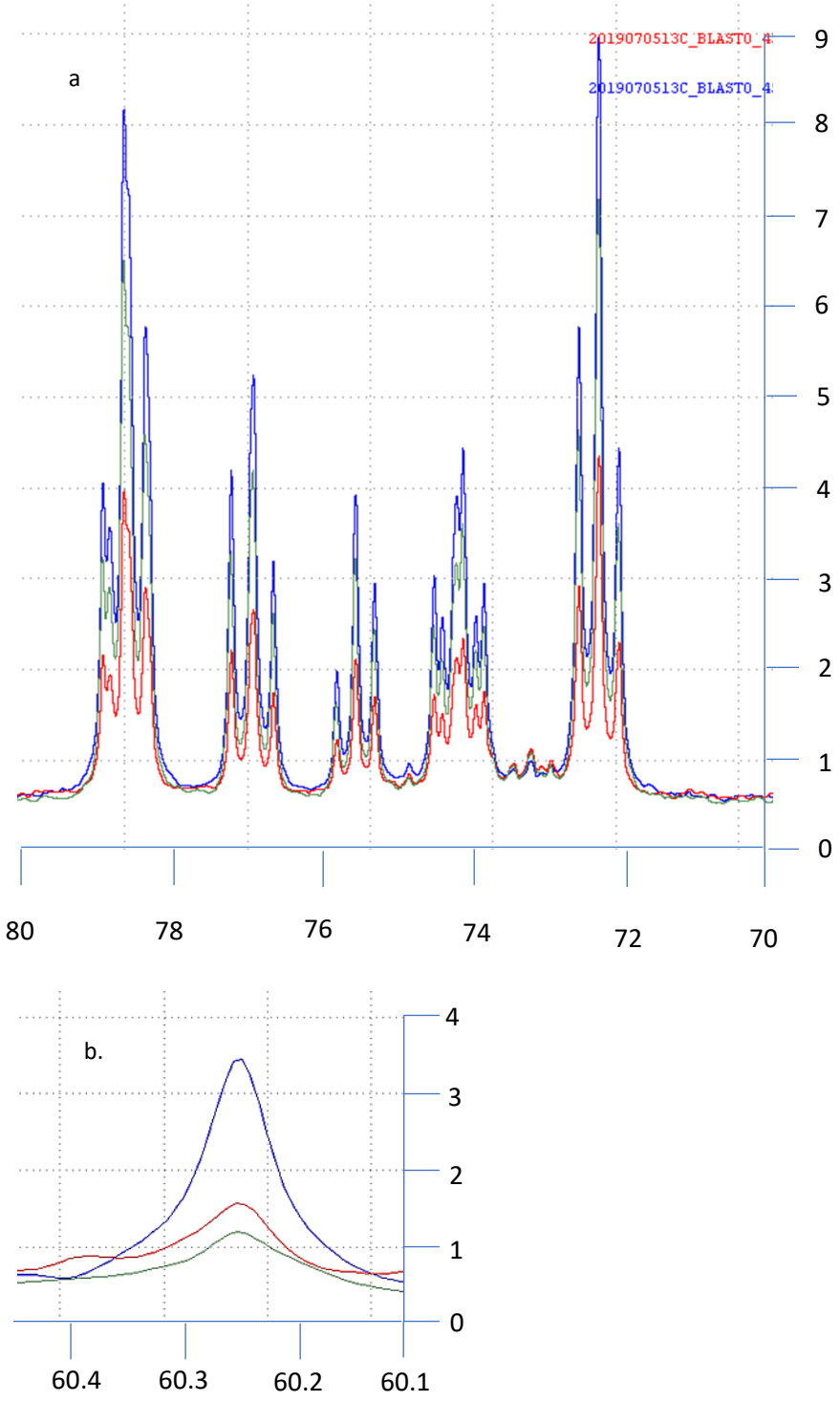

Figure S4 a. 1D-^{13}C NMR spectral overlay between 70 ppm and 80 ppm of the one hour, two hour and three hour incubations of *Blastocytis* in lockes solution + 25mM ^{13}C-Glucose. This spectral overlay shows a selection of Glucose peaks **b.** Spectral overlay showing Ethanol peaks from the one hour, two hour and three hour incubations of *Blastocytis* in lockes solution + 25mM ^{13}C-Glucose.

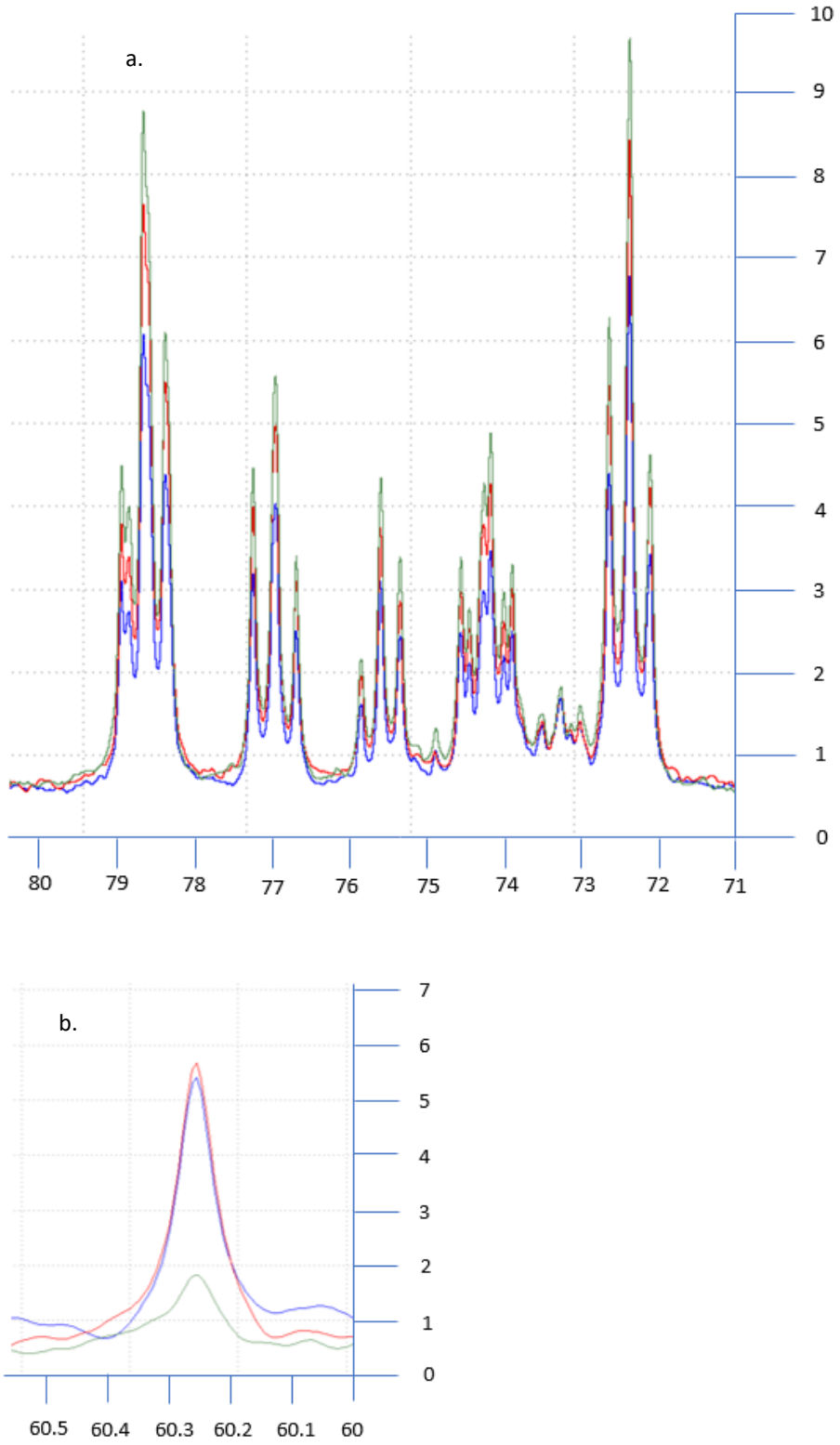

Figure S5 a. 1D-^{13}C NMR spectral overlay between 70 ppm and 80 ppm of the one hour, two hour and three hour incubations of *Blastocytis* in lockes solution + 25mM ^{13}C-Glucose. This spectral overlay shows a selection of Glucose peaks **b.** Spectral overlay showing Ethanol peaks from the one hour, two hour and three hour incubations of *Blastocytis* in lockes solution + 25mM ^{13}C-Glucose.

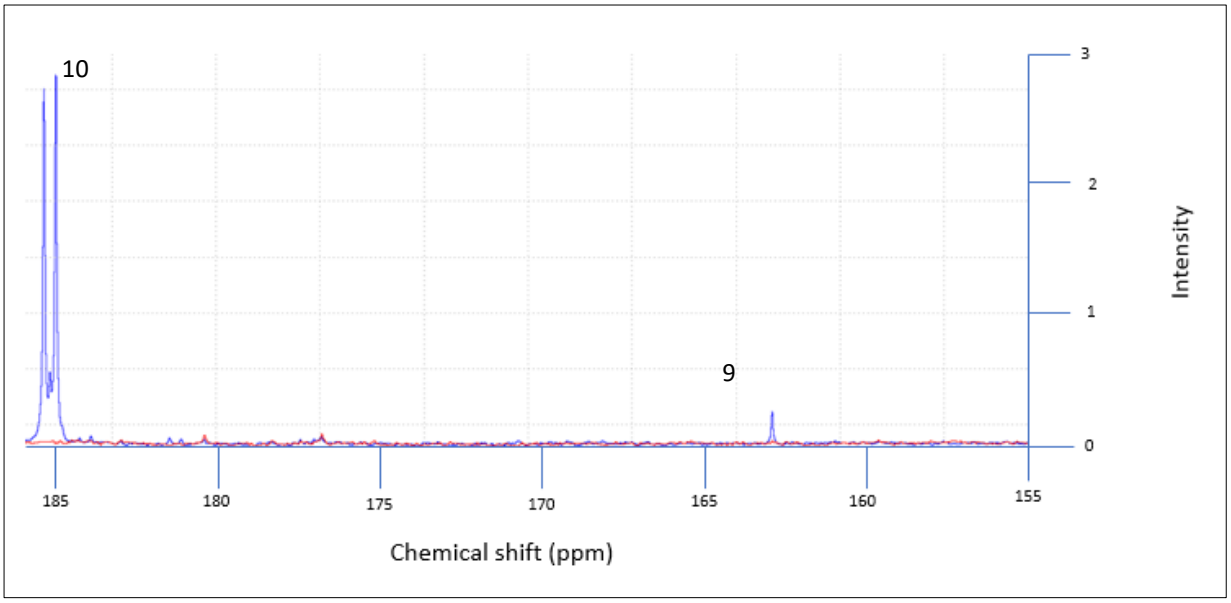

Figure S6. Region of spectral overlay between 155 ppm and 186 ppm of *Blastocystis*' Glucose metabolic footprint. Before (T1) and after (T2) incubation of *Blastocytis.* Numbers 9 and 10 correspond with the peak assignments in **table 10**

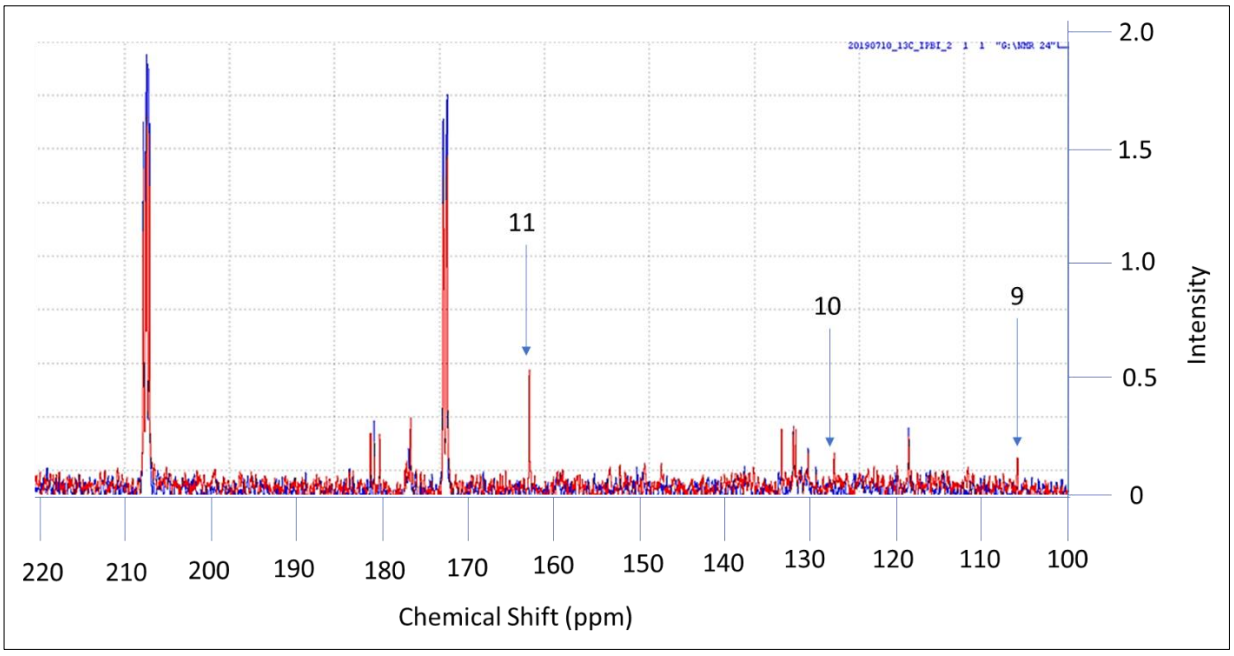

Figure S7. Region of spectral overlay between 100 ppm and 220 ppm of *Blastocystis*' pyruvate metabolic footprint. Before (T1) and after (T2) incubation of *Blastocytis.* Numbers 9,10 and 11 correspond with peak assignments in **table 11.**

Bibliography

[1] D. J. STENZEL1* AND P. F. L. BOREHAM2, "*Blastocystis* hominis Revisited," *Clin. Microbiol. Rev.*, vol. 9, no. 4, pp. 563–584, 1996.

[2] NOBUKO ARISUE et al "Phylogenetic Position of *Blastocystis hominis* and of Stramenopiles Inferred from Multiple Molecular Sequence Data," *J. Eukaryot. Microbiol.,* vol. 49, no. 1, pp. 42–53, 2002.

[3] V. P. Edgcomb *et al.*, "Molecular Phylogenies of *Blastocystis* Isolates from Different Hosts: Implications for Genetic Diversity, Identification of Species, and Zoonosis," *J. Clin. Microbiol.*, vol. 43, no. 1, pp. 348–355, 2005.

[4] C. R. Stensvold and C. G. Clark, "Current status of Blastocystis: A personal view," *Parasitol. Int.*, vol. 65, no. 6, pp. 763–771, 2016.

[5] K. S. W. Tan, "New insights on classification, identification, and clinical relevance of *Blastocystis spp*.," *Clin. Microbiol. Rev.*, vol. 21, no. 4, pp. 639–665, 2008.

[6] A. Duda, D. Kosik-Bogacka, N. Lanocha-Arendarczyk, L. Kołodziejczyk, and A. Lanocha, "The prevalence of *Blastocystis* hominis and other protozoan parasites in soldiers returning from peacekeeping missions," *Am. J. Trop. Med. Hyg.*, vol. 92, no. 4, pp. 805–806, 2015.

[7] Y. Taşova, B. Şahin, S. Koltaş, and S. Paydaş, "Clinical significance and frequency of *Blastocystis hominis* in Turkish patients with hematological malignancy," *Acta Medica Okayama*, vol. 54, no. 3. pp. 133–136, 2000.

[8] A. M. Martín-Sánchez, A. Canut-Blasco, J. Rodriguez-Hernandez, I. Montes-Martínez, and J. A. García-Rodríguez, "Epidemiology and clinical significance of *Blastocystis hominis* in different population groups in Salamanca (Spain)," *Eur. J. Epidemiol.*, vol. 8, no. 4, pp. 553–559, 1992.

[9] M. Mardani Kataki, M. Tavalla, and M. Beiromvand, "Higher prevalence of *Blastocystis hominis* in healthy individuals than patients with gastrointestinal symptoms from Ahvaz, southwestern Iran," *Comp. Immunol. Microbiol. Infect. Dis.*, vol. 65, no. May, pp. 160–164, 2019.

[10] M. A. Alfellani, C. R. Stensvold, A. Vidal-Lapiedra, E. S. U. Onuoha, A. F. Fagbenro-Beyioku, and C. G. Clark, "Variable geographic distribution of *Blastocystis* subtypes and its potential implications," *Acta Trop.*, vol. 126, no. 1, pp. 11–18, 2013.

[11] Y. H *et al.*, "Genomic analysis of *Blastocystis hominis* strains isolated from two long-term health care facilities," *J. Clin. Microbiol.*, vol. 38, no. 4, pp. 1324–30, 2000.

[12] I. Requena, Y. Hernández, M. Ramsay, C. Salazar, and R. Devera, "Prevalencia de *Blastocystis hominis* en vendedores ambulantes de comida del municipio Caroní, Estado Bolívar, Venezuela," *Cad. Saude Publica*, vol. 19, no. 6, pp. 1721–1727, 2003.

[13] H. R. Salim *et al.*, "*Blastocystis* in animal handlers," *Parasitol. Res.*, vol. 85, no. 12, pp. 1032–1033, 1999.

[14] P. W. Doyle, M. M. Helgason, R. G. Mathias, and E. M. Proctor, "Epidemiology and pathogenicity of *Blastocystis hominis*.," *J. Clin. Microbiol.*, vol. 28, no. 1, pp. 116–21, 1990.

[15] F. Dogruman-Al, H. Yoshikawa, S. Kustimur, and N. Balaban, "PCR-based subtyping of *Blastocystis* isolates from symptomatic and asymptomatic individuals in a major hospital in Ankara, Turkey," *Parasitol. Res.*, vol. 106, no. 1, pp. 263–268, 2009.

[16] K. H. S. Wong, G. C. Ng, R. T. P. Lin, H. Yoshikawa, M. B. Taylor, and K. S. W. Tan, "Predominance of subtype 3 among *Blastocystis* isolates from a major hospital in Singapore," *Parasitol. Res.*, vol. 102, no. 4, pp. 663–670, 2008.

[17] L. Souppart *et al.*, "Molecular epidemiology of human *Blastocystis* isolates in France,"

Parasitol. Res., vol. 105, no. 2, pp. 413–421, 2009.

[18] E. M. Hussein, A. M. Hussein, M. M. Eida, and M. M. Atwa, “Pathophysiological variability of different genotypes of human *Blastocystis hominis* Egyptian isolates in experimentally infected rats,” *Parasitol. Res.*, vol. 102, no. 5, pp. 853–860, 2008.

[19] H. Yoshikawa *et al.*, “Polymerase chain reaction-based genotype classification among human *Blastocystis hominis* populations isolated from different countries,” *Parasitol. Res.*, vol. 92, no. 1, pp. 22–29, 2004.

[20] D. J. Stenzel, L.A. Dunn, P.F.L. Boreham, “Ultrastructural variation of *Blastocystis hominis* stocks in culture,” *Int. J. Parasitol.*, vol. 19, no. 1, pp. 43–56, 1989.

[21] J. A. Yason, Y. R. Liang, C. W. Png, Y. Zhang, and K. S. W. Tan, “Interactions between a pathogenic *Blastocystis* subtype and gut microbiota: In vitro and in vivo studies,” *Microbiome*, vol. 7, no. 30, pp. 1–13, 2019.

[22] L. Eme, E. Gentekaki, B. Curtis, J. M. Archibald, and A. J. Roger, “Lateral Gene Transfer in the Adaptation of the Anaerobic Parasite *Blastocystis* to the Gut,” *Curr. Biol.*, vol. 27, no. 6, pp. 807–820, 2017.

[23] S. Isshiki *et al.*, “Cloning, expression, and characterization of a novel UDP-galactose:β- N-acetylglucosamine β1,3-galactosyltransferase (β3Gal-T5) responsible for synthesis of type 1 chain in colorectal and pancreatic epithelia and tumor cells derived therefrom,” *J. Biol. Chem.*, vol. 274, no. 18, pp. 12499–12507, 1999.

[24] Anthony P. Moran*, “Relevance of fucosylation and Lewis antigen expression in the bacterial gastroduodenal pathogen *Helicobacter pylori*,” *Carbohydr. Res.*, vol. 253, no. 1, pp. 1952–1965, 2008.

[25] C. Wunder *et al.*, “Cholesterol glucosylation promotes immune evasion by *Helicobacter pylori*,” *Nat. Med.*, vol. 12, no. 9, pp. 1030–1038, 2006.

[26] S. CHANDRAMATHI, K. SURESH, S. SHUBA, A. MAHMOOD, and U. R. KUPPUSAMY, “ High levels of oxidative stress in rats infected with *Blastocystis hominis* ,” *Parasitology*, vol. 137, no. 4, pp. 605–611, 2010.

[27] L. O. Andersen, I. Bonde, H. B. Nielsen, and C. R. Stensvold, “A retrospective metagenomics approach to studying *Blastocystis*,” *FEMS Microbiol. Ecol.*, vol. 91, no. 7, pp. 1–9, 2015.

[28] M. Arumagum *et al*, “Enterotypes of the human gut microbiome,” *Nature*, vol. 473, no. 1, pp. 174–180, 2011.

[29] Céline Nourrisson *et al*, “Blastocystis Is Associated with Decrease of Fecal Microbiota Protective Bacteria: Comparative Analysis between Patients with Irritable Bowel Syndrome and Control Subjects,” *PLoS One*, vol. 9, no. 11, pp. 1–9, 2014.

[30] Y. Lantsman, K. S. W. Tan, M. Morada, and N. Yarlett, “Biochemical characterization of amitochondrial-like organelle from *Blastocystis sp*. subtype 7,” *Microbiology*, vol. 154, no. 9, pp. 2757–2766, 2008.

[31] A. Stechmann *et al.*, “Organelles in *Blastocystis* that Blur the Distinction between Mitochondria and Hydrogenosomes,” *Curr. Biol.*, vol. 18, no. 8, pp. 580–585, 2008.

[32] M. Müller *et al.*, “Biochemistry and evolution of anaerobic energy metabolism in eukaryotes.,” *Microbiol. Mol. Biol. Rev.*, vol. 76, no. 2, pp. 444–95, 2012.

[33] Takashi Makiuchi, Tomoyoshi Nozaki “Highly divergent mitochondrion-related organelles in anaerobic parasitic protozoa,” *Biochimie*, vol. 100, no. 1, pp. 3–17, 2014.

[34] F. Denoeud *et al.*, “Genome sequence of the stramenopile *Blastocystis*, a human anaerobic parasite,” *Genome Biol.*, vol. 12, no. 3, p. R29, 2011.

[35] S. W. H. Van Weelden, J. J. Van Hellemond, F. R. Opperdoes, and A. G. M. Tielens, “New functions for parts of the krebs cycle in procyclic *Trypanosoma brucei*, a cycle not operating as a cycle,” *J. Biol. Chem.*, vol. 280, no. 13, pp. 12451–12460, 2005.

[36] J. J. van Hellemond, F. R. Opperdoes, and A. G. M. Tielens, “The extraordinary mitochondrion and unusual citric acid cycle in *Trypanosoma brucei*,” *Biochem. Soc. Trans.*, vol. 33, no. 5, p. 967, 2005.

[37] T. Narayanese, WikiUserPedia, YassineMrabet, “File:Citric acid cycle with aconitate 2.svg,” 2008. [Online]. Available: https://commons.wikimedia.org/wiki/File:Citric_acid_cycle_with_aconitate_2.svg.

[38] D. B. Ramsden *et al.*, “Human neuronal uncoupling proteins 4 and 5 (UCP4 and UCP5): Structural properties, regulation, and physiological role in protection against oxidative stress and mitochondrial dysfunction,” *Brain Behav.*, vol. 2, no. 4, pp. 468–478, 2012.

[39] Brigitte Boxma *et al*, “An anaerobic mitochondrion that produces hydrogen,” *Nature*, vol. 434, no. 1, pp. 74–79, 2005.

[40] C. R. Bártulos *et al.*, “Mitochondrial glycolysis in a major lineage of eukaryotes,” *Genome Biol. Evol.*, vol. 10, no. 9, pp. 2310–2325, 2018.

[41] L. V. Hooper and J. I. Gordon, “Glycans as legislators of host-microbial interactions: Spanning the spectrum from symbiosis to pathogenicity,” *Glycobiology*, vol. 11, no. 2, pp. 1–10, 2001.

[42] C. J. Day *et al.*, “Differential Carbohydrate Recognition by *Campylobacter jejuni* Strain 11168: Influences of Temperature and Growth Conditions,” *PLoS One*, vol. 4, no. 3, pp. 1–11, 2009.

[43] J. Xu *et al.*, “A Genomic View of the Human-Bacteroides *thetaiotaomicron* Symbiosis,” *Science (80-.).*, vol. 299, no. 5615, pp. 2074–2076, 2003.

[44] M. Stahl *et al.*, “L-Fucose utilization provides *Campylobacter jejuni* with a competitive advantage,” *Proc. Natl. Acad. Sci.*, vol. 108, no. 17, pp. 7194–7199, 2011.

[45] C. W. Stairs *et al.*, “A SUF Fe-S cluster biogenesis system in the mitochondrion-related organelles of the anaerobic protist Pygsuia,” *Curr. Biol.*, vol. 24, no. 11, pp. 1176–1186, 2014.

[46] P. Meza-Cervantez *et al.*, “Pyruvate: Ferredoxin oxidoreductase (PFO) is a surface-associated cell-binding protein in *Trichomonas vaginalis* and is involved in trichomonal adherence to host cells,” *Microbiology*, vol. 157, no. 12, pp. 3469–3482, 2011.

[47] M. Hoffmeister *et al.*, “*Euglena gracilis* rhodoquinone:ubiquinone ratio and mitochondrial proteome differ under aerobic and anaerobic conditions,” *J. Biol. Chem.*, vol. 279, no. 21, pp. 22422–22429, 2004.

[48] A. J. R. Michelle M. Leger., Ryan M. R. Gawryluk., Michael W. Gray, “Evidence for a Hydrogenosomal-Type Anaerobic ATP Generation Pathway in *Acanthamoeba castellanii*,” *PLoS One*, vol. 8, no. 9, pp. 1–13, 2013.

[49] Y. Aqeel, R. Siddiqui, M. Farooq, and N. A. Khan, “Anaerobic respiration: In vitro efficacy of Nitazoxanide against mitochondriate *Acanthamoeba castellanii* of the T4 genotype,” *Exp. Parasitol.*, vol. 157, pp. 170–176, 2015.

[50] N. A. Khan, “*Acanthamoeba*: Biology and increasing importance in human health,” *FEMS Microbiol. Rev.*, vol. 30, no. 4, pp. 564–595, 2006.

[51] P. D. Scanlan and C. R. Stensvold, “*Blastocystis*: Getting to grips with our guileful guest,” *Trends Parasitol.*, vol. 29, no. 11, pp. 523–529, 2013.

[52] E. Gentekaki, “Extreme genome diversity in the hyper-prevalent parasitic eukaryote Blastocystis,” *PLoS Biol.*, vol. 15, no. 9, pp. 1–42, 2017.

[53] P. D. Scanlan *et al.*, “The microbial eukaryote *Blastocystis* is a prevalent and diverse member

of the healthy human gut microbiota," *FEMS Microbiol. Ecol.*, vol. 90, no. 1, pp. 326–330, 2014.

[54] C. D. Dehaven, A. M. Evans, H. Dai, and K. A. Lawton, "Organization of GC/MS and LC/MS metabolomics data into chemical libraries," *J. Cheminform.*, vol. 2, no. 1, pp. 1–12, 2010.

[55] F. Fathi *et al.*, "NMR-based identification of metabolites in polar and non-polar extracts of avian liver," *Metabolites*, vol. 7, no. 4, pp. 1–9, 2017.

[56] J. Li, T. Vosegaard, and Z. Guo, "Applications of nuclear magnetic resonance in lipid analyses: An emerging powerful tool for lipidomics studies," *Prog. Lipid Res.*, vol. 68, no. August, pp. 37–56, 2017.

[57] C. Bruno *et al.*, "The combination of four analytical methods to explore skeletal muscle metabolomics: Better coverage of metabolic pathways or a marketing argument?," *J. Pharm. Biomed. Anal.*, vol. 148, pp. 273–279, 2018.

[58] A. Beltran *et al.*, "Assessment of compatibility between extraction methods for NMR- and LC/MS-based metabolomics," *Anal. Chem.*, vol. 84, no. 14, pp. 5838–5844, 2012.

[59] M. A. Salem, J. Jüppner, K. Bajdzienko, and P. Giavalisco, "Protocol: A fast, comprehensive and reproducible one-step extraction method for the rapid preparation of polar and semi-polar metabolites, lipids, proteins, starch and cell wall polymers from a single sample," *Plant Methods*, vol. 12, no. 1, pp. 1–15, 2016.

[60] F. M. Geier, E. J. Want, A. M. Leroi, and J. G. Bundy, "Cross-platform comparison of *caenorhabditis elegans* tissue extraction strategies for comprehensive metabolome coverage," *Anal. Chem.*, vol. 83, no. 10, pp. 3730–3736, 2011.

[61] W. Li, R. E. Lee, R. E. Lee, and J. Li, "Methods for acquisition and assignment of multidimensional high-resolution magic angle spinning NMR of whole cell bacteria," *Anal. Chem.*, vol. 77, no. 18, pp. 5785–5792, 2005.

[62] O. Beckonert *et al.*, "Metabolic profiling, metabolomic and metabonomic procedures for NMR spectroscopy of urine, plasma, serum and tissue extracts.," *Nat. Protoc.*, vol. 2, no. 11, pp. 2692–2703, 2007.

[63] C. Gómez-Gallego *et al.*, "Human breast milk NMR metabolomic profile across specific geographical locations and its association with the milk microbiota," *Nutrients*, vol. 10, no. 10, 2018.

[64] L. C. Tan, W. J. Yang, W. P. Fu, P. Su, J. K. Shu, and L. M. Dai, "1 H-NMR-based metabolic profiling of healthy individuals and high-resolution CT-classified phenotypes of COPD with treatment of tiotropium bromide," *Int. J. COPD*, vol. 13, pp. 2985–2997, 2018.

[65] M. Vermathen, J. Müller, J. Furrer, N. Müller, and P. Vermathen, "1H HR-MAS NMR spectroscopy to study the metabolome of the protozoan parasite *Giardia lamblia*," *Talanta*, vol. 188, no. May, pp. 429–441, 2018.

[66] O. A. Snytnikova, A. A. Khlichkina, R. Z. Sagdeev, and Y. P. Tsentalovich, "Evaluation of sample preparation protocols for quantitative NMR-based metabolomics," *Metabolomics*, vol. 15, no. 6, p. 84, 2019.

[67] P. Giavalisco *et al.*, "Elemental formula annotation of polar and lipophilic metabolites using 13C, 15N and 34S isotope labelling, in combination with high-resolution mass spectrometry," *Plant J.*, vol. 68, no. 2, pp. 364–376, 2011.

[68] M. A. Anwar *et al.*, "Optimization of metabolite extraction of human vein tissue for ultra performance liquid chromatography-mass spectrometry and nuclear magnetic resonance-based untargeted metabolic profiling," *Analyst*, vol. 140, no. 22, pp. 7586–7597, 2015.

[69] S. SCHÄFER, T. PAALME, R. VILU, and G. FUCHS, "13C-NMR study of acetate assimilation

in *Thermoproteus neutrophilus*," *Eur. J. Biochem.*, vol. 186, no. 3, pp. 695–700, 1989.

[70] J. G. Zeikus, M. K. Jain, and P. Elankovan, "Biotechnology of succinic acid production and markets for derived industrial products," *Appl. Microbiol. Biotechnol.*, vol. 51, no. 5, pp. 545–552, 1999.

[71] J. B. McKinlay, Y. Shachar-Hill, J. G. Zeikus, and C. Vieille, "Determining *Actinobacillus succinogenes* metabolic pathways and fluxes by NMR and GC-MS analyses of 13C-labeled metabolic product isotopomers," *Metab. Eng.*, vol. 9, no. 2, pp. 177–192, 2007.

[72] Y. Kwon, S. Park, J. Shin, and D. C. Oh, "Application of 13C-labeling and 13C-13C COSY NMR experiments in the structure determination of a microbial natural product," *Arch. Pharm. Res.*, vol. 37, no. 8, pp. 967–971, 2014.

[73] A. Peksel, N. Torres, J. Liu, G. Juneau, and C. Kubicek, "13C-NMR analysis of glucose metabolism during citric acid production by *Aspergillus niger*," *Appl. Microbiol. Biotechnol.*, vol. 58, no. 2, pp. 157–163, 2002.

[74] C. Rotte, F. Stejskal, G. Zhu, J. S. Keithly, and W. Martin, "Pyruvate: NADP+ oxidoreductase from the mitochondrion of *Euglena gracilis* and from the apicomplexan *Cryptosporidium parvum*: A biochemical relic linking pyruvate metabolism in mitochondriate and amitochondriate protists," *Mol. Biol. Evol.*, vol. 18, no. 5, pp. 710–720, 2001.

[75] Eugen Kubala et al, "Hyperpolarized 13C Metabolic Magnetic Resonance Spectroscopy and Imaging," *J. Vis. Exp.*, vol. 118, no. 1, 2016.

[76] J. Liu *et al.*, "Sparse 13C labelling for solid-state NMR studies of P. pastoris expressed eukaryotic seven-transmembrane proteins," *J. Biomol. NMR*, vol. 65, no. 1, pp. 7–13, 2016.

[77] C. Peng, T. Viana, M. A. Petersen, F. H. Larsen, and N. Arneborg, "Metabolic footprint analysis of metabolites that discriminate single and mixed yeast cultures at two key time-points during mixed culture alcoholic fermentations," *Metabolomics*, vol. 14, no. 7, pp. 1–12, 2018.

[78] R. Calvani *et al.*, "Fecal and urinary NMR-based metabolomics unveil an aging signature in mice," *Exp. Gerontol.*, vol. 49, no. 1, pp. 5–11, 2014.

[79] Ece Mutlu et al, "Intestinal dysbiosis: a possible mechanism of alcohol-induced endotoxemia and alcoholic steatohepatitis in rats," *Natl. isntitue Heal.*, vol. 33, no. 10, pp. 1836–1846, 2009.

[80] Arthur Yan et al, "Enteric Dysbiosis Associated with a Mouse Model of Alcoholic Liver Disease," *Natl. Institutes Heal.*, vol. 53, no. 1, pp. 96–105, 2011.

[81] S. A. Kurola P, Tapiainen T, Kaijalainen T, Uhari M, "Xylitol and capsular gene expression in *Streptococcus pneumoniae*.," *J. Med. Microbiol.*, vol. 58, no. 11, pp. 1470–1473, 2009.

[82] A Scheinin KK Makinen E Tammisalo M Rekola, "Turku sugar studies XVIII. Incidence of dental caries in relation to 1-year consumption of xylitol chewing gum," *Scand. Dent. Act*, vol. 33, no. 5, pp. 269–278, 1975.

[83] K. Shekhawat, H. Patterton, F. F. Bauer, and M. E. Setati, "RNA-seq based transcriptional analysis of *Saccharomyces cerevisiae* and *Lachancea thermotolerans* in mixed-culture fermentations under anaerobic conditions," *BMC Genomics*, vol. 20, no. 1, pp. 1–15, 2019.

[84] Y. Lantsman, K. S. W. Tan, M. Morada, and N. Yarlett, "Biochemical characterization of amitochondrial-like organelle from *Blastocystis sp*. subtype 7," *Microbiology*, vol. 154, no. 9, pp. 2757–2766, 2008.

[85] C. Bourriaud *et al.*, "Lactate is mainly fermented to butyrate by human intestinal microfloras but inter-individual variation is evident," *J. Appl. Microbiol.*, vol. 99, no. 1, pp. 201–212, 2005.

[86] A. Shikano *et al.*, "Effects of *Lactobacillus plantarum* Uruma-SU4 fermented green loofah on plasma lipid levels and gut microbiome of high-fat diet fed mice," *Food Res. Int.*, vol. 121, no.

September 2018, pp. 817–824, 2019.

[87] K. Takahashi, H. Terashima, K. Kohno, and N. Ohkohchi, “A stand-alone synbiotic treatment for the prevention of D-lactic acidosis in short bowel syndrome,” *Int. Surg.*, vol. 98, no. 2, pp. 110–113, 2013.

[88] C. R. S. Lee O’Brien Andersen, “*Blastocystis* in Health and Disease: Are We Moving from a Clinical to a Public Health Perspective?,” *J. Clin. Microbiol.*, vol. 54, no. 3, pp. 524–528, 2019.

[89] Ece Mutlu et al, “Intestinal dysbiosis: a possible mechanism of alcohol-induced endotoxemia and alcoholic steatohepatitis in rats,” *NIH Public Access*, vol. 33, no. 10, pp. 1836–1846, 2009.

[90] A. W. Yan. et Al, “Enteric Dysbiosis Associated with a Mouse Model of Alcoholic Liver Disease,” *NIH Public Access*, vol. 53, no. 1, pp. 96–105, 2011.

[91] KK Makinen, “Possible mechanisms for the cariostatic effect of xylitol,” *Int. Mag. Vitam. Nutr. Res. Suppl.*, vol. 15, no. 1, pp. 368–380, 1976.

[92] AF Silva et al, “In Vitro Inhibition of Adhesion of *Escherichia coli* Strains by Xylitol,” *Brazilian Arch. Biol. Technol.*, vol. 54, no. 2, pp. 235–241, 2011.

[93] L. W. Parfrey *et al.*, “Communities of microbial eukaryotes in the mammalian gut within the context of environmental eukaryotic diversity,” *Front. Microbiol.*, vol. 5, no. JUN, pp. 1–13, 2014.

[94] N. G. Rossen *et al.*, “Low prevalence of *Blastocystis sp*. in active ulcerative colitis patients,” *Eur. J. Clin. Microbiol. Infect. Dis.*, vol. 34, no. 5, pp. 1039–1044, 2015.

[95] C. Wright, G. Herbert, R. Pilkington, M. Callaghan, and S. McClean, “Real-time PCR method for the quantification of Burkholderia cepacia complex attached to lung epithelial cells and inhibition of that attachment,” *Lett. Appl. Microbiol.*, vol. 50, no. 5, pp. 500–506, 2010.

[96] S. H. Lee, B. K. Choi, and Y. J. Kim, “The cariogenic characters of xylitol-resistant and xylitol-sensitive *Streptococcus mutans* in biofilm formation with salivary bacteria,” *Arch. Oral Biol.*, vol. 57, no. 6, pp. 697–703, 2012.

[97] P Kurola et al, “Effect of xylitol and other carbon sources on *Streptococcus pneumoniae* biofilm formation and gene expression in vitro.,” *APMIS*, vol. 119, no. 2, pp. 135–142, 2011.